AD-A055 179 AIR FORCE INST OF TECH WRIGHT-PATTERSON AFB OHIO SCH--ETC F/G 19/5
AN EXTENDED KALMAN FILTER FIRE CONTROL SYSTEM AGAINST AIR-TO-AI--ETC(U)
DEC 77 S J CUSUMANO, M DE PONTE

UNCLASSIFIED AFIT/GE/EE/77-13-VOL-1 NL

1 OF 2
AD A055179

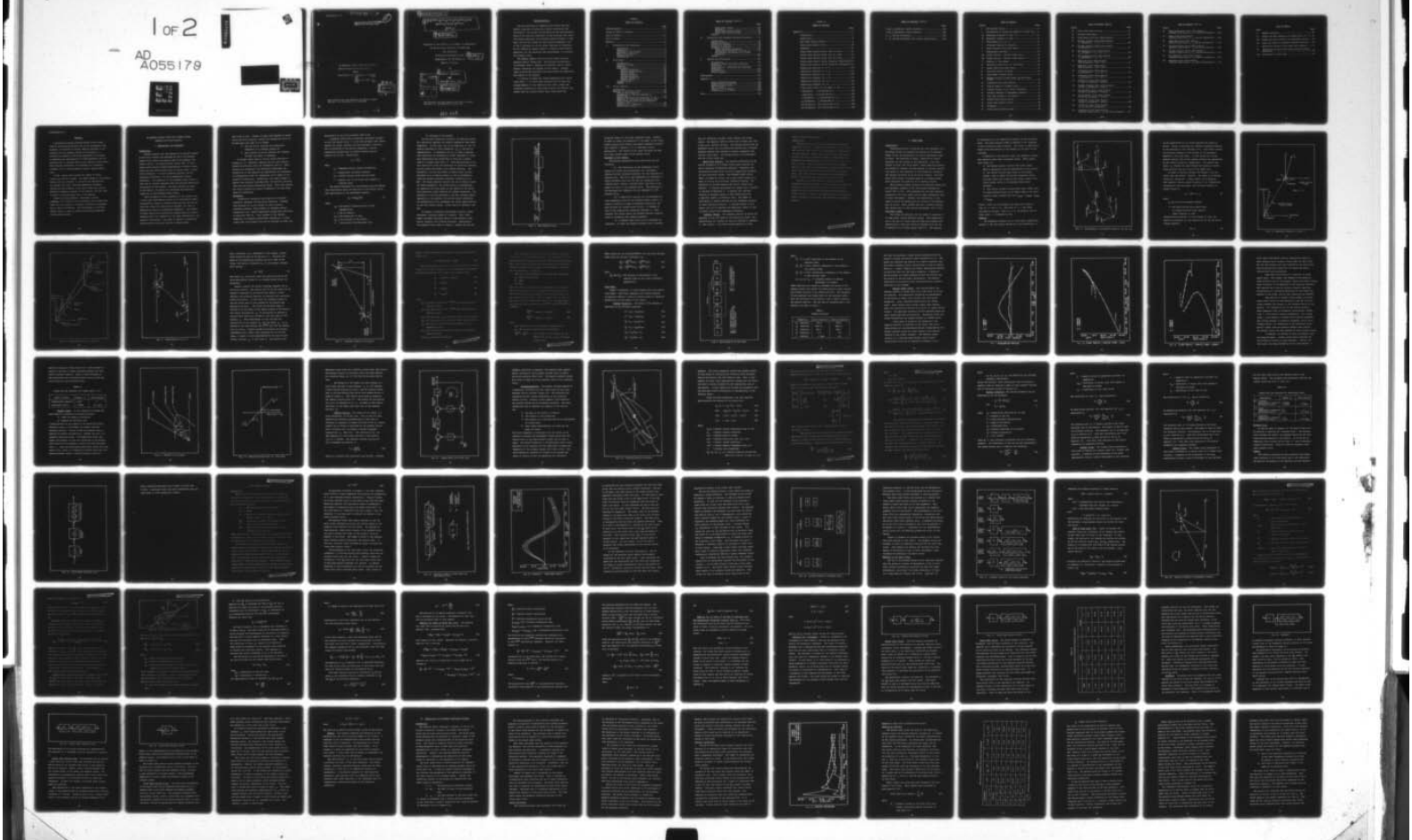

AFIT/GE/EE/77-13

AN EXTENDED KALMAN FILTER FIRE CONTROL SYSTEM AGAINST AIR-TO-AIR MISSILES (U)

THESIS

AFIT/GE/EE/77-13 Salvatore J. Cusumano
Capt USAF
and
Manuel De Ponte, Jr.
Capt USAF

(14) AFIT/GE/EE/77-13 - VOL-1

(6) AN EXTENDED KALMAN FILTER FIRE CONTROL SYSTEM AGAINST AIR-TO-AIR MISSILES, VOLUME I,

(9) Master's THESIS,

Presented to the Faculty of the School of Engineering

of the Air Force Institute of Technology

Air University

in Partial Fulfillment of the

Requirements for the Degree of

Master of Science

(12) 144 p.

by

(10) Salvatore J. Cusumano

and

Manuel De Ponte, Jr

Graduate Engineering

(11) December 1977

Acknowledgements

The work performed in completing this thesis has been greatly supported by people who deserve recognition from the authors. The project was sponsored by the Laser Analysis Group of the Avionics Laboratory, Wright-Patterson AFB, Ohio. The authors appreciate the direction given by Captain J. Gary Reid, who was the liaison for the Avionics Laboratory, and is now a professor at the Air Force Institute of Technology. We are indebted to Captain Robert N. Lutter of the Avionics Laboratory for his assistance and encouragement in following his original study.

The immense support given by our two thesis advisors deserves special recognition. The patience and dedication of Professor Peter S. Maybeck and Professor James E. Negro greatly influenced the outcome of this thesis. Through their guidance and assistance they have earned the admiration and respect of the authors.

In closing, we thank Mrs. Connie Weatherford for typing final draft. It is with great pleasure that we share the accomplishments of this labor with our wives, Linda, who graciously sketched all hand drawn figures, and Carolyn, who helped type the original draft, many, many drafts ago.

Volume I

Table of Contents

Table of Contents (Cont'd)

Volume II

Table of Contents

Table of Contents (Cont'd)

List of Figures

List of Figures (Cont'd)

List of Figures (Cont'd)

List of Tables

Abstract

A previously designed Extended Kalman Filter, based upon the proportional guidance law and an aerodynamic drag equation, is modified to include complete modeling of the autopilot and the guidance system of the missile. A sensitivity analysis of three key parameters is performed to determine the observability of these parameters and the possible need to estimate them in less complex filter models. This analysis establishes the advantages for reasonable estimates of all three parameters during a high-g trajectory.

A less complex model reduces the number of filter states from eleven to eight. The seeker dynamics, the guidance system, and the autopilot of a missile are approximated by a first order lag. The three parameters estimated include the time constant of the first order lag, the proportional navigation constant of the missile, and the ratio of mass to cross-sectional area of the missile.

Under the high-g scenario, reasonably accurate estimates of the states and the parameters are accomplished. Under the low-g scenario, parameter estimates are degraded due to lack of excitation. This performance of the parameters, however, does not hinder the accurate estimation of the missile states.

AN EXTENDED KALMAN FILTER FIRE CONTROL SYSTEM AGAINST AIR-TO-AIR MISSILES

I. Introduction and Background

Introduction

Current research into the defense of an aircraft against an air-to-air missile has proposed the use of an Extended Kalman Filter within the control loop of an automatic fire control system. An Extended Kalman Filter (EKF) in such a system would process incoming measurements of missile range, range rate and line-of-sight angle to achieve both: current state estimation - to aid in pointing accuracy, and for trajectory prediction - to aid in probability-of-kill assessment. The capability of the Extended Kalman Filter in this role is directly dependent upon the accurate modeling of the dynamics of the missile. The more accurate the model of the missile, the better the estimation and prediction capability of the Extended Kalman Filter.

Early attempts at state estimation of air targets used a first order Gauss-Markov process as an acceleration model. An appropriate choice of process noise strength and correlation time, along the three axes of movement, was used in modeling the target's acceleration components. The results of these studies have consistently implied that the filter's estimates were very sensitive to the least mismodeling of the target's acceleration. The model is generic in nature and has provided satisfactory results in several cases

(Ref 2:366; 8:323). However to apply this approach in modeling an air-to-air missile, ignores two assumptions which can be made about this type of air target:

1) most air-to-air missiles use proportional navigation as a guidance system and,
2) many current air-to-air missiles are "boosted to Mach" and coast to intercept.

In current thesis work at the Air Force Institute of Technology, an alternate approach has met with moderate success by utilizing these two assumptions (Ref 5). These results were incomplete, but definitely established the feasibility of this approach and demonstrated the advantages of incorporating these two assumptions into a model of the missile's acceleration. Essentially, the model attempts to exploit more physical knowledge about the missile's acceleration than the generic Gauss-Markov model. This study extends the results obtained by Lutter in Reference 5 by also using these two assumptions.

Background

Proportional navigation has proven to be straightforward to implement and tactically effective. Although this guidance law is not optimal for most realistic intercept problems, those attempts to implement optimal guidance on-line, usually approximate proportional navigation in some form (Ref 12). Also, because of the inherent simplicity to mechanize proportional navigation, it seems likely that this guidance law will be retained for some time,

particularly in air-to-air missiles (Ref 11:18).

A guidance system with prcportional navigation attempts to null the angular rate, $\dot{\theta}$, of the line-of-sight (LOS) vector between the target (ownship) and the interceptor (missile). This is performed by the missile commanding a lateral acceleration proportional to closing velocity and the angular rate of LOS. Analytically,

$$a_c = nV_c\dot{\theta} \tag{1}$$

where

a_c = commanded missile lateral acceleration

n = proportional navigation constant

V_c = closing velocity along the LOS vector

$\dot{\theta}$ = angular rate of LOS vector with respect to inertial space.

The second hypothesis of a non-thrusting missile implies that acceleration along the body axis of the missile can be well approximated by the aerodynamic equation

$$a_D = \tfrac{1}{2}\rho C_D V_m^2 S/M \tag{2}$$

where

a_D = the missile acceleration due to drag (deceleration)

ρ = the air density

C_D = the coefficient of drag

V_m = the velocity of the missile

S = the missile cross-sectional area

M = the mass of the missile.

As with most engineering problems, the benefits gained by a particular approach are usually tempered by some added complexity. In this case, the use of Equations (1) and (2) require knowledge of three parameters; C_D, n, and M/S for implementation. An expression for C_D in terms of measureable quantities was developed by Lutter (Reference 5) which well approximates the coefficient of drag for a generic missile at speeds above Mach 1.1. This approximation is not very restrictive since the velocities of air-to-air missiles are well above this speed in all combat scenarios. The parameters n and M/S may either be chosen using a priori knowledge of an attacking missile or may be estimated by using the unknown parameter estimation capability of an EKF. The former approach includes the use of nominal values for these parameters. The latter choice is accomplished by augmenting the state model of the missile in the filter with additional states modeling the unknown parameters. The estimation of the two parameters n and M/S, although adding complexity to the problem, can provide useful information for probability-of-kill assessment and threat identification to the fire control system. Lutter chose to estimate n and M/S.

To conduct a meaningful performance analysis, Lutter developed a realistic model of a missile. This "truth model" included significant detail of the missile's kinematics, dynamics, and internal structure. Specifically, the guidance strip, shown in Figure 1, modeled the lag and

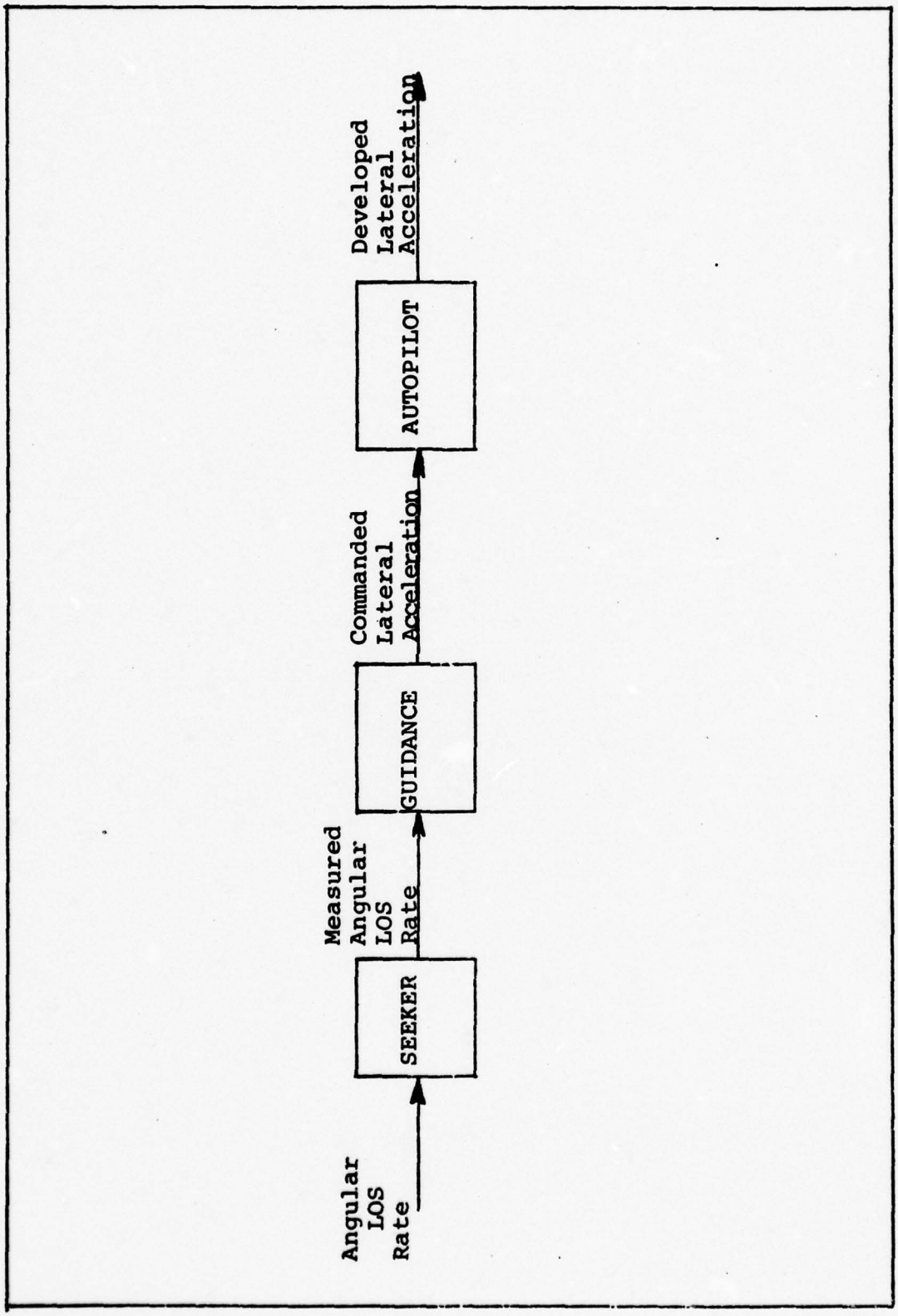

Fig. 1. The Guidance Strip

filtering effects of the three components shown. However, in order to reduce the complexity of the model in the filter, Lutter ignored these effects and equated commanded acceleration (defined in Equation (1)) to developed lateral acceleration. The results of his study indicated the need for a more refined model of the guidance strip.

Statement of the Problem

The problems addressed by this thesis work are the following:

(1) The feasibility of the fundamental Filter design has already been established, but a benchmark, showing the best estimation possible, was not considered in previous work. The first topic addressed will determine a proper benchmark which will be used for comparison with "reduced order" filters ("reduced order" referring to the number of states of the guidance strip). The designing of the benchmark will emphasize the key components of the guidance strip.

(2) A sensitivity analysis will be performed for those parameters which are not normally known a priori, or cannot be defined in terms of observable quantities, and must be known for reduced order filters. An example of this is the proportional navigation constant, n. This analysis will better define the tradeoff between a nominal value or estimating each unknown parameter.

(3) A reduced order filter will be designed and evaluated. To model the complete guidance strip, assuming

that all parameters are known, would require five filter states. The approach taken by Lutter was to model this with a zero order transfer function. The insights gained from the benchmark design and the sensitivity analysis will influence proposed reduced order designs of greater complexity than the zero order model. The minimum design to be considered will be a first order lag.

Monte Carlo Analysis. The accurate description of the missile kinematics in a proper filter model required the use of nonlinear differential equations. Therefore, the conventional Kalman Filter was not an appropriate estimator for this particular system. The Extended Kalman Filter (EKF), as chosen by Lutter, was a good initial choice as a means of solving this nonlinear estimation problem. The evaluation of the EKF requires the use of a Monte Carlo analysis. A complete description of a Monte Carlo analysis is included in Reference 6. In general this analysis involves an ensemble average of the filter error over a specified number of simulation runs. The number of runs chosen is usually dictated by the confidence required in these compiled statistics. A related problem in this thesis work will be choosing the approriate number of runs to obtain results with reasonable confidence.

Software Changes. The software provided by Lutter was modified to suit the needs of this particular study. The modifications and reasons for each are included in Appendix A. The results of the Lutter design appearing in this

thesis include these changes.

Organization

The body of this thesis has been arranged into four additional chapters. Chapter Two summarizes the key ideas and equations used by Lutter in developing the truth model for this problem. Chapter Three includes the development of the basic filter derived by Lutter. In addition, the benchmark and reduced order filters gerenated in this study are presented. The sensitivity analysis of the unknown parameters as well as the estimation analysis of the reduced order filter with parameter estimation comprise Chapter Four. The final results, conclusions and suggestions for further analysis conclude this work in Chapter Five.

Appendix B was constructed to contain all plots produced during the analysis. It was necessary to make this a separate volume becuase of the large number of plots generated from the myriad of changes performed during the filter analysis. However, the important plots are contained within the body of this report when necessary as supportive material.

II. TRUTH MODEL

Introduction

Oversimplification in modeling the "true dynamics" of a non-linear system can degrade the analysis of an Extended Kalman Filter and misrepresent its actual performance capabilities. The attention to detail should be an overall qualifier for the results of the simulation. With this thought in mind, the "truth model" (those equations defining the system of interest) has been modeled to include significant detail in the simulation of the kinematics, dynamics, and internal structure of an air-to-air missile. The truth model also includes a flexible model of an ownship target which simulates the maneuvers of an evading aircraft.

The following chapter presents the coordinate frames and the engagement geometry of the truth model developed by Lutter (Ref 5:7-50). Also presented are the most important equations of the truth model with the basic assumptions used in their development. However, the presentation in this report is brief and serves only as a review of the development by Lutter. Those readers desiring a complete development should refer to this earlier development (Ref 5:7-50).

Coordinate Frames

The filter was designed with the intent of applying it to cases which involve multiple targets. This design goal led to the use of a local inertial frame which reduces the computational burden that would be necessary with the use of multiple line-of-sight frames (Ref 5:1). The analysis

is restricted to a two dimensional scenario in the horizontal plane. The local inertial frame is defined to lie parallel to this horizontal plane of motion. The origin is arbitrarily chosen to be the position of the ownship at the start of the intercept.

In addition to the inertial frame, the geometric development exploits three other coordinate frames. These coordinate frames are

1) the ownship tracker line-of-sight frame (TLOS), used in conjunction with the measurements of the missile

2) the initial line-of-sight frame of the missile (IMLOS), used to define the missile kinematics within the truth model and to measure the angular rates of the line-of-sight vector to the ownship (maneuvering aircraft)

3) the initial tracker line-of-sight frame (ITLOS) used to relate missile motion in the IMLOS frame to the local inertial frame, defined such that $X_{ITLOS} = -X_{IMLOS}$, $Y_{ITLOS} = -Y_{IMLOS}$.

Figure 2 shows the relationship for these four frames at time (t) = 0 and t = t_1. Note that at t = 0 the ITLOS and TLOS are aligned. Also, at t = 0, the missile line-of-signt angle, θ, is defined as zero.

Geometry

The engagement geometry may at first appear complicated because of the many angles defined but, once understood, it

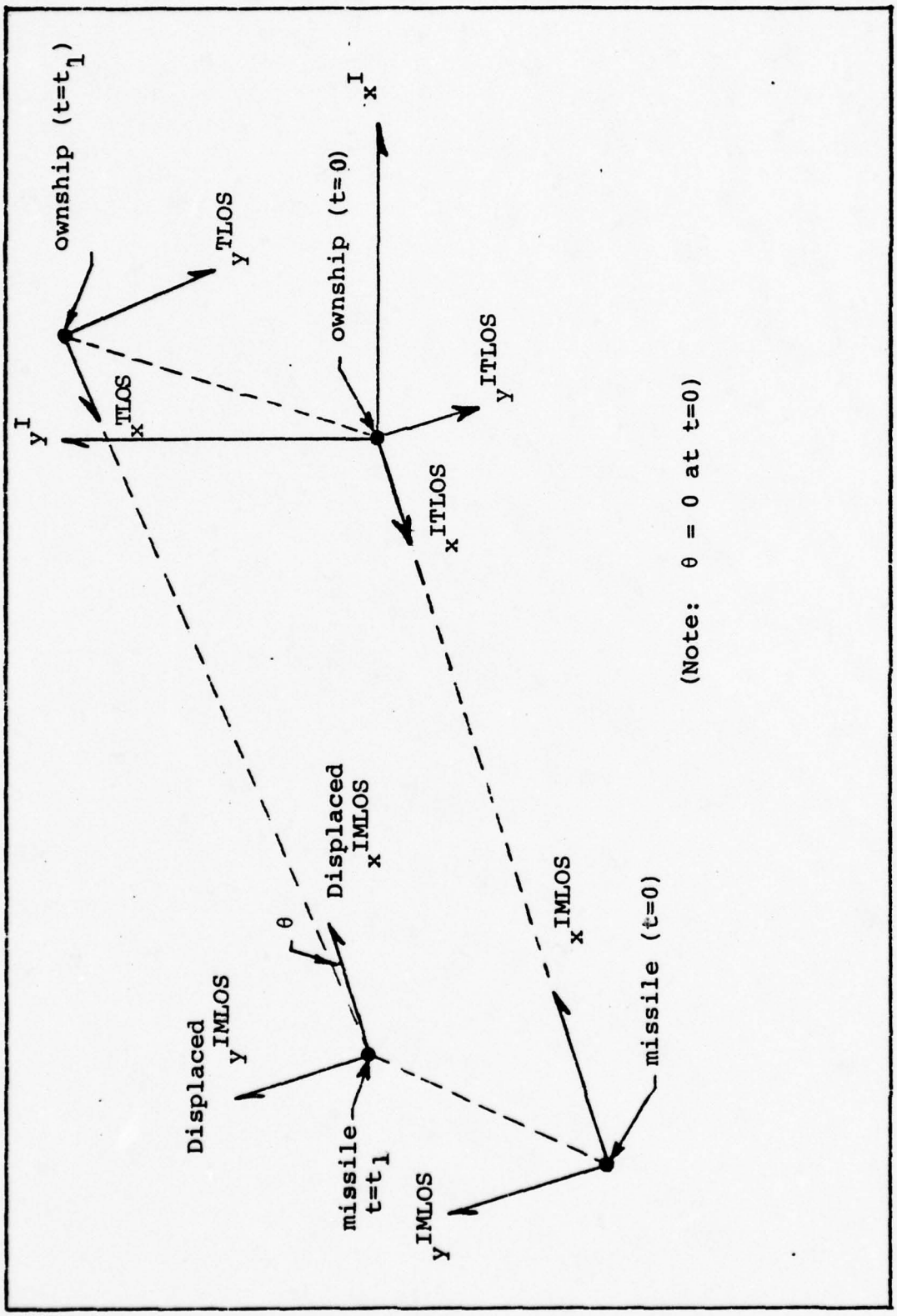

Fig. 2. Relationship of Coordinate Frames at t=0 and $t=t_1$

can be appreciated for its direct approach and versatile nature. Figure 3a describes the complete engagement geometry at the beginning of the intercept (t=0). This figure relates the intercept geometry of the missile to the engagement geometry of the truth model. In this figure the initial missile velocity and initial ownship velocity are represented by the vectors V_m and V_T, respectively. The missile lead angle, θ_L, defines the angle between the missile's current velocity vector and the X-axis of the IMLOS frame.

In order to actively estimate the change in the LOS vector that the missile observes, the angle θ_T is defined (Figure 3a, Figure 3b). Using a basic law of geometry, that opposite interior angles formed by a line intersecting two parallel lines are equal, the following equation is formed (Figure 4)

$$\theta_T - 180 = \theta + \phi \tag{3}$$

where

θ_T and θ are as previously defined

ϕ = the angle through which IMLOS frame is rotated from the local inertial frame (constant in time)

Differentiating Equation (3) with respect to time, the desired relationship for the angular rate of the LOS vector becomes apparent.

$$\dot{\theta}_T = \dot{\theta} \tag{4}$$

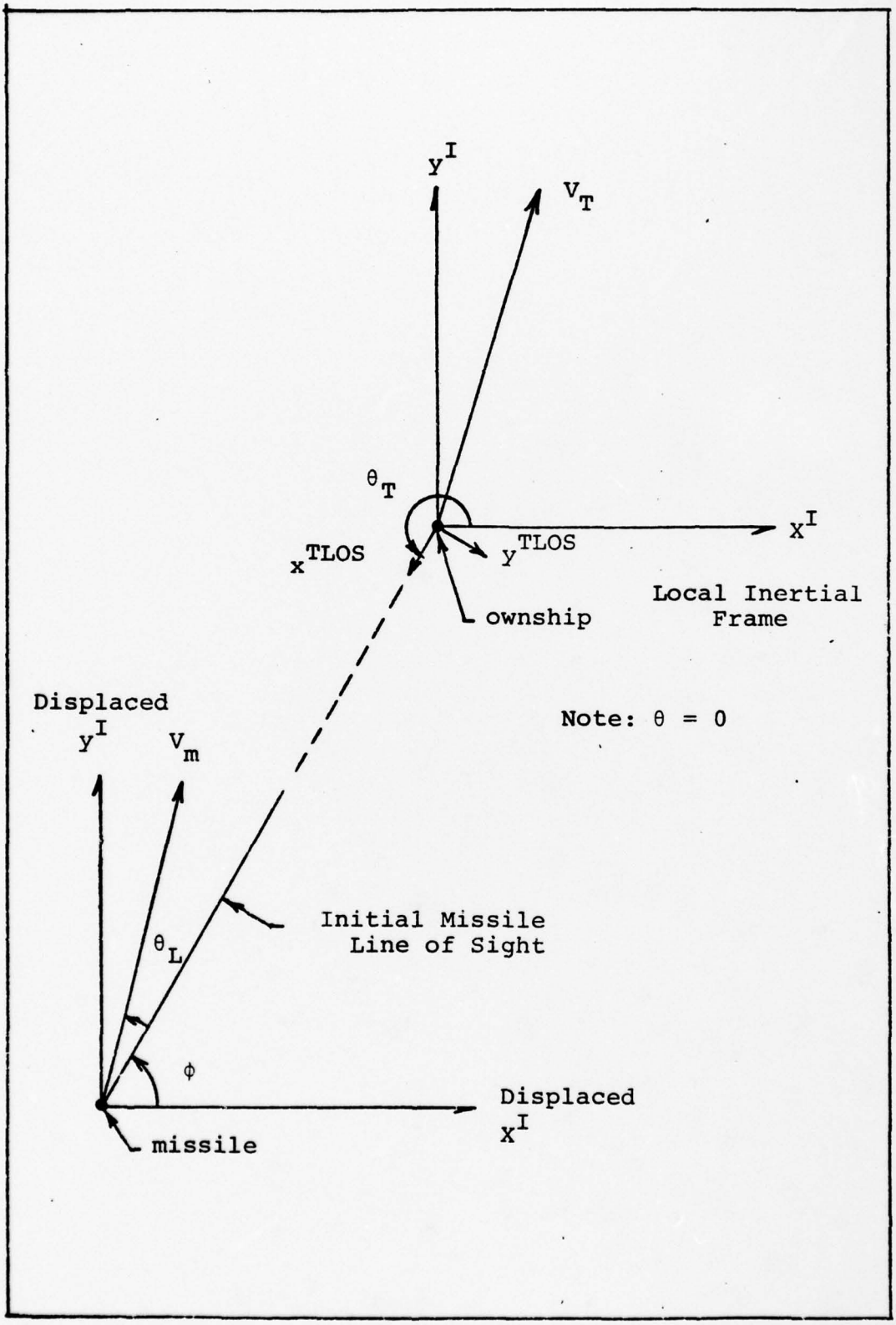

Fig. 3a Engagement Geometry at Time = 0

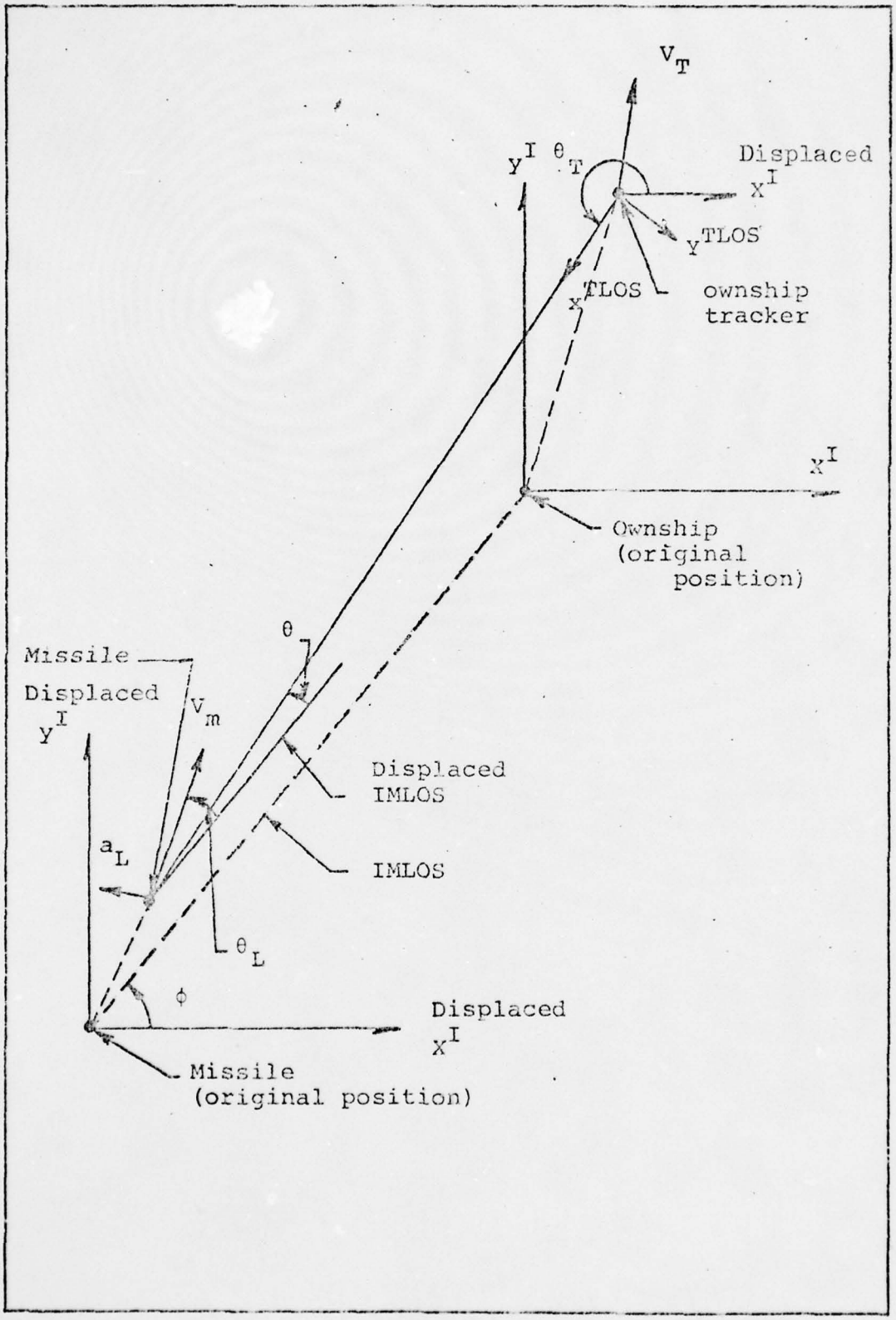

Fig. 3b. Engagement Geometry at Time >0

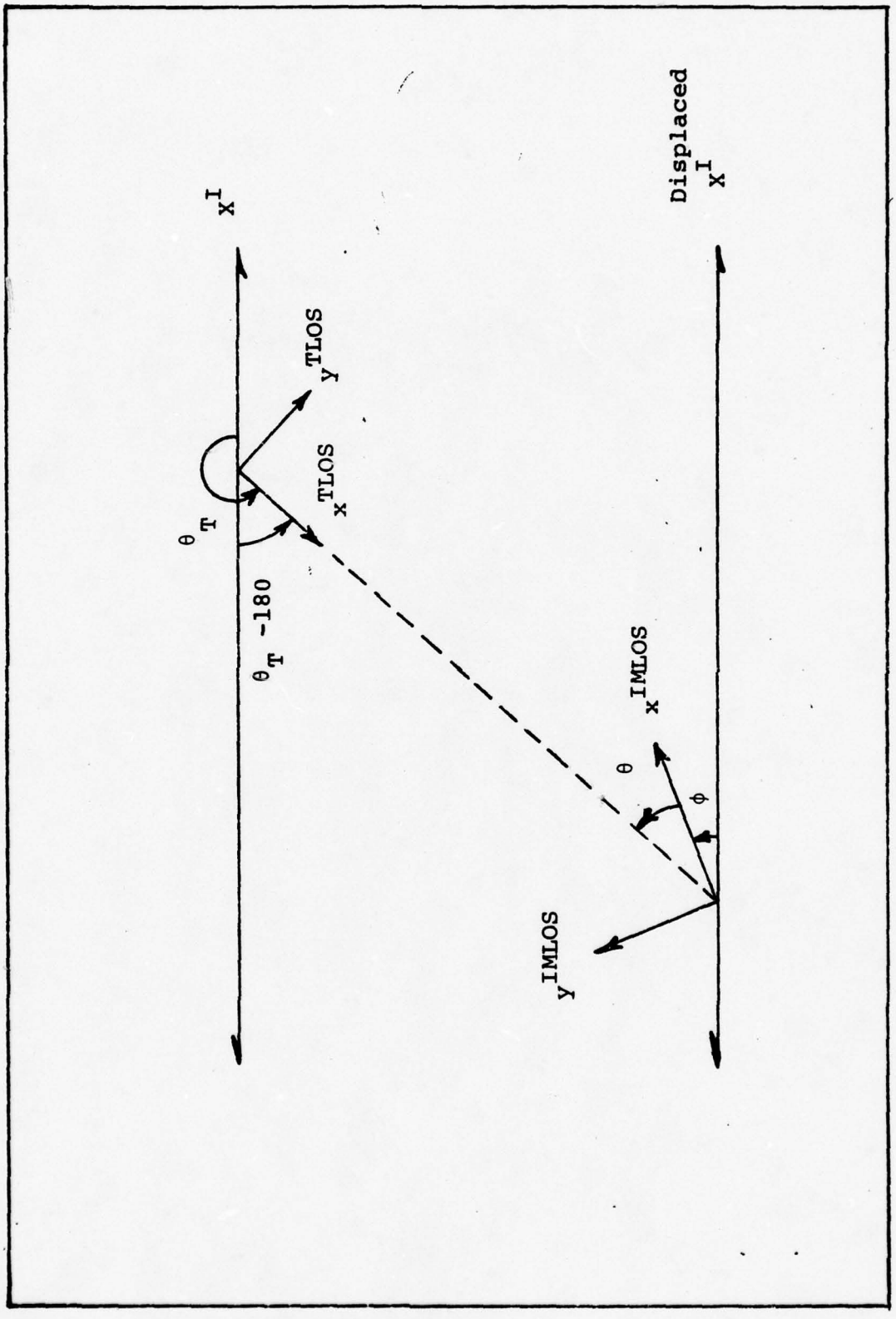

Fig. 4. Relationship of θ_T to θ

Thus, variations in θ_T, measurable at the ownship, reflect those variations seen by the missile in θ. Recalling the model of the proportional guidance law to be used in the filter, the merits of measuring θ_T, in this manner, becomes quite obvious:

$$a_L = nV_c\dot{\theta} \tag{1}$$

This angle, θ_T, along with range and range rate will be the three measurements passed to the Extended Kalman Filter for processing.

Figure 5 depicts the typical intercept geometry for an air-to-air missile. The angular rate of the LOS vector to the ownship is measured by the missile with respect to some arbitrary *non-rotating reference* for missiles with inertially stabilized seekers. In this case, the reference chosen is the LOS vector that is first sighted by the missile upon beginning intercept. The origin of the IMLOS frame is defined to be the center of the seeker antenna of the missile. The lateral acceleration, a_L, of the missile is defined as positive when causing an increase in the lead angle of the missile, θ_L. This relationship is also true for the acceleration of the ownship, a_T, and the angle, θ_A. θ_A is defined as the angle between the X^{IMLOS} axis and the ownship velocity vector. Missile guidance controllers are usually implemented with a small angle approximation for the LOS angle, θ, where θ is well approximated by the ratio of the lateral distance, y_d, to the range, R. The missile truth

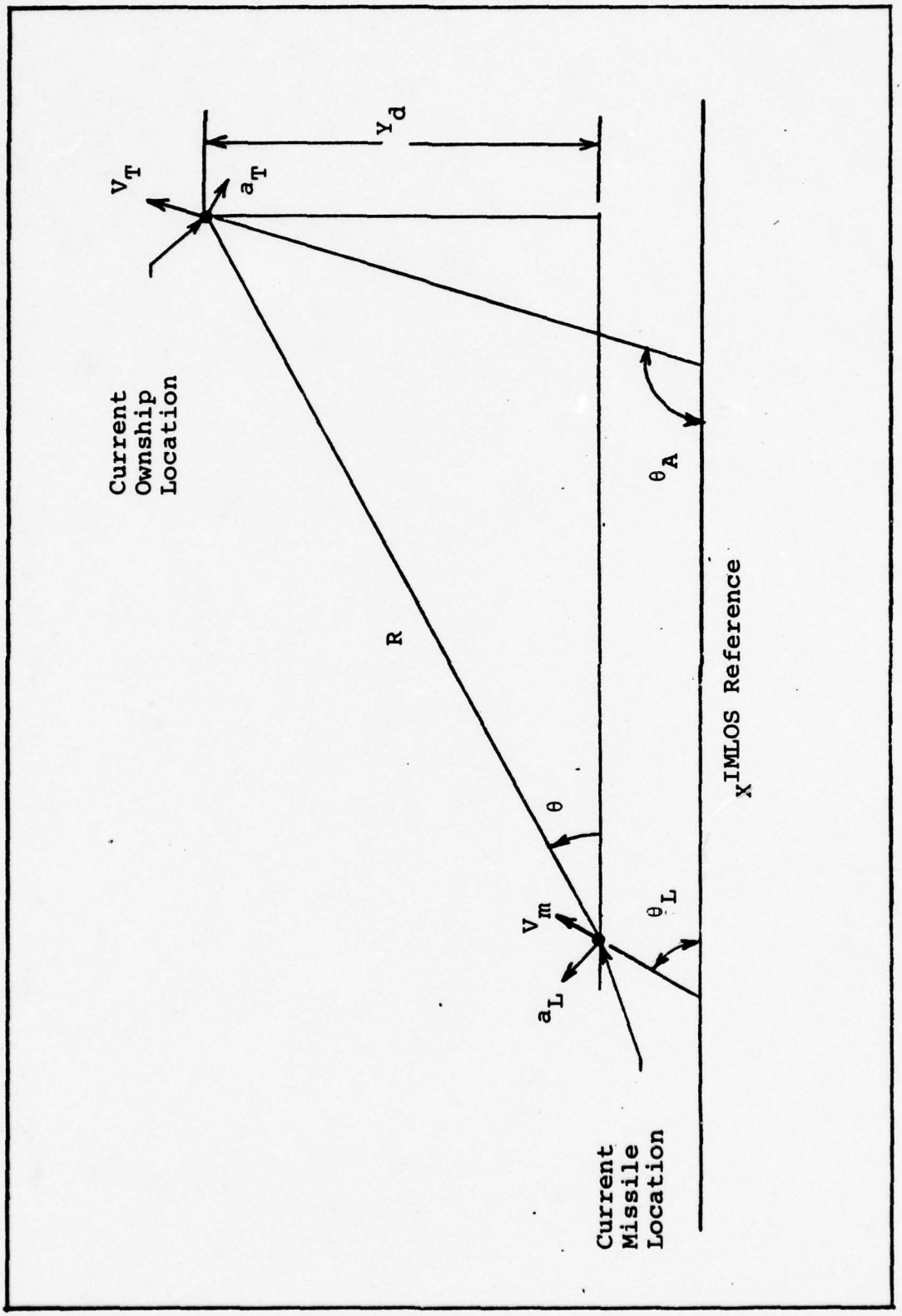

Fig. 5. Intercept Geometry for Missile

model in this simulation does include the small angle approximation for θ

$$\theta = \arcsin (y_d/R) \cong y_d/R \tag{5}$$

The intercept geometry for an air-to-air missile is used to define four state variables of the truth model, all quantities being referenced with respect to the IMLOS frame.

$$\dot{y}_d = V_T \sin\theta_A - V_m \sin\theta_L \tag{6}$$

$$\dot{\theta}_L = a_L g/V_m \tag{7}$$

$$\dot{\theta}_A = a_T g/V_T \tag{8}$$

$$\dot{R}^{-1} = -V_c R^{-2} \tag{9}$$

where

θ_A = the angle between the $-x^{IMLOS}$ axis and the ownship velocity vector

θ_L = the angle between the X^{IMLOS} axis and the missile velocity vector

V_T = the magnitude of the velocity vector of the ownship

V_m = the magnitude of the velocity vector of the missile

a_T = the tracker acceleration perpendicular to V_T expressed in g's

V_c = the realtive closing velocity between the missile and the tracker

R and y_d as defined previously

The origin of the ownship LOS frame (TLOS) is defined as the center of its measuring antenna. The antenna of the ownship is assumed to point without error and without lag effects. This simplification assumes that the possible errors arising from the dynamics of the antenna are negligible as compared to the measurement uncertainty.

Thus far, three coordinate frames have been discussed:

1) Local inertial frame
2) IMLOS
3) TLOS

Since the filter estimates will be described with respect to the inertial frame, the true missile velocity and position must also be defined with respect to the inertial frame for an estimate of true error. This is accomplished by relating the current missile acceleration vectors in the IMLOS frame to the ITLOS frame (recalling that $x^{ITLOS} = -x^{IMLOS}$, $y^{ITLOS} = -y^{IMLOS}$):

$$\dot{V}_{mx}^{ITLOS} = a_D \cos\theta_L + a_L \sin\theta_L \tag{10}$$

$$\dot{V}_{my}^{ITLOS} = a_D \sin\theta_L - a_L \cos\theta_L \tag{11}$$

where

a_D = the missile drag acceleration (deceleration)

a_L = the lateral acceleration of the missile

V_{mx}^{ITLOS}, V_{my}^{ITLOS} = the velocity of the missile in the ITLOS frame in the x and y direction respectively

These quantities are then coordinitized into the local inertial frame using the initial θ defined as θ_0.

$$V_{mx}^{I} = V_{mx}^{ITLOS}\cos\theta_0 - V_{my}^{ITLOS}\sin\theta_0 \quad (12)$$

$$V_{my}^{I} = V_{mx}^{ITLOS}\sin\theta_0 - V_{my}^{ITLOS}\cos^{\theta}{}_0 \quad (13)$$

where

V_{mx}^{I} and V_{my}^{I} = the velocity of the missile in the inertial frame in the x and y direction respectively.

Truth Model

Figure 6 represents, in block diagram form, the overall truth model. Each block represents the logical grouping of equations modeling a specific function which is addressed sequentially as they appear in the figure.

Ownship Kinematics. The motion of the ownship is described by the following equations:

$$x^{I} = k_1 t + k_2\cos(\omega t) \quad (14)$$

$$y^{I} = k_3 t + k_4\sin(\omega t) \quad (15)$$

$$V_x^{I} = k_1 - k_2\omega\sin(\omega t) \quad (16)$$

$$V_y^{I} = k_3 + k_4\omega\cos(\omega t) \quad (17)$$

$$a_x^{I} = -k_2\omega^2\cos(\omega t) \quad (18)$$

$$a_y^{I} = -k_r\omega^2\sin(\omega t) \quad (19)$$

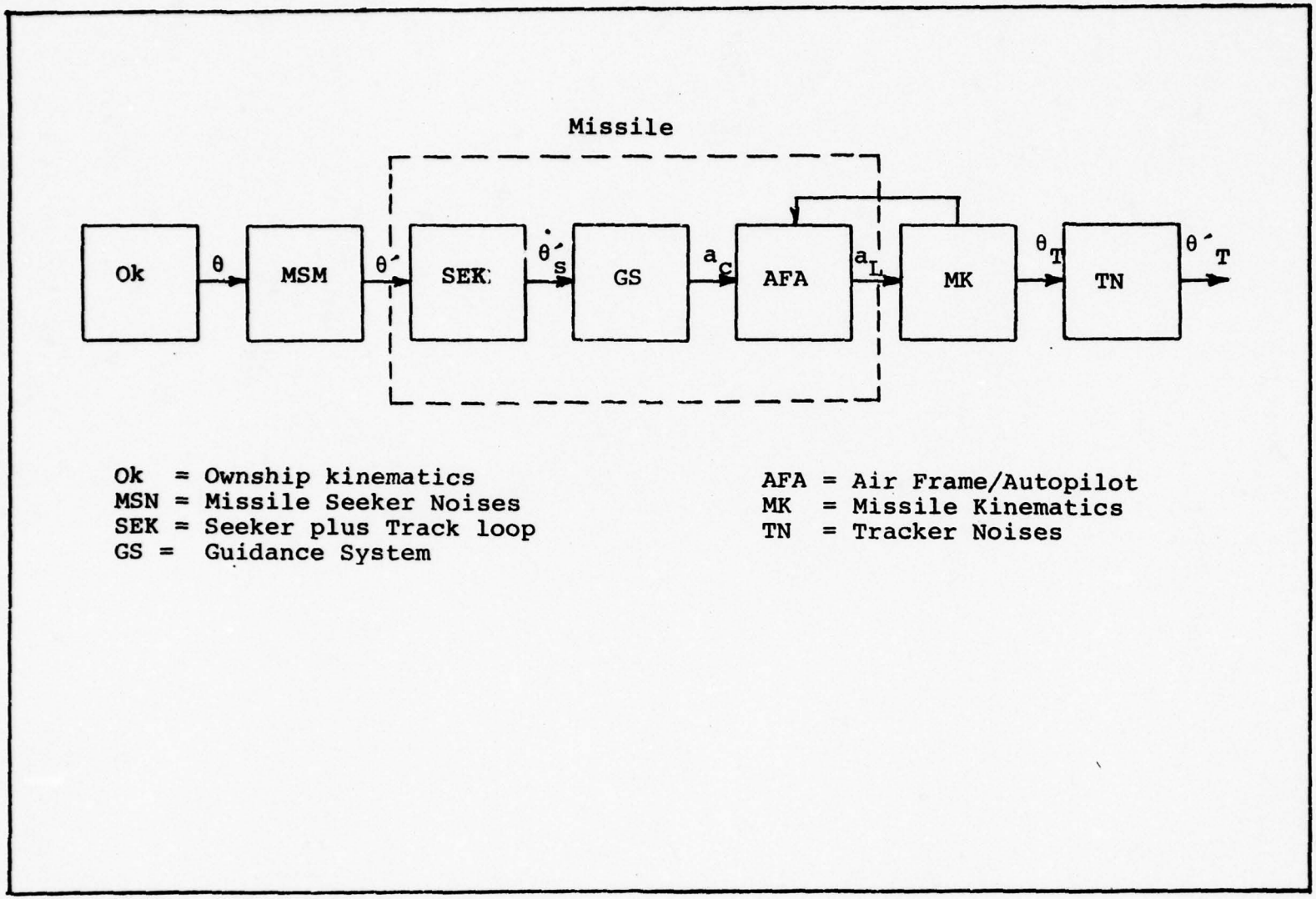

Fig. 6. Block Diagram of the Truth Model

where

X^I, Y^I = X and Y positions of the ownship in the inertial frame.

V_x^I, V_y^I = X and Y velocity components of the ownship in the inertial frame

a_x^I, a_y^I = X and Y acceleration components of the ownship in the inertial frame

k_1, k_2, k_3, k_4, ω = variables chosen for desired performance of ownship

These equations were chosen to represent the motion of the ownship because they embody the characteristic high-g turning and jinking maneuvers of an evading aircraft. The variables of the equations were chosen more for the resultant effect upon the trajectory of the missile, than to model a particular evasion maneuver. The two sets of variables used in the analysis are shown in Table I.

Table I

Ownship Variables

Parameters	Low-g-trajectory	High-g-trajectory
k_1 (feet/sec)	500.0	500.0
k_2 (feet/sec)	2864.51	2864.51
k_3 (feet/sec)	800.0	800.0
k_4 (feet/sec)	0.0	0.0
ω (rad/sec)	0.17455	0.4

The first set produced a rather benign trajectory with the missile's lateral acceleration never exceeding six g's. The second set subjected the missile to a high-g trajectory with the missile reaching lateral accelerations as high as twenty-three g's. Figure 7 depicts the lateral acceleration profiles for both the low-g and the high g scenarios. Figures 8a and 8b present the flight profiles of both the aircraft and the missile in low and high-g trajectories. The marking identifiers on the profile plots are positioned at constant intervals of 0.56 seconds.

Missile Seeker Noises. This section models the dominant aspects of seeker noise for a wide class of air-to-air missiles. The uncertainty corrupting the measurements of the missile's seeker can be placed into three broad categories: glint, amplitude scintillation and thermal noise. Those effects which corrupt seeker angle measurements are collectively referred to as glint (or angle scintillation). The amplitude variations of the received signal are aptly termed amplitude scintillation. Background noises and system inaccuracies are grouped together as thermal noise.

Glint noise is caused by the wandering of the apparent centroid of radiation of the target (Ref 13:97). These effects are time-correlated and are interpreted by the missile guidance system as actual changes in the angular velocity of the target (ownship). The dominant characteristic of a time-correlated process such as angle scintillation noise can be captured by modeling it as a

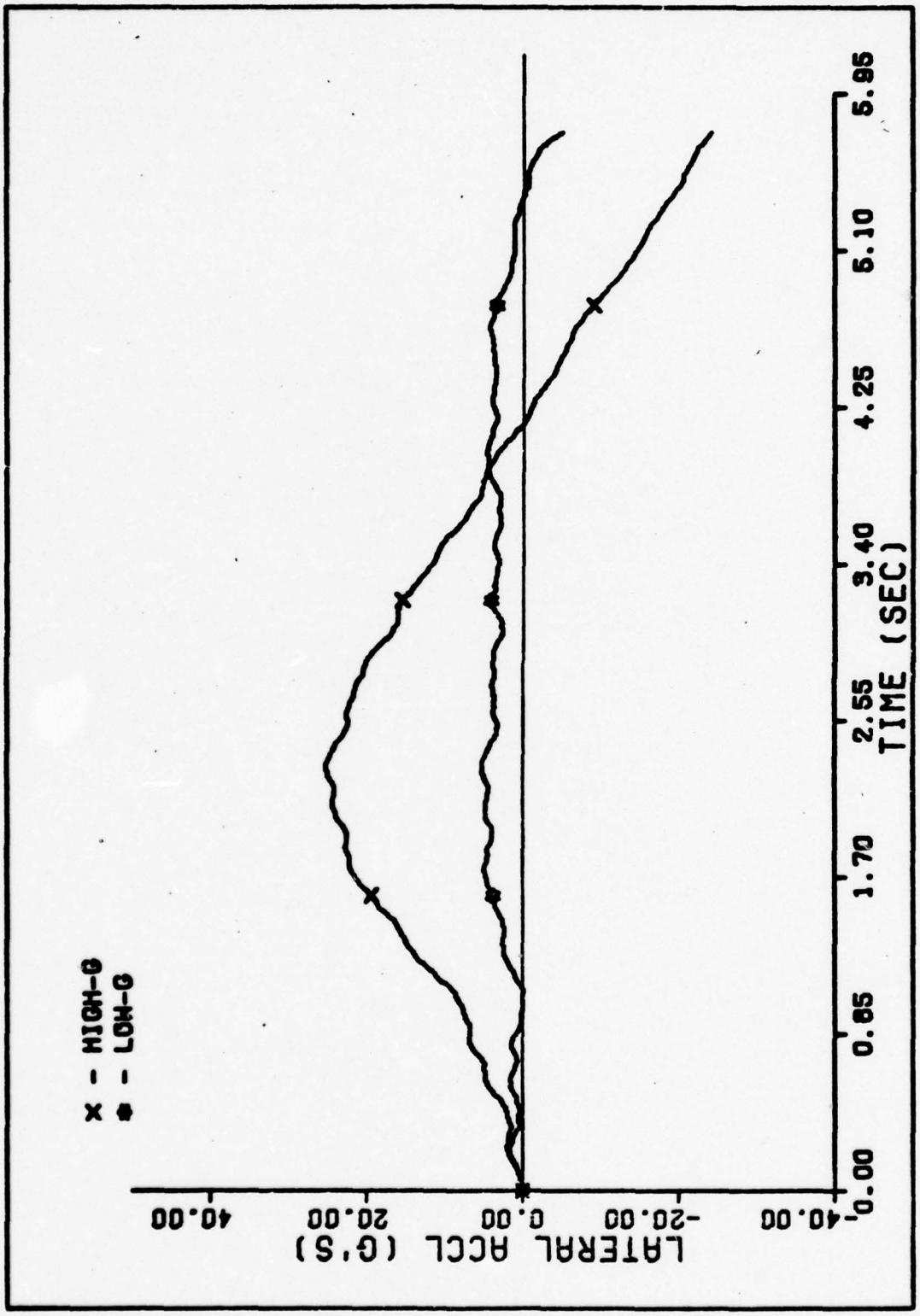

Fig. 7 ACCELERATION PROFILES

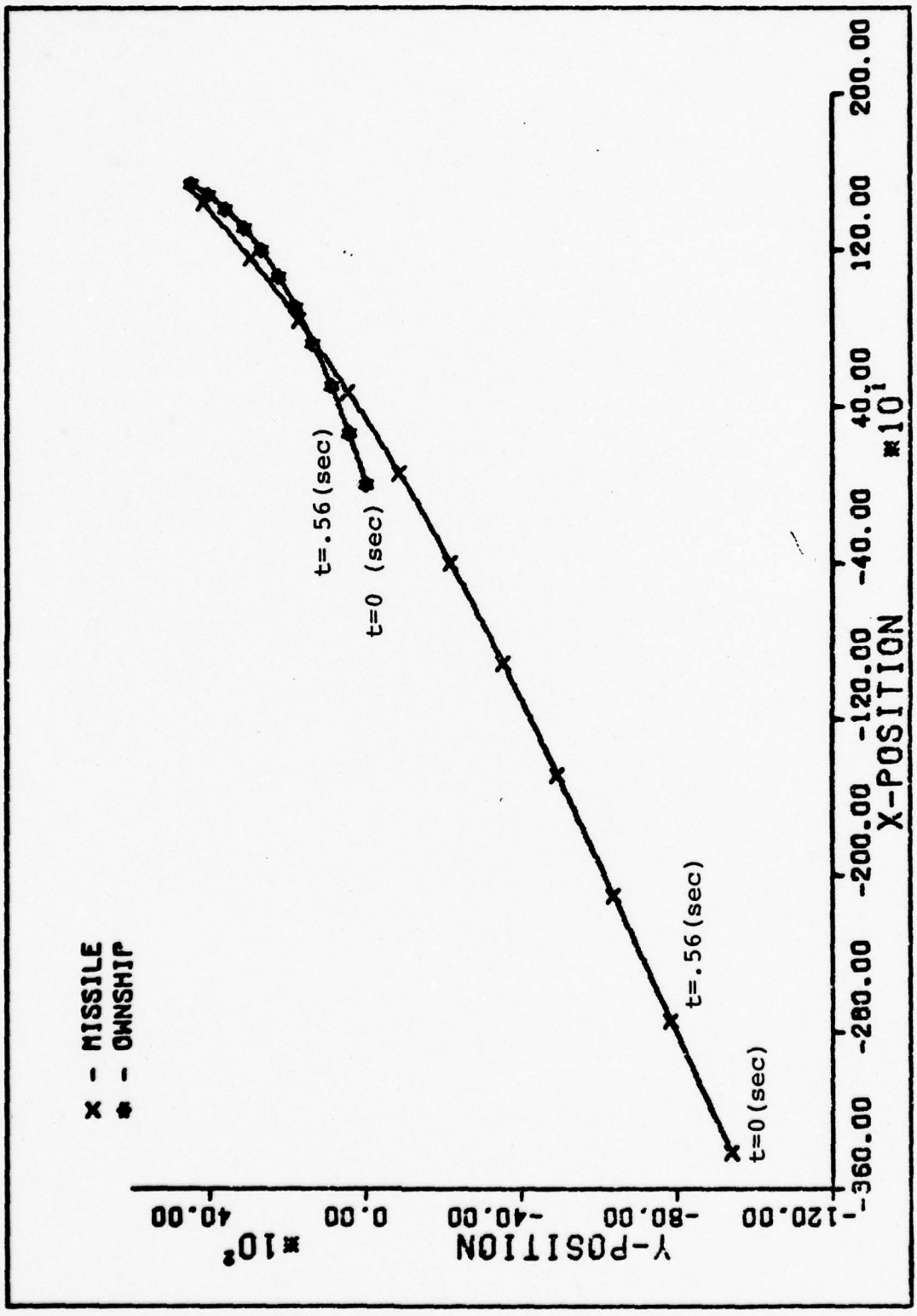

Fig. 8a. FLIGHT PROFILE ; INERTIAL FRAME . LOW-G

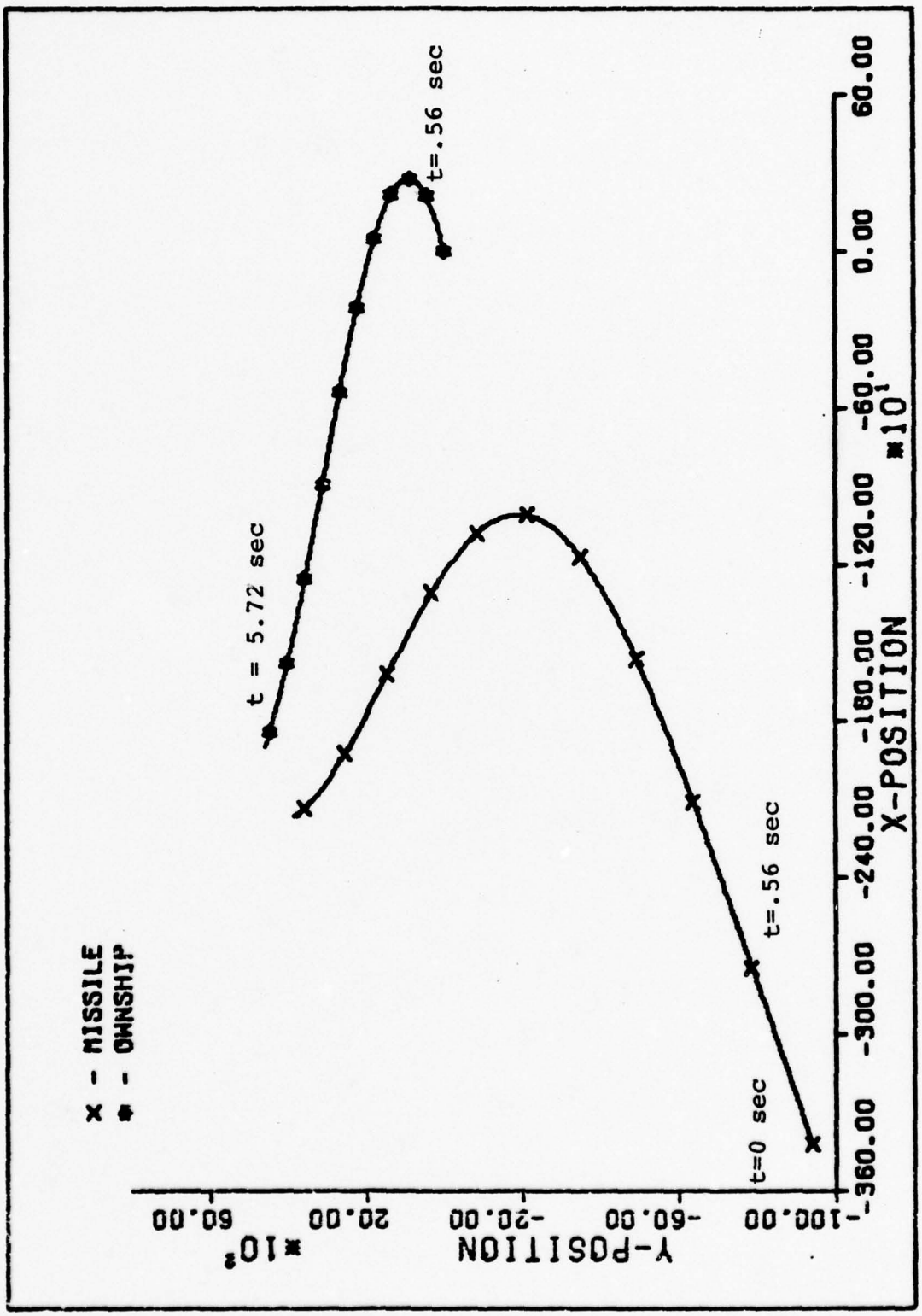

Fig. 8b FLIGHT PROFILE : INERTIAL FRAME . HIGH-G

first order Gauss-Markov process, generated by passing a white Gaussian noise through a first order lag (Ref 6:192). The lag time constant and input strength of the white noise must be appropriately chosen for the target and system uncertainties being considered.

Amplitude scintillation is a function of target aspect angle. More simply, the changes in the effective cross-sectional area of the ownship, facing the missile seeker, cause variations in the amplitude of the received radiation. The inaccuracies in missile guidance caused by amplitude scintillation are considered negligible for the ranges considered in this study, and for this reason are not modeled.

The modeling of thermal noise attempts to include those effects which are uncorrelated in time and are relatively wideband with respect to the "guidance strip" of the missile. The "guidance strip" of the missile includes those components used in processing line-of-sight information, $\dot{\theta}'$, into missile lateral acceleration. For a radar seeker, a good example of thermal noise would be unexplainable voltage changes in electronic equipment, while for an infrared seeker, the temperature of the background atmosphere or under cover are possible thermal noise sources. The thermal noises have been modeled as white Gaussian noises.

In general, the effects of glint and thermal noise are range dependent: thermal noise effects decrease and glint effects increase as range decreases. However, for this study, the range dependency has not been modeled. A

realistic strength of these noises for a radar system at a range of 2,000 feet is chosen and held constant over the entire intercept scenario. Table II shows strengths of the uncorrelated and correlated noises as well as the lag time constant of the correlated noise.

Table II

Sigmas and Time Constants for Seeker Noise ($\theta'-\theta$)

Types of Noises	Sigmas (σ)	Time Constant
uncorrelated (Thermal)	0.003	---
correlated (Glint)	0.00894	0.1 (Sec)

Missile Seeker. In this analysis the seeker has been modeled to perform the following functions:

1) track the ownship continuously
2) measure the LOS angle rate.

A characteristic of all seekers is the distortion effect, aberration error, of the radome (or irdome) upon the received radiation. Figure 9 shows the geometry used in modeling the seeker and explicitly defines the error, θ_r, caused by aberration error. With aberration error, the seeker now attempts to align the centerline of the antenna with the LOS to the ownship by nulling the false boresight error ε'. Since the aberrration angle error varies with look angle ($\theta-\theta_m$), there is a coupling of missile pitch rate with measured ownship motion. Figure 10 depicts a plot of

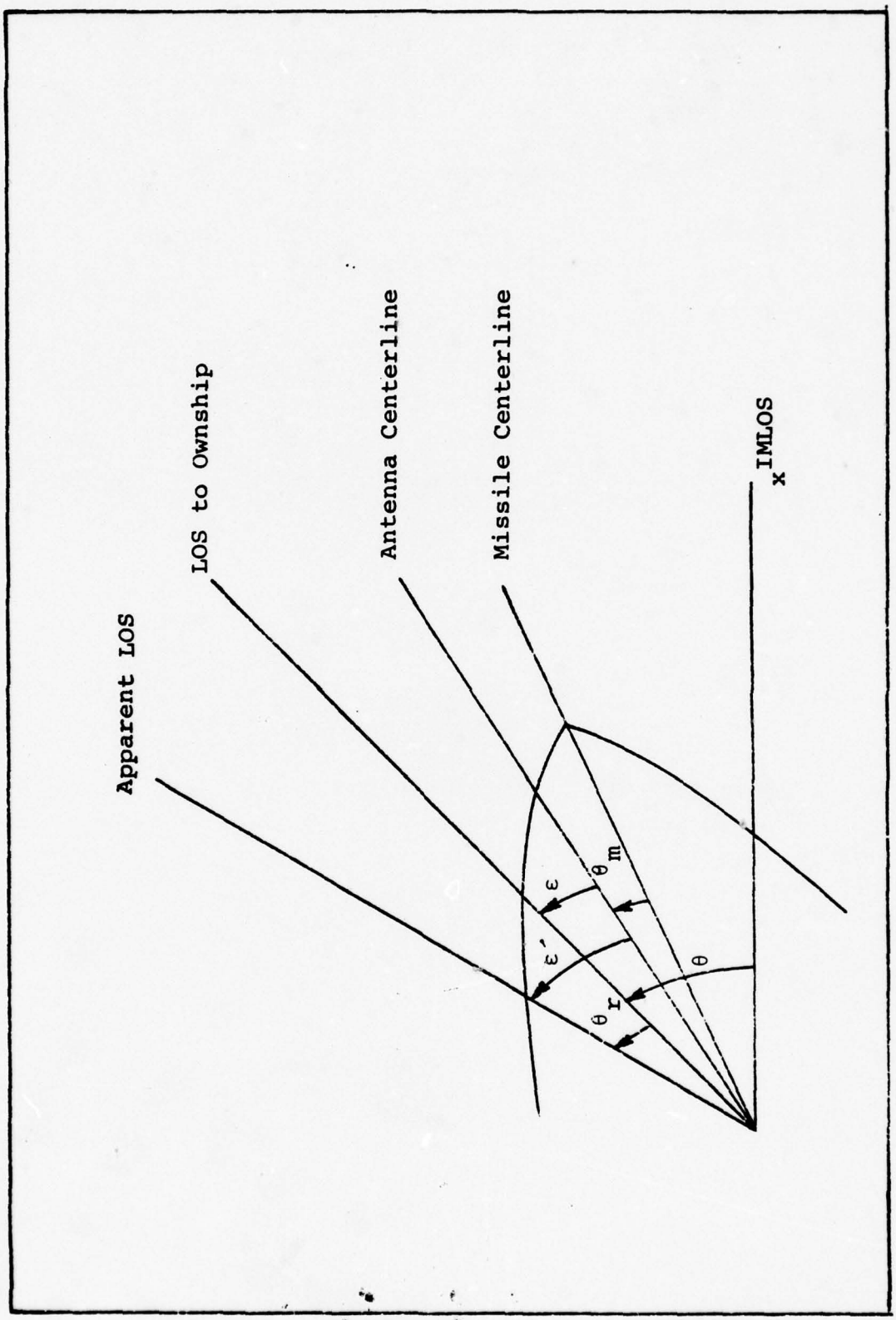

Fig. 9. Geometry of the Seeker

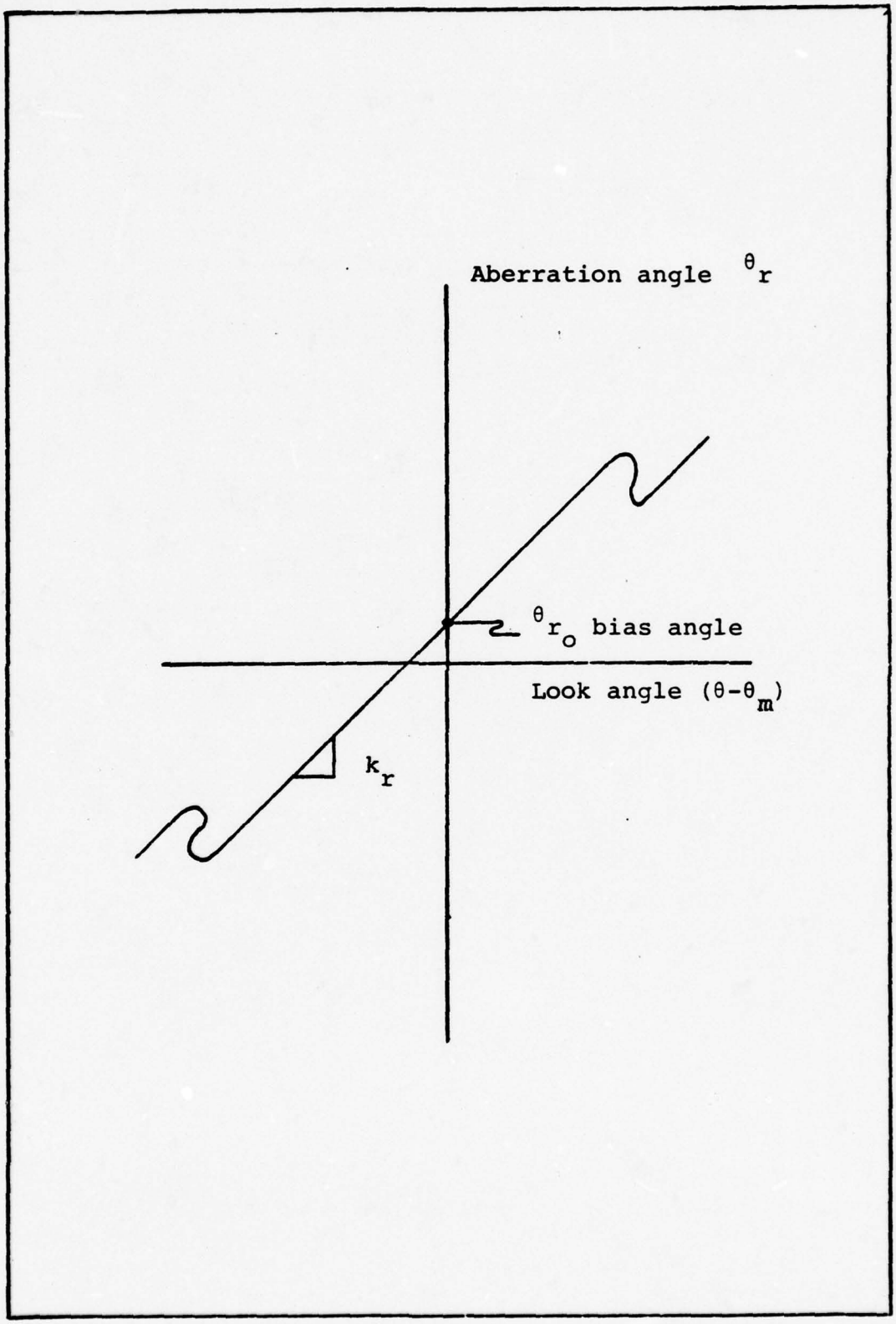

Fig. 10. Aberration Angle Error vs. Look Angle

aberration angle error as a function of look angle (Ref 10:A-6). The dominant aspects of aberration error have been modeled as a constant slope, k_r, of .001 and with an angle bias of zero.

The dynamics of the seeker have been modeled as a first order lag with a time constant, τ_1, of .075 seconds. A block diagram showing the input θ and the coupling effect that k_r has upon missile body motion with ownship motion is shown in Figure 11. This effect can be seen by examining the summing junction prior to ε' and noting the contribution of θ_m to θ is canceled if $k_r = 0$. As shown in this figure, the output of the seeker and track loop is the measured LOS rate, $\dot{\theta}'_s$.

Missile Guidance. The output of the seeker is a noisy measurement of the LOS rate. This is true for most missiles and therefore implementation of some form of filtering is necessary to reduce the noise on the $\dot{\theta}'_s$ signal. Usually the filtering is performed by the guidance system, with a variable gain, to produce a desired commanded acceleration, a_c (Ref 11:1). The filtering of $\dot{\theta}'_s$ has been modeled as a first order lag with a time constant (τ_2) of .3 seconds. The complete transfer function for $\dot{\theta}'_s$ to commanded acceleration is

$$a_c = \frac{nV_c\dot{\theta}'_s}{s\tau_2 + 1} \tag{20}$$

where all variables have previously been defined. Although

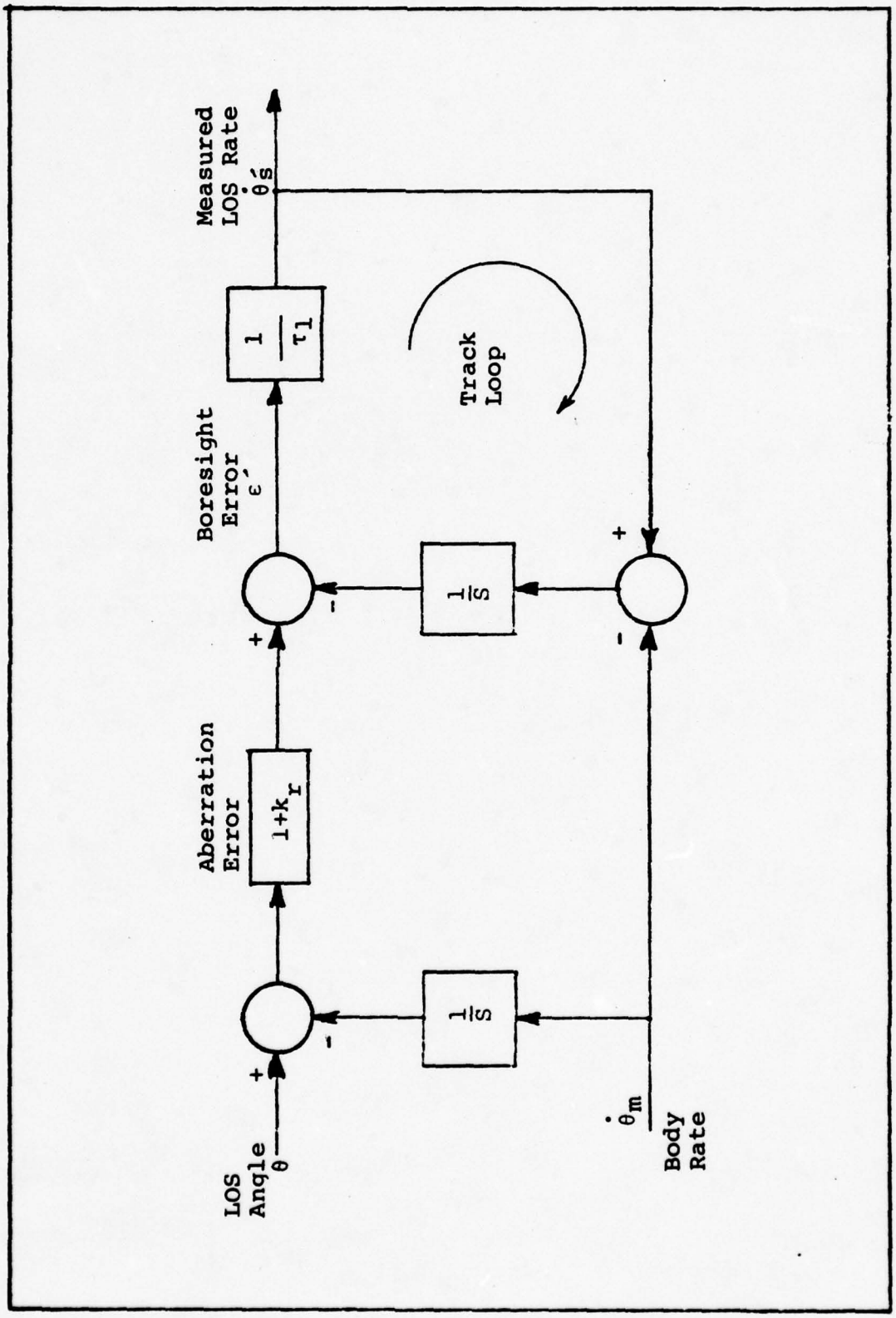

Fig. 11. Seeker Model plus Track Loop

somewhat simplified in approach, this modeling does approximately characterize some guidance systems found in modern air-to-air missiles (Ref 11:42). The missile guidance system will later be shown to be the dominant block of the "guidance strip."

Airframe/Autopilot. The missile airframe modeled is a symetrical cruciform with four fixed wings and four rear moveable control surfaces (Figure 12). The cruciform configuration permits lateral maneuvering in any direction without rolling. Because of this symmetry, the horizontal and vertical planes can be considered uncoupled. The major assumptions used in modeling the dynamics of the missile are

1) the mass of the missile is constant
2) the missile is roll stabilized
3) the missile is a rigid body and can be represented as a point mass
4) small angle approximations are valid for the angle of attack.

The first assumption is consistent with the intent of the problem to consider the aerodynamic forces acting upon the missile after it has been boosted to Mach and its fuel is spent. The second assumption is nonrestrictive since a wide class of air-to-air missiles are roll stabilized to reduce the complexity of the guidance system (Ref 1:235; 11:23). The third assumption considers all forces to act through the center of gravity as well as neglecting all rotational

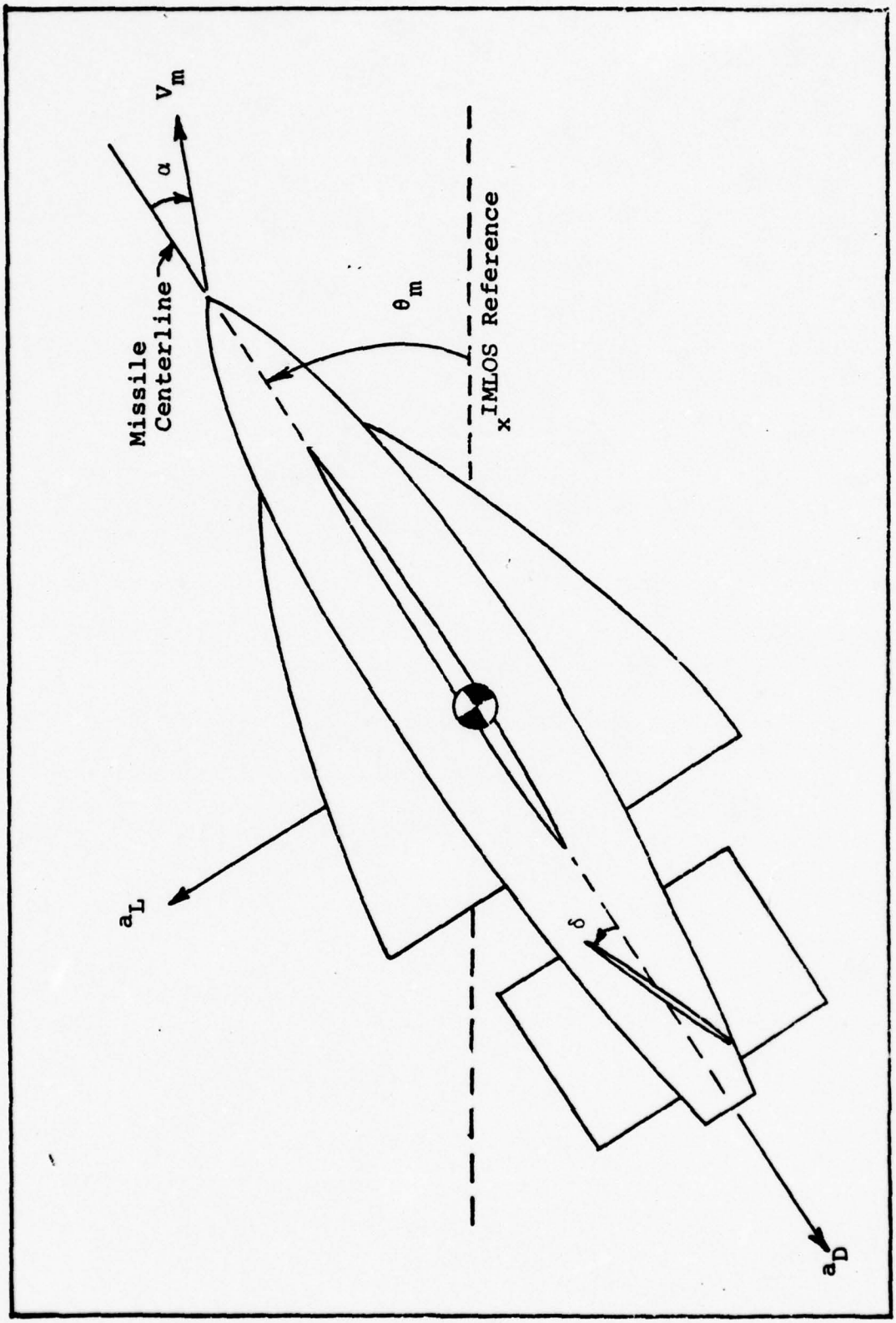

Fig. 12. Cruciform Missile Airframe

dynamics. The fourth assumption ignores the nominal values of drag caused by increasing the effective cross sectional area of the missile into the effective wind. This is true because the small angle approximation assumes that the effective wind is always aligned with the longitudinal axis of the missile. It also enables one to make the assumption that the developed lateral acceleration is perpendicular to the velocity vector.

Given the above assumptions, the four equations which describe the dynamics of the missile are

$$a_L(t) = -V_m \{\dot{\alpha}(t) - q(t)\} \tag{21}$$

$$\dot{q}(t) = M_q q(t) + M_\alpha \alpha(t) + M_\delta \delta(t) \tag{22}$$

$$\dot{\alpha}(t) = q(t) - L_\alpha \alpha(t) - L_\delta \delta(t) \tag{23}$$

$$\dot{\delta}(t) = -\lambda \delta(t) + \lambda u(t) \tag{24}$$

where

$a_L(t)$ = missile lateral acceleration due to lift

V_m = missile velocity magnitude

$\alpha(t)$ = missile angle of attack

$q(t)$ = missile pitch rate, note: $\dot{\theta}_m = q(t)$

$\delta(t)$ = control surface deflection

$u(t)$ = control command (commanded value of δ)

$-\lambda$ = actuator pole (bandwidth)

M_q, M_α, M_δ, L_α, L_δ = Missile stability derivatives

(Ref 4:14; 5:20-21; 9: Chap. 8, p.3)

The control command, u(t), is modeled as a function of commanded acceleration, pitch rate and lateral acceleration.

$$u(t) = k_\delta a_c(t) - h_2 a_L(t) - h_1 q(t) \tag{25}$$

After some algebraic manipulation, equations (21) through (25) can be formed into the system of equations

$$\begin{bmatrix} \dot{a}_L(t) \\ \dot{q}(t) \\ \dot{\delta}(t) \end{bmatrix} = \begin{bmatrix} -(L_\alpha + h_2 \lambda V_m L_\delta) & \dfrac{(V_m L_\alpha - h_1 \lambda V_m L_\delta)}{g} & -\dfrac{(\lambda V_m L_\delta)}{g} \\ \dfrac{g M_\alpha}{V_m L_\alpha} & M_q & M_\delta - \dfrac{M_\alpha L_\delta}{L_\alpha} \\ -g h_2 \lambda & -h_1 \lambda & -\lambda \end{bmatrix} \begin{bmatrix} a_L(t) \\ q(t) \\ \delta(t) \end{bmatrix}$$

$$+ \begin{bmatrix} k_\delta \lambda V_m L \\ 0 \\ g \lambda k_\delta \end{bmatrix} a_c(t) \tag{26}$$

where the gravity unit g = 32.2 ft/sec has been included for proper scaling.

The missile has been modeled with an adaptive autopilot which varies the gain k_δ and feedback gains h_1, h_2 to maintain a specific pole placement of the airframe response. The desired response is described by the second order system

$$\frac{a_L}{a_c} = \frac{\omega_n^2}{s^2 + 2\zeta\omega_n s + \omega_n^2} \tag{27}$$

where

$$\zeta = .707$$

$$\omega_n = 7.07 \text{ rad/sec.}$$

To accomplish this k_δ, h_1 and h_2 are varied according to the following equations

$$k_\delta = \frac{h_1}{V_m} + h_2 - \frac{1}{V_m} \cdot \frac{M_\alpha + L_\alpha M_q}{L_\alpha M_\delta - M_\alpha L_\delta} \tag{28}$$

$$h_1 = \frac{-L_\alpha \{M_\alpha - \frac{M_\delta}{L_\delta} L_\alpha + \omega^2 + (2\zeta\omega + M_q)(\frac{M_\delta}{L_\delta} + M_q)\}}{M_\delta (M_\alpha - \frac{M_\delta}{L_\delta} L_\alpha + \omega^2) + (M_q + 2\zeta\omega)(L_\delta M_\alpha - M_\delta L_\alpha)} \tag{29}$$

$$h_2 = \frac{L_\delta M_\alpha (L_\alpha - 2\zeta\omega - M_q) + M_\delta \{L_\alpha (2\zeta\omega - L_\alpha) - \omega^2 - M_\alpha\}}{V_m L_\delta \{M_\delta (M_\alpha - \frac{M_\delta}{L_\delta} L_\alpha + \omega^2) + (M_q + 2\zeta\omega)(L_\delta M_\alpha - M_\delta L_\alpha)\}} \tag{30}$$

The stability coefficients and stability derivatives are determined within the simulation by use of a cubic fit, obtained from the Air Force Avionic Laboratory (AFAL), to a set of empirical data from actual flight tests of an air-to-air missile. This method provides accurate estimates of these coefficients and derivatives for the adaptive gains used in the autopilot. Equation (26) will later be used to define the airframe/autopilot transfer function. By assuming time invariant coefficients, the Laplace transform of this transfer function may be found to be

$$\frac{a_L}{a_c} = \frac{a_2 S^2 + a_1 S + a_0}{S^3 + b_2 S^2 + b_1 S + b_0} \tag{31}$$

where

a_2, a_1, a_0, b_2, b_1, b_0, are defined as the airframe/autopilot coefficients

During the analysis, these coefficients were calculated at specific times to generate a model of this transfer function. This is discussed further in Chapter III.

Missile Kinematics. The missile kinematics can be described by the two equations

$$a_D = \frac{1}{2} \rho \frac{S}{M} C_D V_m^2 \tag{32}$$

and

$$\dot{\theta}_L = a_L g / V_m \tag{7}$$

where a_D = acceleration magnitude due to drag

ρ = density of the air

S = cross sectional reference area

M = mass of the missile

C_D = coefficient drag

V_m = velocity magnitude of the missile

a_L = lateral acceleration

g = 32.2 ft/sec^2

Equation (7) was originally introduced with the interecept geometry. The coefficient of drag can be well approximated for speeds greater than 1.1 Mach by the following:

$$C_D = \frac{2(A)^{\frac{1}{2}}}{(V_m)^{\frac{1}{2}}} + \frac{C_L^2}{C_{N\alpha}} \tag{33}$$

where

A = speed of sound at appropriate altitude, air temperature

$C_{N\alpha}$ = coefficient of normal force with respect to the angle of attack

C_L = coefficient of lift (Ref 5:7-50)

The coefficient of lift, C_L, may be defined as

$$C_L = \frac{2a_L}{\rho V_m^2} \cdot \frac{M}{S} \tag{34}$$

By substituting Equation (32) into Equation (33) C_D is expressible as

$$C_D = \frac{2(A)^{\frac{1}{2}}}{(V_m)^{\frac{1}{2}}} + \frac{2a_L}{C_{N\alpha}\rho V_m^2} \cdot \frac{M}{S} \tag{35}$$

The reference area, S, is usually defined as the cross sectional area of the missile. This makes it easy to scale for different missiles. From Equation (35) it is seen that C_D is a function of S. From this realtionship any S will yield an appropriate C_D when solving for the a_D in Equation (32). With this, both equations of the missile kinematics are completely defined.

Tracker Noises. The tracker being considered in this study is modeled as a typical radar for a fighter type aircraft. A modeling of the uncertainty of the radar measurements follows a similar development as was described

where

A = speed of sound at appropriate altitude, air temperature

$C_{N\alpha}$ = coefficient of normal force with respect to the angle of attack

C_L = coefficient of lift (Ref 5:7-50)

The coefficient of lift, C_L , may be defined as

$$C_L = \frac{2a_L}{\rho V_m^2} \cdot \frac{M}{S} \tag{34}$$

By substituting Equation (32) into Equation (33) C_D is expressible as

$$C_D = \frac{2(A)^{\frac{1}{2}}}{(V_m)^{\frac{1}{2}}} + \frac{2a_L}{C_{N\alpha}\rho V_m^2} \cdot \frac{M}{S} \tag{35}$$

The reference area, S, is usually defined as the cross sectional area of the missile. This makes it easy to scale for different missiles. From Equation (35) it is seen that C_D is a function of S. From this realtionship any S will yield an appropriate C_D when solving for the a_D in Equation (32). With this, both equations of the missile kinematics are completely defined.

Tracker Noises. The tracker being considered in this study is modeled as a typical radar for a fighter type aircraft. A modeling of the uncertainty of the radar measurements follows a similar development as was described

for the glint scintillation and thermal noises of the missile seeker. The strengths and correlation times for the tracker noises are given in Table III.

Table III

Sigmas and Time Constants for Measurement Noise

Measurement	Sigmas (σ)	Time Constant
θ_T (radians)		
uncorrelated (Thermal)	0.00126	---
correlated (Glint)	0.00168	0.5(sec)
R (feet)		
uncorrelated (Thermal)	11.7	---
correlated (Glint)	10.0	0.5 (sec)
$\dot{R}$ (feet/sec)		---
uncorrelated (Thermal)	7.0	
correlated (Glint)	4.242	1.0 (sec)

Guidance Strip

As will be shown in Chapter III, the major thrust will be directed at modeling the "guidance strip." The guidance strip includes the seeker, the guidance system and the autopilot/airframe dynamics of the missile. It is the set of components which process the LOS rate, $\dot{\theta}$, into a developed lateral acceleration. Figure 13 shows the complete truth model guidance strip.

Summary

This chapter presented the major equations and assumptions contained in the truth model used in the simulation. The explicit development of the equations has been omitted

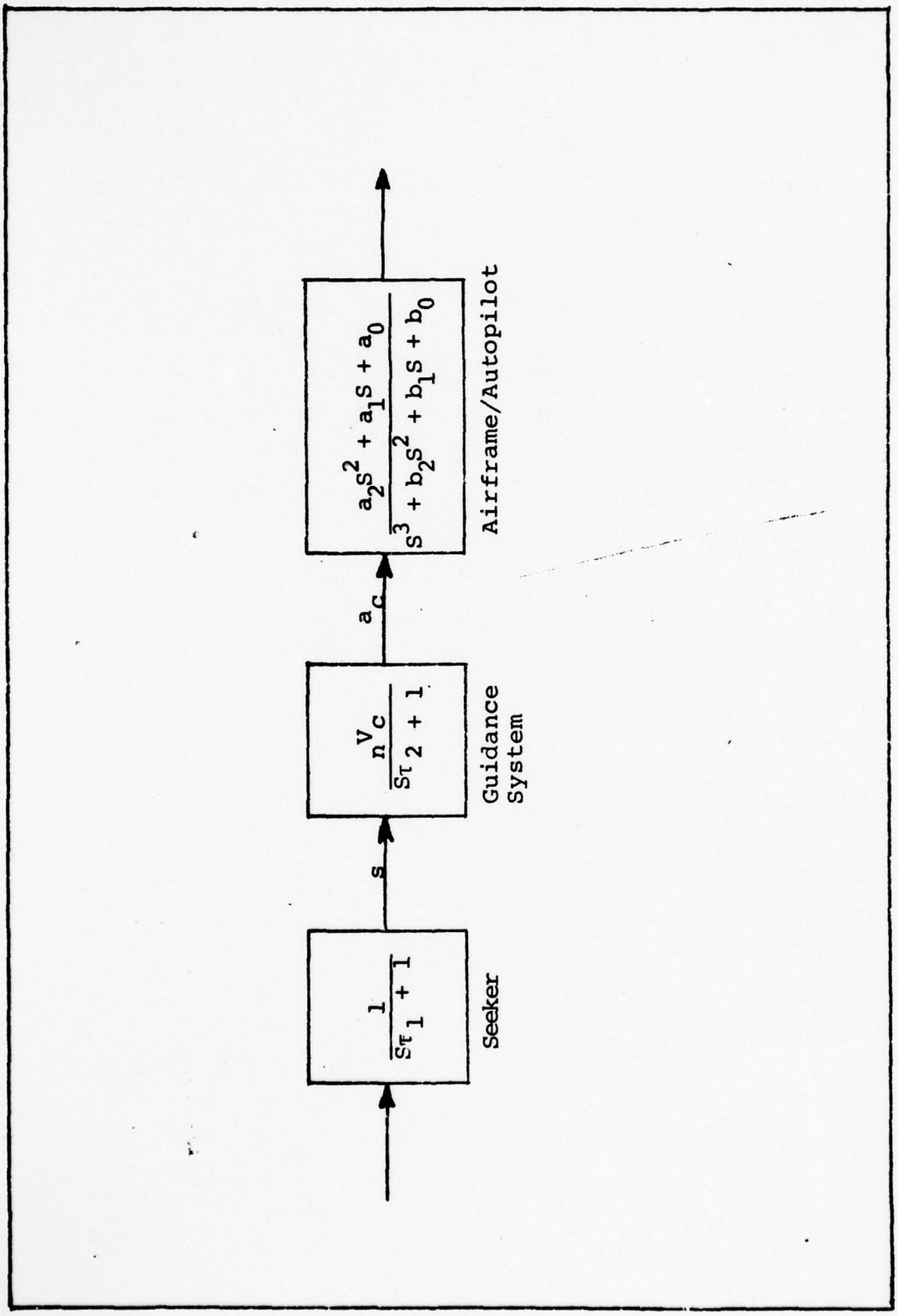

Fig. 13. Truth Model Guidance Strip

since a detailed derivation can be found in Lutter (Ref 5:7-50). Significant detail has been incorporated into the truth model to yield appropriate results.

III. FILTER MODELING

Introduction

The basic filter model considered within this study was originally developed by Lutter in Reference 5. This filter modeled the following four dynamic states, and two parameters of an air-to-air missile.

- θ_T - LOS angle as seen by the ownship
- R - range
- $\dot{R}$ - range rate (relative closing velocity, where by convention: $\dot{R} = -V_c$)
- V_{mx}^I - x-velocity of missile in inertial frame
- n - proportional navigation constant
- M/S - ratio of the mass of the missile to cross sectional reference area

These modeled states and parameters are collectively referred to within this report as the "basic filter," since they serve as the basis for all other designs presented.

A modeling assumption within this filter ignored the prefiltering of the guidance system along with the lag effects of the seeker and autopilot. This assumption was used to develop the simplest filter model possible. It was argued, that if the results of this filter were unsatisfactory, a more refined model would be proposed. The assumption essentially equated lateral acceleration to commanded acceleration. Recalling the proportional navigation law, this assumption is expressed in the following equation.

$$a_L = nV_c\dot{\theta} \tag{36}$$

As previously discussed in Chapter 2, the term "guidance strip" refers to those components which process LOS information, $(\dot{\theta}')$, into developed lateral acceleration. Figure 14 shows the actual guidance strip in the missile along with the model based upon Equation (36) and used by Lutter in Reference 5. The effects of aberration error and seeker noise upon θ in the truth model are indicated by the use a prime. Also, the subscript "s" has been used to indicate the effects of the seeker dynamics upon $\dot{\theta}'$.

The analysis within this report continues to use the basic filter developed by Lutter with various models of the guidance strip inserted into the filter. For purposes of identification, these various models of the guidance strip are used to define the "order of the missile," which is modeled in the filter. The number of poles in the guidance strip transfer function determines the missile order. In this way, the basic filter designed by Lutter is called the "zero order missile filter."

The performance of the zero order filter was considered inadequate for accurate pointing and tracking, which was the original design goal for the filter. Figure 15 shows the estimation of the V_{mx}^I state for the zero order filter when it was given perfect knowledge of n and M/S. In general, knowledge of these parameters will not be available and the filter will have to estimate their value. Thus, Figure 15

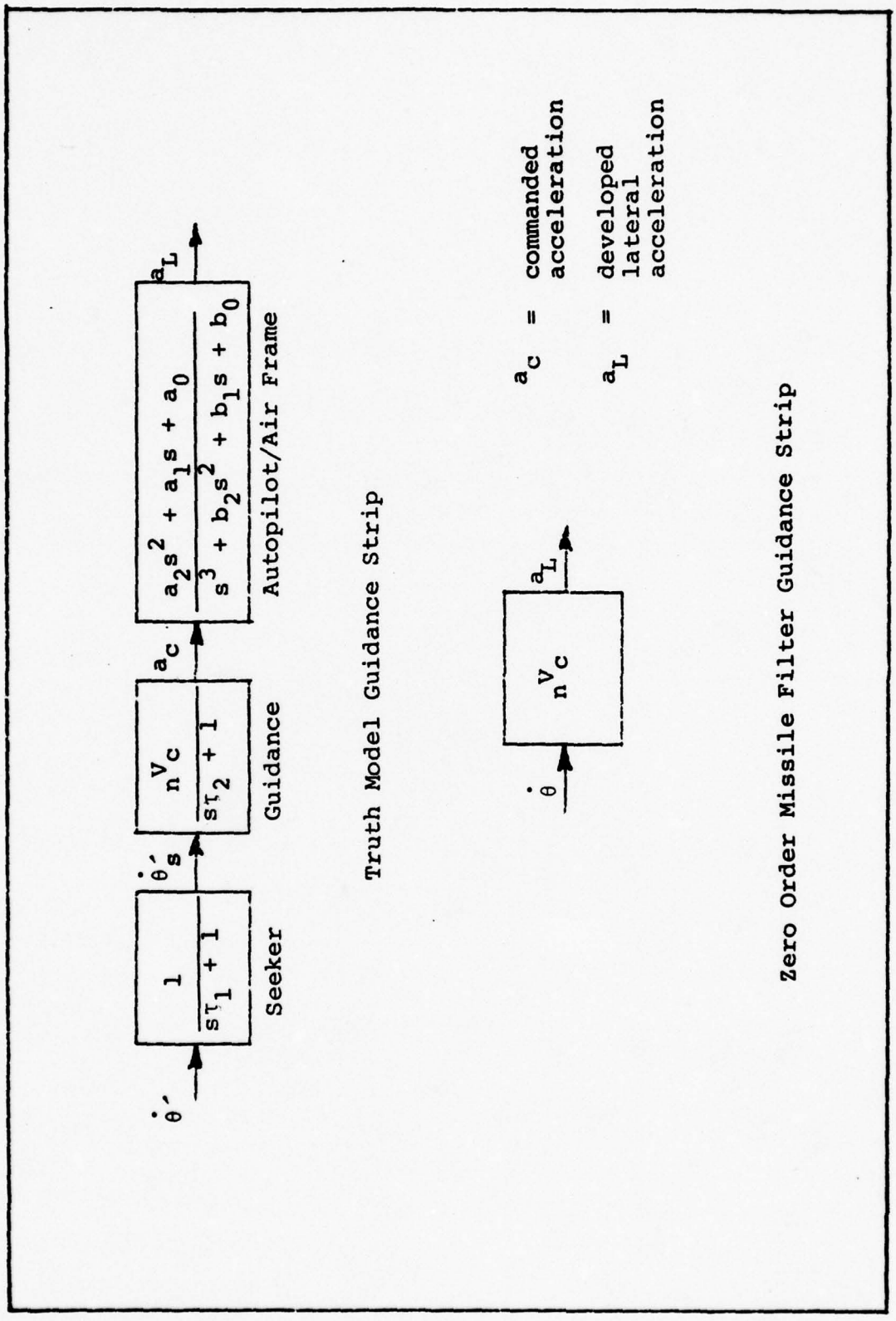

Fig. 14. Guidance Strips of Truth Model and Zero Order Filter

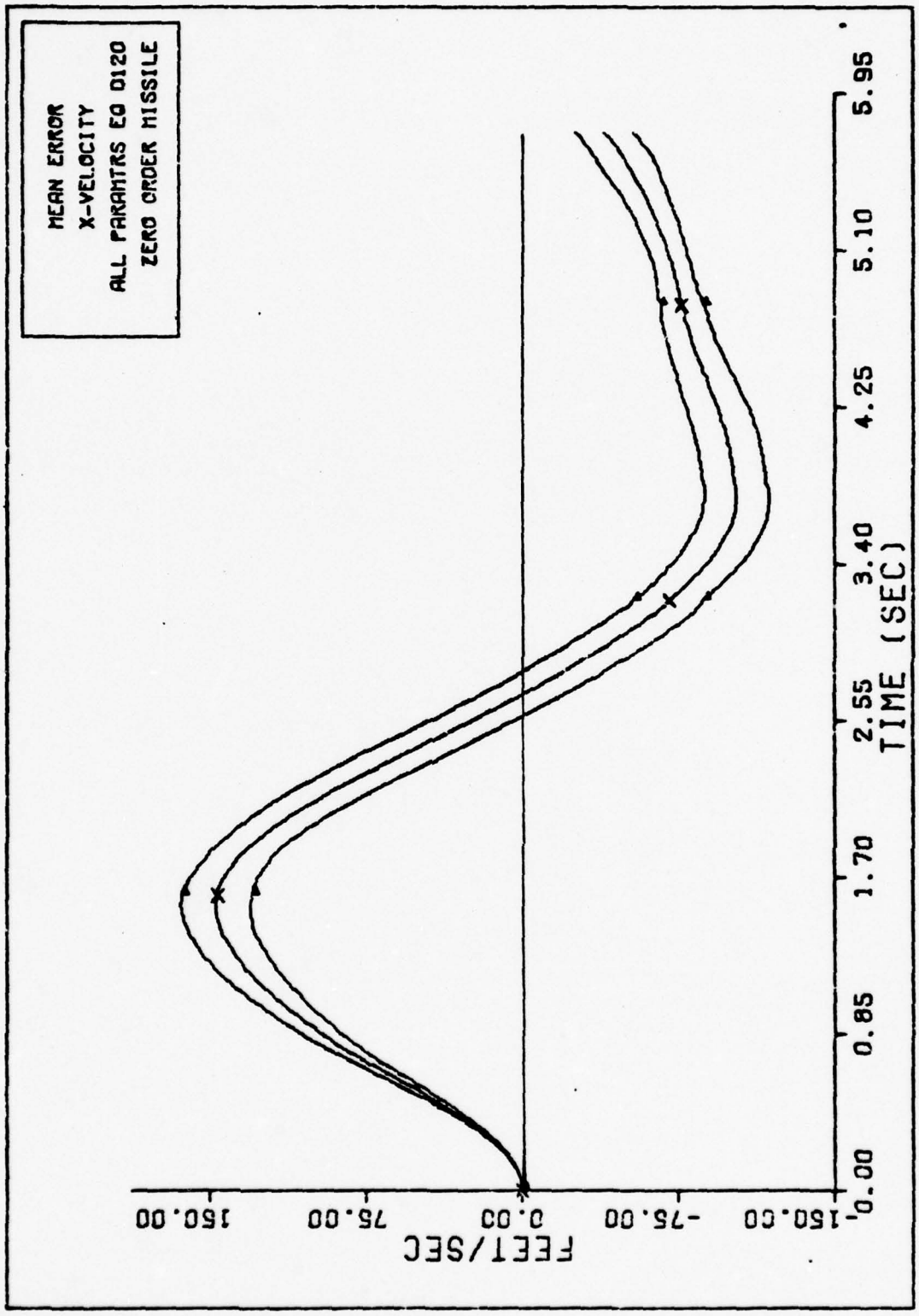

Fig. 15. X-VELOCITY ZERO ORDER MISSILE

is portraying the best estimation possible for the zero order filter when the missile flies a high-g trajectory. The box in the upper right hand corner of the figure contains the important information about the curve. For this plot, it indicates that the center curve is the "mean error" of the V^I_{mx} state (x-velocity) when all parameters were set equal to their true values. It also indicates the use of data set 120 for the zero order missile filter. The data sets are explained in Appendix B. The center curve is an ensemble average of the mean error made by the filter over 20 simulations of the high-g intercept scenario. The mean error is enveloped by plus and minus one standard deviation. Thus, for a time of approximately 1.7 seconds in the time history of this curve, the filter error in the V^I_{mx} state can be observed to be 150 ft/sec with a one sigma confidence of 25 ft/sec. The x-velocity state, V^I_{mx}, of each filter designed in this report was the most sensitive state to filter changes. For this reason, it will be used to represent the overall performance of the various filters to be discussed.

It was suggested by Lutter that modeling the lag effects of the autopilot would improve the estimates achievable by the zero order filter. This conclusion was based upon the observation that the filter was estimating too large an initial deceleration value of the missile in the X^I - direction, causing an initial positive bias. This condition occurred because of the zero delay for lateral

acceleration modeled in the filter (Ref 5:84-85).

The initial modeling effort in this report was aimed at acquiring a proper benchmark. The benchmark would include as complex a model as necessary to provide accurate state estimation. In this way the benchmark would represent a lower bound for filter error and would be used as a comparison when evaluating reduced order filters. The approach taken in designing the benchmark was based upon the suggestion made by Lutter, but it encoumpassed a more exhaustive set of possible models for the guidance strip. Figure 16 represents the possible models that were considered for each component of the guidance strip. A column labeled "a_c transferred" is also included in this figure. This column was used only in conjunction with an autopilot model and refers to an ad hoc procedure in which the truth model value of commanded acceleration, a_c, is passed directly to the autopilot of the filter. This procedure was used in designing a benchmark and will be discussed in depth later in this chapter. Combining a model choice from each component column or choosing an autopilot model with commanded acceleration transferred, defines a proper benchmark design.

Once a benchmark had been decided upon, the insights gained from its performance inspired the development of two filters, a fourth order missile filter and a first order missile filter. The fourth order missile filter included exact models of the guidance system and autopilot. This filter was used to determine filter sensitivity to the

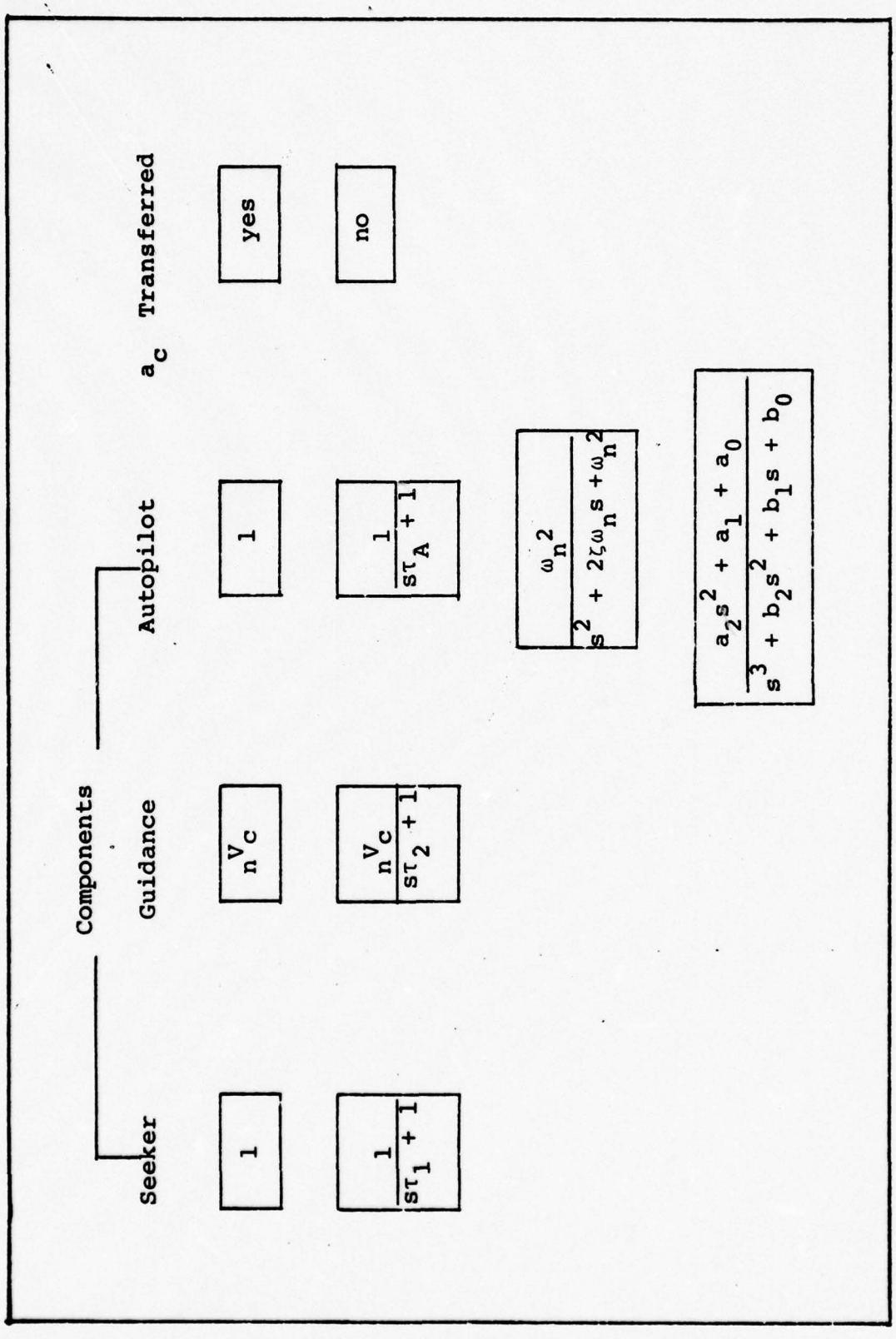

Fig. 16. Possible Models of Guidance Strip

navigation constant, n, the M/S ratio, and the bandwidth of the guidance strip. It also established the best estimation possible when given perfect knowledge of these parameters.

The first order filter was proposed as a reduced order filter which would provide accurate estimation of the missile's states and three of its key parameters. This filter used a first order lag to approximate the complete guidance strip of the missile. The performance of the first order filter was unexpectedly impressive, considering that the first order missile model in the filter was approximating the entire fifth order guidance strip. A complete discussion as to why this filter performed so well will be deferred until Chapter IV; however, a foundation for its understanding can be gained from the modeling presentation given in this chapter.

Figure 17 presents the guidance strips of all filters that were analyzed in this report. The guidance strips are arranged in order of complexity starting with the zero order filter. This chapter will discuss the rationale for each design in chronological order of their development, after reviewing the modeling of the basic filter.

Modeling of the Basic Filter

The use of the Extended Kalman Filter algorithm requires that the system of interest be described by a set of first order ordinary differential equations and that the random disturbances, which model the system uncertainty, be input in a linear additive fashion (Ref 7:179). Equation (37)

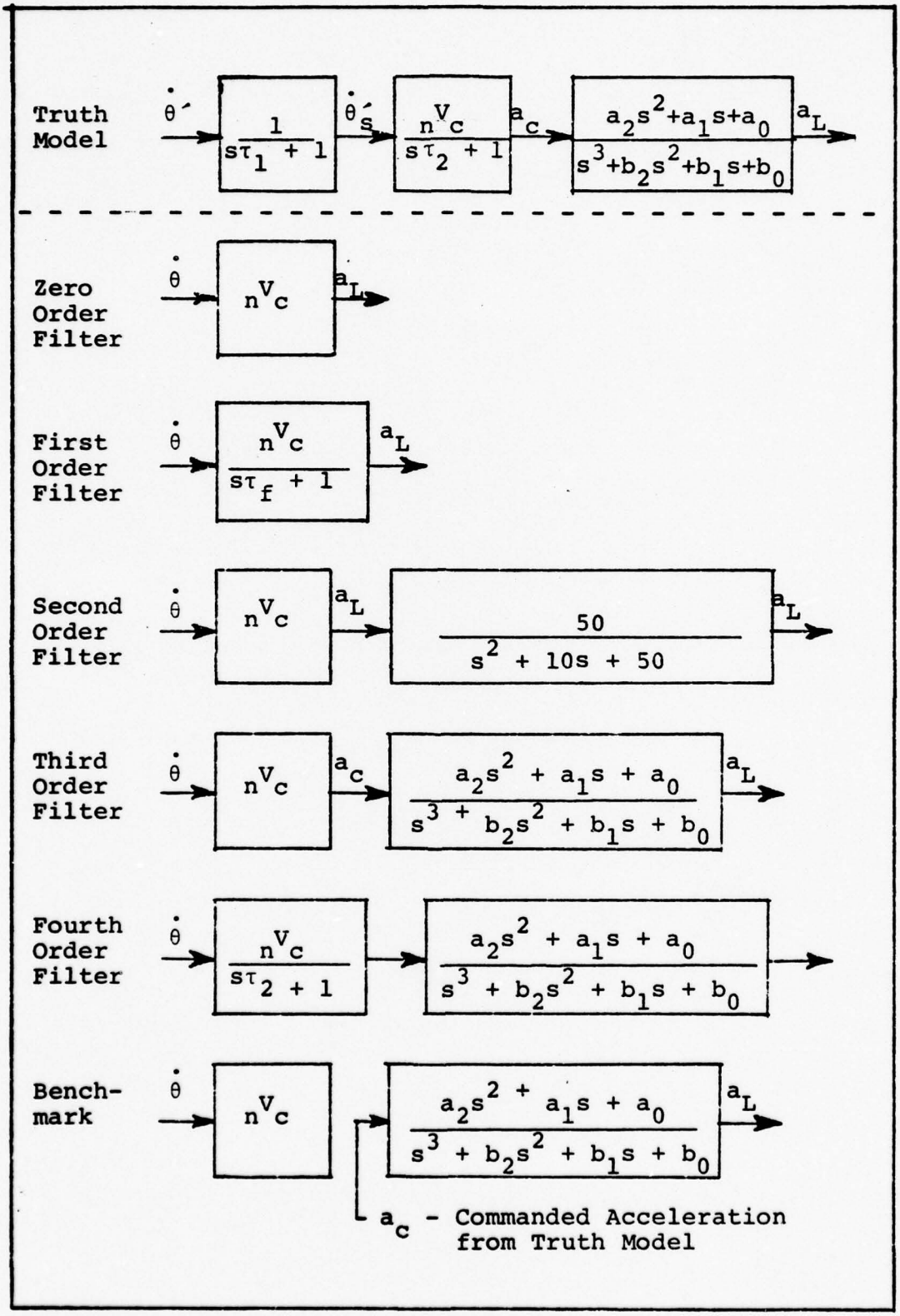

Fig. 17. Guidance Strips of all Filters Analyzed

expresses this modeling approach in vector notation

$$\dot{\underline{x}}(t) = \underline{f}(\underline{x}(t),\underline{u}(t),t) + \underline{G}(t)\underline{w}(t) \tag{37}$$

where

$\underline{x}(t)$ = n-dimensional state vector (the underscoring indicates that the variable is a vector)

$\underline{w}(t)$ = zero mean white Gaussian noise

with

$$E\{\underline{w}(t)\underline{w}^T(t+\tau)\} = \underline{Q}(t)\delta(\tau)$$

Restricting the modeling for the filter to this general form, the following subparagraphs develop and define the first six states.

Line of Sight Angle (θ_T). Figure 18 presents the inertial frame with a depiction of the ownship and missile at some time after the start of the intercept. In this figure, the position of the ownship and missile are defined by the two inertial vectors $\underline{R}_{OT}$, and $\underline{R}_{OM}$ respectively. The vector $\underline{R}$, is aligned with the x-axis of the ownship antenna and is the range of the missile from the ownship. Using vector addition

$$\underline{R}_{OM} = \underline{R}_{OT} + \underline{R} \tag{38}$$

Utilizing the theorem of Coriolis, and notation established in reference 14, the inertial velocity of the missile is found to be

$$P_I\underline{R}_{OM} = P_{TLOS}\underline{R}_{OM} + \omega_{I(TLOS)} \times \underline{R}_{OM} \tag{39}$$

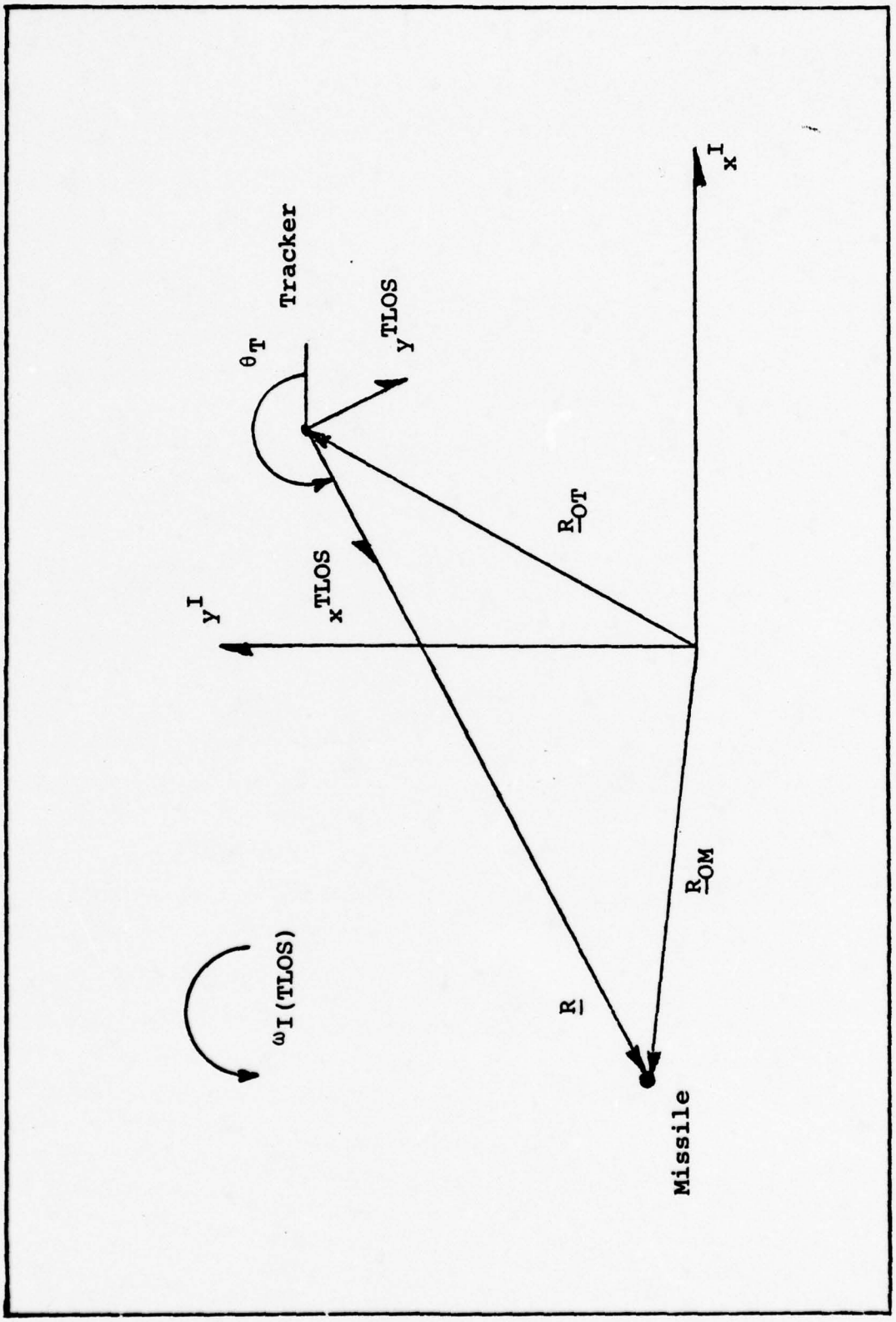

Fig. 18. Inertial Geometry of Engagement Scenario

After substituting Equation (38) into (39) and reducing, Equation (39) can be written as

$$P_I \underline{R}_{OM} = P_I \underline{R}_{OT} + P_{TLOS} \underline{R} + \underline{\omega}_{I(TLOS)} \times \underline{R} \tag{40}$$

or equivalently, coordinatized in the I frame,

$$\underline{V}_m^I = \underline{V}_T^I + \dot{\underline{R}}^I + (\underline{\omega}_{I(TLOS)} \times \underline{R}) \tag{41}$$

where

P_I = time derivative with respect to the inertial frame

P_{TLOS} = time derivative with respect to the TLOS frame

$\dot{\underline{R}}$ = relative closing velocity between missile and ownship

$\underline{V}_m^I$ = inertial velocity vector of the missile

$\underline{V}_T^I$ = inertial velocity vector of the tracker

$\underline{\omega}_{I(TLOS)}$ = the angular rate between the I frame and the TLOS frame

Expressing Equation (41) in terms of its components, and solving for the magnitude of $\omega_{I(TLOS)}$, the following two equations can be found.

$$\omega_{I(TLOS)} = \frac{\dot{R}}{R} \cot\theta_T + \frac{V_{Tx}^I - V_{mx}^I}{R} \csc\theta_T \tag{42a}$$

$$\omega_{I(TLOS)} = -\frac{\dot{R}}{R} \tan\theta_T + \frac{V_{my}^I - V_{Ty}^I}{R} \sec\theta_T \tag{42b}$$

where by definition (see Figure 18)

$$\omega_{I(TLOS)} = \dot{\theta}_T \tag{43}$$

the desired modeling of LOS angle has been achieved. It was decided to use Equation (42a) when $\sin \theta_T \geq .707$ and Equation (42b) when $\sin \theta_T < .707$ to avoid the singularities of $\dot{\theta}_T$.

Equations (42a) and (42b) are also used to define an important relationship which will be used to solve for the y-component of the missile velocity in the inertial frame. By setting Equations (42a) and (42b) equal to one another, solving for V^I_{my} yields

$$V^I_{my} = \frac{\dot{R}\cos^2\theta_T + V^I_{Tx}\cos\theta_T - V^I_{mx}\cos\theta_T + \dot{R}\sin\theta_T + V^I_{Ty}}{\sin\theta_T} \tag{44}$$

Equation (44) shows that V^I_{my} can be found directly with knowledge of V^I_{mx}, θ_T, and $\dot{R}$. This equation is used outside the structure of the filter and thus eliminates the need for estimating both components of the inertial velocity of the missile. The modeling in this analysis assumed that no conditions exist which would favor estimating one component of inertial velocity over the other. The x-component of the velocity was estimated in all cases.

X-component of Inertial Velocity of Missile (V^I_{mx}). Modeling V^I_{mx} as a first order differential equation can be accomplished by resolving the acceleration acting upon the missile into its x and y components. Figure 19 shows a

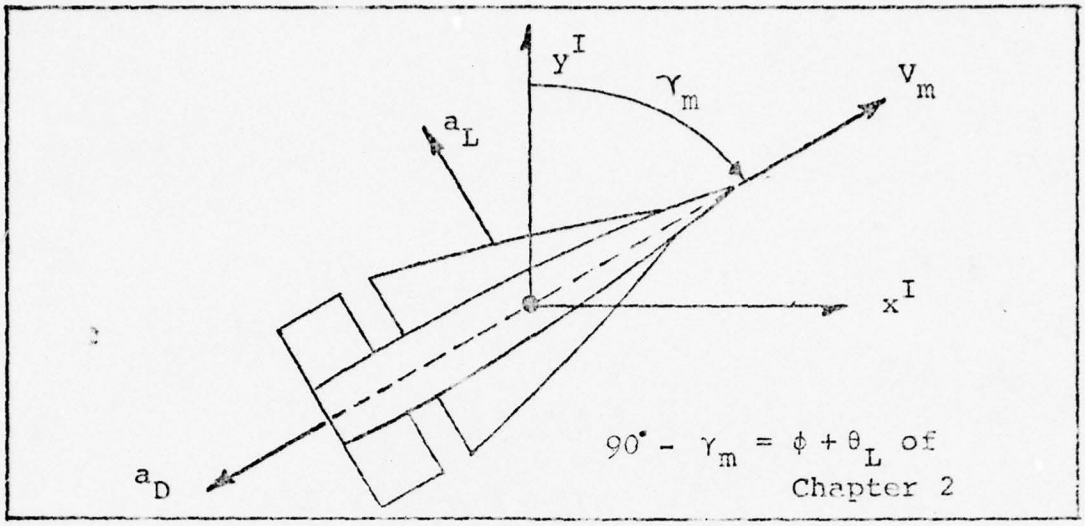

Fig. 19. Free Body Diagram of the Missile

free body diagram of the missile drawn in the inertial frame. Solving for $\dot{V}^I_{mx}$ and $\dot{V}^I_{my}$,

$$\dot{V}^I_{mx} = -a_D \text{ Sin } \gamma_m - a_L \cos\gamma_m \tag{45a}$$

$$\dot{V}^I_{my} = -a_D \cos \gamma_m + a_L \text{ Sin}\gamma_m \tag{45b}$$

where

a_D = total drag acting upon the missile

a_L = lateral acceleration due to lift

γ_m = angle defining incidence of inertial velocity of missile to x-axis of inertial frame.

It is important to emphasize here that the modeling assumptions introduced in Chapter I allow for specification of the acceleration terms in Equations (45a) and (45b). Repeated again, these assumptions are:

1) that the missile will be using proportional navigation

2) that the missile is non-thrusting.

Equation for $\dot{V}^I_{my}$ is developed the same as $\dot{V}^I_{mx}$ for use in defining the range rate state in the following section. Proceeding with the development of $\dot{V}^I_{mx}$, an expression for a_D is determined starting with the basic aerodynamic equation for total drag.

$$a_D = \tfrac{1}{2}\rho C_D V_m^2 \, S/M \tag{46}$$

The use of Equation (46) is dependent upon knowledge of (1/(M/S)) and C_D. The other terms can be considered known or can be obtained from measurements of the missile's kinematics. The term (M/S) is given special attention in a later discussion and for the moment will be considered known. Thus the coefficient of drag, C_D, remains to be defined in terms which are observable to the ownship either directly or through some filtering process. This approach is assuming that apriori knowledge of C_D is not available.

The coefficient of drag can be expressed as the sum of the zero lift drag and the induced drag coefficients.

$$C_D = C_{DO} + C_{DI} \tag{47}$$

where

C_{DO} = coefficient of zero-lift drag

C_{DI} = coefficient of induced drag

The approximation chosen to represent C_{DO} and C_{DI} are

$$C_{DO} = \frac{2\sqrt{A}}{\sqrt{V_m}} \tag{48}$$

where

A = speed of sound at the appropriate altitude (Ref 5:63)

$$C_{DI} = \frac{4M^2}{\rho^2 S^2 A} \cdot \frac{a_L^2}{V_m^3} \tag{49}$$

Substituting in the total expression for C_D into Equation (46) and rearranging terms yields

$$a_D = \tfrac{1}{2}\rho S/M \left\{\frac{2A^{\frac{1}{2}}}{V_m^{\frac{1}{2}}} + \frac{4M^2}{\rho^2 S^2 A} \frac{a_L^2}{V_m^3}\right\} V_m^2 \tag{50}$$

In the above equation ρ and A are considered known and for this analysis are held constant for an altitude of 10,000 feet above sea level for a clear, standard day. Incorporating the complete expression for a_D into Equations (45a) and (45b) yields the desired relationship.

$$\dot{V}_{mx}^I = - \left\{\rho A^{\frac{1}{2}} V_m^{\frac{3}{2}} \left(\frac{S}{M}\right) + \left(\frac{2}{\rho A}\right) \left(\frac{M}{S}\right) \frac{a_L^2}{V_m}\right\} \sin\gamma_m - a_L \cos\gamma_m \tag{51}$$

The modeling for a_L in Equation (51) is described separately for each filter since the definition of this state will vary among the different models of the guidance strip.

The total inertial velocity of the missile V_m and the angle γ_m are calculated with the current estimates of V_{mx}^I and V_{my}^I by the following equations:

$$V_m = \sqrt{(V_{mx}^I)^2 + (V_{my}^I)^2} \tag{52}$$

$$\gamma_m = \tan^{-1} \left(\frac{V^I_{mx}}{V^I_{my}}\right) \tag{53}$$

The term M/S is an unknown parameter in Equation (51) and is estimated by the filter. The modeling for this term will be discussed later in this chapter.

Modeling for Range and Range Rate $(R,\dot{R})$. The modeling for range rate is obtained by taking the derivative of Equation (40), (repeated here)

$$P_I \underline{R}_{OM} = P_I \underline{R}_{OT} + P_{TLOS} \underline{R} + \underline{\omega}_{I(TLOS)} \times \underline{R} \tag{40}$$

with respect to the I-frame. Applying the Theorem of Coriolis, Equation (54) is derived

$$P_I^2 \underline{R}_{OM} = P_I^2 \underline{R}_{OT} + P^2_{TLOS} \underline{R} + 2\underline{\omega}_{I(TLOS)} \times P_{TLOS} \underline{R}$$

$$+ P_{TLOS} \underline{\omega}_{I(TLOS)} \times \underline{R} + \underline{\omega}_{I(TLOS)} \times (\underline{\omega}_{I(TLOS)} \times \underline{R}) \tag{54}$$

Equation (54) can be coordinatized in the I-frame and re-written as

$$\underline{a}^I_m = \underline{a}^I_T + \ddot{\underline{R}}^I + 2 (\underline{\omega}_{I(TLOS)} \times \dot{\underline{R}})^I + (P_{TLOS} \underline{\omega}_{I(TLOS)} \times \underline{R})^I$$

$$+ (\underline{\omega}_{I(TLOS)} \times (\underline{\omega}_{I(TLOS)} \times \underline{R}))^I \tag{55}$$

where

$\underline{a}_m^I$ = inertial missile acceleration

$\underline{a}_T^I$ = inertial tracker acceleration

$\ddot{\underline{R}}^I$ = relative acceleration along the LOS

$\underline{\omega}_{I(TLOS)} \times \dot{\underline{R}}$ = Coriolis acceleration term

$P_{TLOS}\ \underline{\omega}_{I(TLOS)} \times \underline{R}$ = tangential acceleration term

$\underline{\omega}_{I(TLOS)} \times (\underline{\omega}_{I(TLOS)} \times \underline{R})$ = centripetal acceleration term.

The Coriolis and tangential acceleration components are perpendicular to the X^{TLOS} direction and do not contribute to the X^{TLOS} acceleration component. Equation (55) then reduces to:

$$\underline{a}_m^I = \underline{a}_T^I + \ddot{\underline{R}}^I + (\underline{\omega}_{I(TLOS)} \times (\underline{\omega}_{I(TLOS)} \times \underline{R}))^I \qquad (56)$$

Coordinatizing in the TLOS frame, and solving for $\ddot{R}$ (acceleration along the X^{TLOS} axis), the desired equation for modeling range rate is derived.

$$\ddot{R} = \omega^2 R + a_{mx}^{TLOS} - a_{Tx}^{TLOS} \qquad (57)$$

where

$\omega = \underline{\omega}_{I(TLOS)}$

The acceleration term a_{Tx}^{TLOS} is considered known through a coordinate transformation of the accelerations obtained from

the inertial navigation unit on board the ownship. The accelerations obtained from the navigation unit are considered deterministic since the precision of these measurements is much greater than that available from a typical aircraft radar. a_{mx}^{TLOS} is found through the use of a direction cosine matrix transforming $\dot{V}_{mx}^{I}$ and $\dot{V}_{my}^{I}$ into the TLOS frame. Recalling that θ_T is a measure of the angle between the TLOS and inertial frame, the proper transformation is

$$a_{mx}^{TLOS} = \dot{V}_{mx}^{I} \cos\theta_T + \dot{V}_{my}^{I} \sin\theta_T \tag{58}$$

Using the expressions for $\dot{V}_{mx}^{I}$ and $\dot{V}_{my}^{I}$ found in the previous section, and substituting the complete expression of a_{mx}^{TLOS} back into Equation (57), the desired state modeling of range rate is obtained:

$$\ddot{R} = \theta_T^2 R + [\{\rho A^{\frac{1}{2}} \text{ (S/M) } V_m^{\frac{3}{2}} \sin\gamma_m - (\tfrac{2}{\rho A}) \text{ (M/S) } \frac{a_L^2}{V_m} \sin\gamma_m - a_L \cos\gamma_m\} \cos\theta_T + \{-\rho A^{\frac{1}{2}} \text{ (S/M) } V_m \cos\gamma_m - (\tfrac{2}{\rho A}) \text{ (M/S) } a_L^2 \cos\gamma_m - a_L \sin\gamma_m\} \sin\theta_T] - a_{Tx}^{TLOS} \tag{59}$$

Equation (59) is modeled in the filter as two first degree equations:

where

$$\frac{d}{dt} R(t) = \dot{R} \tag{60}$$

and

$$\frac{d}{dt}\dot{R}(t) = \text{RHS of Equation (59)} \tag{61}$$

Modeling for the Ratio of the Mass to Reference Area and Proportional Navigation Constant (M/S, n). This study has considered both the M/S ratio and the navigation constant to remain invariant throughout the scenario. For this reason these two parameters could be modeled as random biases.

$$\dot{(M/S)}\ (t) = 0 \tag{62}$$

$$\dot{n}(t) = 0 \tag{63}$$

Once the filter has obtained an initial estimate of the constant, the random bias model causes the Kalman gain to approach zero and essentially ignore available information brought in after this time. Since the complete missile model in the filter is not exact, it is possible for the filter to acquire an incorrect initial estimate of these constants. This behavior, referred to as "learning the wrong state too well," can be avoided by adding a pseudo noise to each channel and thus avoid the condition of having the Kalman gain go to zero on these channels (Ref 3:189; 6:204). Thus, the complete model of these parameters is defined as

$$(\dot{M/S})(t) = w_1(t) \tag{64}$$

$$\dot{n}(t) = w_2(t) \tag{65}$$

where

$$E[w_1(t)\ w_1^T(t+\tau)] = Q_1\delta(\tau)$$

$$E[w_2(t)\ w_2^T(t+\tau)] = Q_2\delta(\tau)$$

with Q_1 and Q_2 suitably chosen during the tuning process.

Searching for a Benchmark. Figure 16, presented in the introduction of this Chapter, laid out the possible alternatives for designing a benchmark. The intent in finding a benchmark was to demonstrate the best performance obtainable from even the most complicated form of a potential filter design. The benchmark is sought not for possible implementation, but more for a comparison between it and reduced order filters. In some cases, as in this analysis, the benchmark is given knowledge of a system's structure along with its exact parameter values, all of which would not be available should its design be considered for implementation. This image of a benchmark is what prompted the development of the three designs that follow. The final design was chosen to represent the benchmark for all possible filter designs that could be implemented.

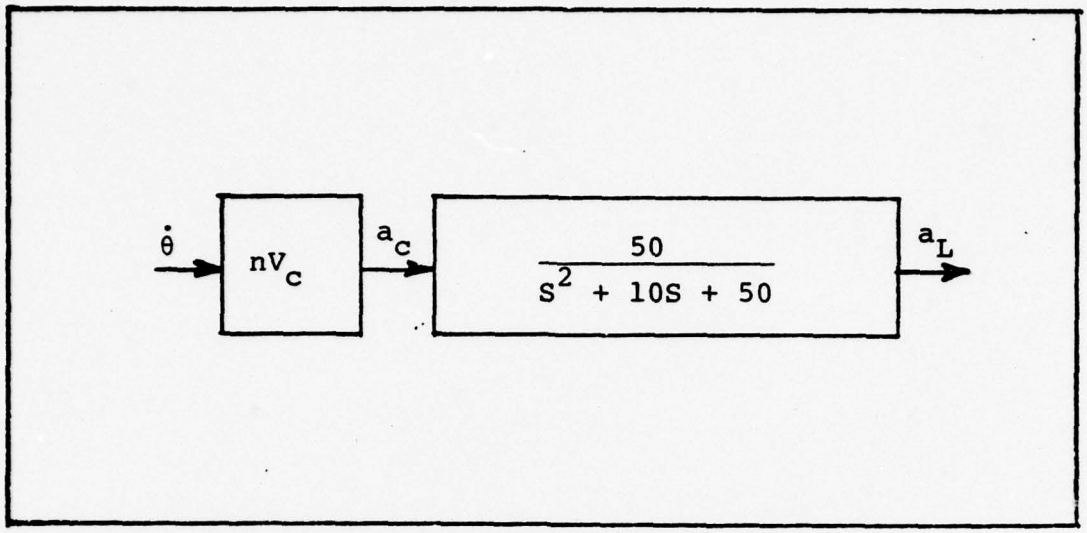

Fig. 20. Second Order Missile Filter

Second Order Design. The first design considered lag characteristics of the autopilot as the most important effect influencing filter performance. Although the actual autopilot was third order, it was adaptively controlled by feedback gains (refer to Chapter II) to respond as a second order system with an effective damping ratio of .707 and a natural frequency of 7.07 rad/sec. These values are based upon previous design work for this missile model (Ref 5:26). The choice of the second order model was, therefore, a reasonable first approach in capturing the lag effects of the autopilot (see Figure 20).

The performance, however, was marginal. The estimates in the V_{mx}^I state were greater then 100 ft/sec. This could hardly be used as a benchmark since this would be admitting that any filter designed for implementation would in the best of circumstances do no better then 100 ft/sec.

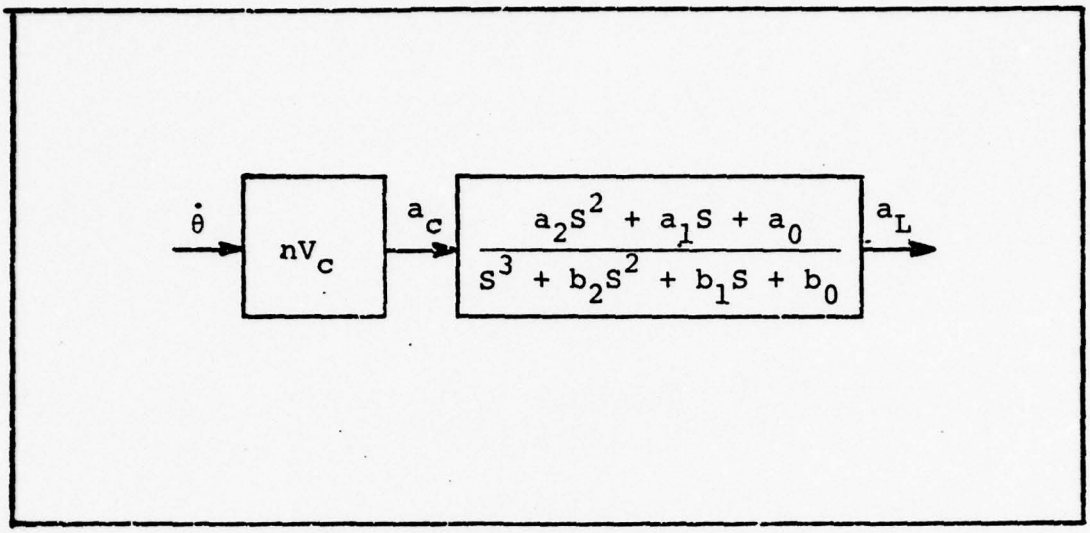

Fig. 21. Third Order Missile Filter

Third Order Design. The second attempt in defining a benchmark, used the exact structure of the autopilot. This approach still considered the lag effects of the autopilot as the essential effect to be modeled. The difference between this approach and the second order design was that the actual autopilot was nonminimum phase. This is usually true of tail-controlled missiles since the initial movement of the rear fins causes acceleration in the opposite direction desired. This "tail-wags-the-dog" characteristic shows up in the autopilot transfer function as a right-half-plane zero. It seemed possible that inclusion of this effect was needed for producing a benchmark (Ref 11:20).

The coefficients of the autopilot transfer function were time varying since it was designed to be adaptive. An ensemble average of each coefficient for six time points of the high-g intercept was made from twenty runs of the simulation. Table IV shows the poles and zeroes of the

Table IV

Poles and Zeroes of Autopilot Transfer Function

	Poles			Zeroes	
Time	1	2	3	1	2
0 sec	-63.34	-21.88	-3.06	-33.44	31.10
1 sec	-60.82	-20.96	-3.19	-33.35	30.96
2 sec	-57.43	-20.02	-3.35	-33.61	31.13
3 sec	-52.21	-18.61	-3.64	-34.63	32.00
4 sec	-49.12	-17.42	-3.89	-35.57	32.88
5 sec	-47.77	-16.69	-4.06	-35.99	33.33

transfer function for the six time points. Even though the coefficients did vary, the actual dominant pole and zero movement was slight enough that one set of coefficients could well approximate the autopilot for the entire scenario. Although this was true for steady state estimates, it was found that using the coefficients for t = 0 slightly reduced the transients in the state error plots. These coefficients were therefore used. The nonminimum phase characteristic of the autopilot was modeled by using constant coefficients and, the ease of implementing this approach made it more attractive compared to the integration of the complete adaptive autopilot (see Figure 21).

Quite unexpectedly, the third order design performance was not much improved over the second order design. The mean error in V_{mx}^{I} channel was still reaching a 110 ft/sec maximum (all plots for this design can be found in Appendix B). Again this design was considered unacceptable for a benchmark. Although no minimum error had previously been decided upon, the fundamental structure of the filter was considered sound and capable of producing better estimates of the V_{mx}^{I} state.

Benchmark. Proceeding with the assumption that the other modeling in the basic filter was adequate, the true a_c of the missile was passed to the filter design which modeled the third order autopilot. This was done in an attempt to determine if more modeling of the guidance strip, prior to the autopilot, was necessary. Also, if this approach failed

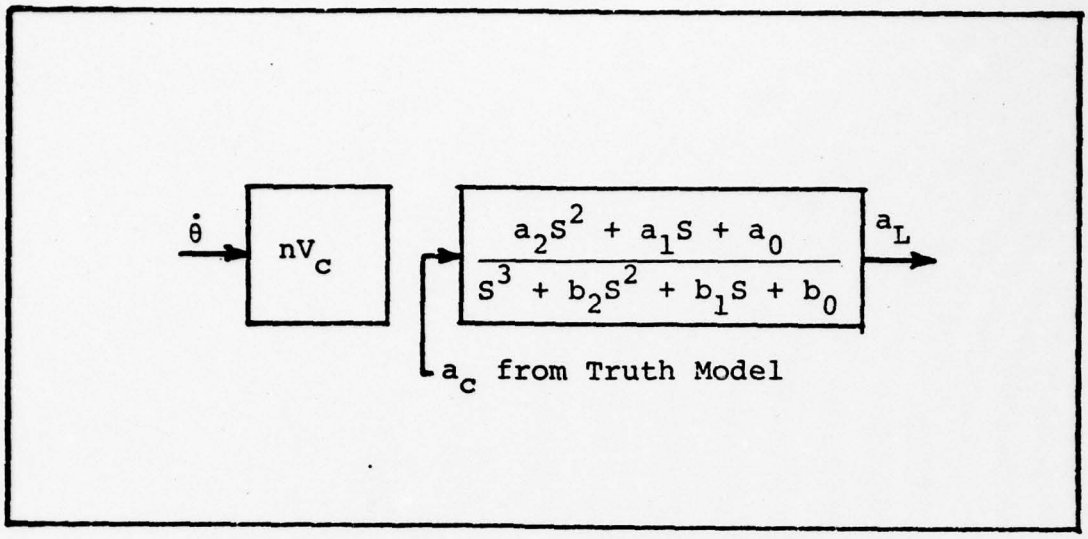

Fig. 22. Benchmark

to produced reasonably accurate estimates, it would indicate a major flaw in the fundamental design structure of the filter. The benchmark is shown in Figure 22.

The performance improvement of this design was dramatic when compared to the second and third order designs. For example, the mean error committed in the V_{mx}^I channel, the most sensitive state, did not exceed 10 ft/sec. This enhancement in performance confirmed the idea that more modeling of the guidance strip was necessary. It also indicated that the autopilot was not the critical subsystem of the guidance strip and that a simpler autopilot model would suffice.

Although this ad hoc design could never be implemented, it was considered to be a proper benchmark and would be used as a comparison for reduced order filters. The small errors committed in each channel would serve as a critical test on

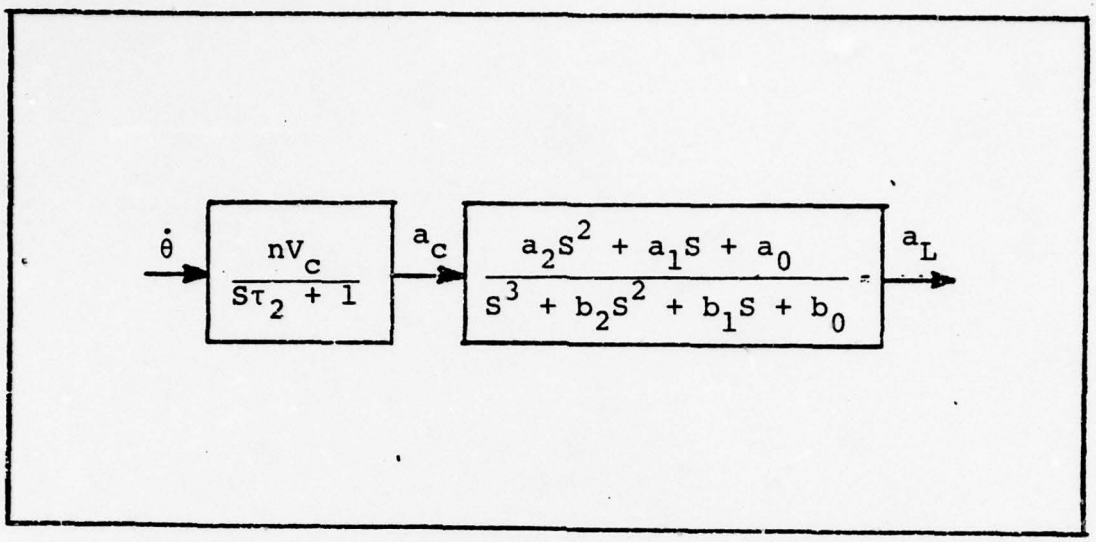

Fig. 23. Fourth Order Missile Filter

the performance of all filters analyzed for implementation. The complete set of benchmark plots are contained in Appendix B.

Fourth Order Missile Model. The benchmark design provided a lower bound for filter errors and indicated the need for more modeling of the guidance strip prior to the autopilot. The ad hoc approach, however, used in this development did not include models of the seeker and guidance system. The development of implementable reduced order filters would need specific knowledge of the dominant effects of these two components. To gain this insight, the fourth order missile model was proposed.

Upon examination of the three components of the guidance strip, it was observed that the guidance system had a limiting bandwidth of 3 rad/sec. Comparing this to the 7 rad/sec bandwidth of the autopilot and the 50 rad/sec bandwidth of the

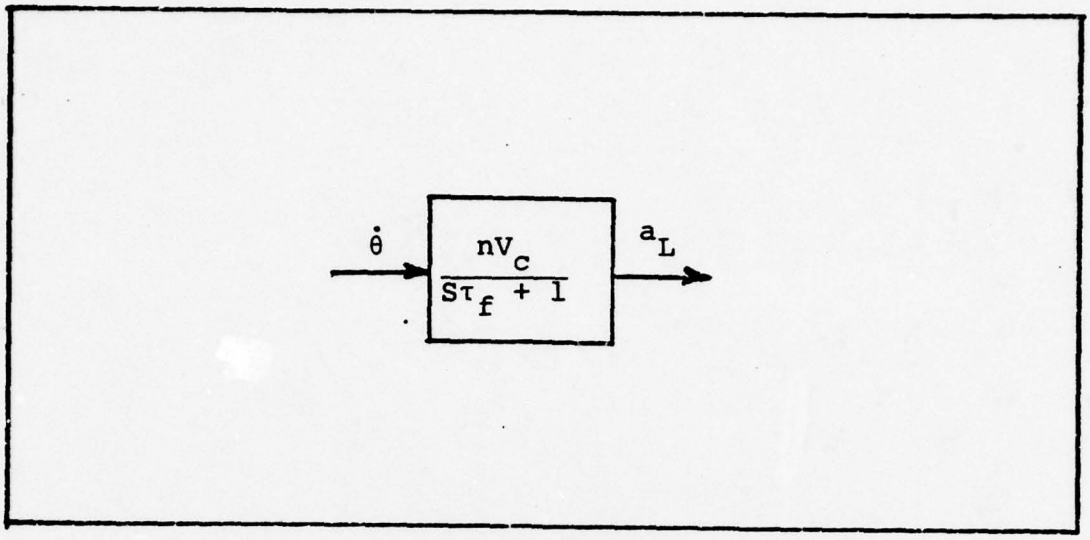

Fig. 24. First Order Missile Filter

seeker, it was hypothesized that the modeling of the guidance strip should include the bandlimiting characteristic of the guidance system. The guidance strip of this filter model is shown in Figure 23.

The fourth order missile filter produced estimates of the V_x^I state with a maximum mean error of 25 ft/sec. This was only 15 ft/sec greater then the benchmark filter, in which a_c was considered to be known exactly. This performance emphasized the need to model the bandlimit effect of the guidance system.

First Order Missile Filter. The significant performance of the fourth order filter suggested the possibility of a reduced order filter which modeled the complete guidance strip as a first order lag. This reasoning followed since the guidance system, itself a first order lag, appeared to be the dominant component of the entire guidance strip. It was, therefore, decided to approximate the complete guidance strip

as a first order lag (Figure 24). With this approach, a fifth order guidance strip, considering time invariant coefficients, was modeled by a first order lag in the filter.

An iterative search was performed to determine a time constant, τ_f, which would produce the least error in the state estimates. During this search, the proportional navigation constant, n, and the M/S ratio were assumed perfectly known. The results of this search showed that the best estimates were obtained with a time constant of .85 seconds. The maximum error of the first order missile model was 35 ft/sec, only 10 ft/sec greater than the fourth order filter and 25 ft/sec greater than the benchmark.

This filter was the first attempt at providing a reduced order model of the guidance strip which could possibly be implemented. However, the design required knowledge of τ_f for the particular missile being tracked. It also needed values for n and M/S. If the filter was insensitive to these parameters, it might be possible to use nominal values for all three. Of course, if the filter was highly sensitive to some or all of these parameters, their estimation might improve the overall performance of the filter. For this case, a random walk would be chosen to model τ_f. This model would portray the essential characteristic of τ_f, which is assumed constant over the entire scenario. As with n and M/S the pseudo noise is added to avoid having the Kalman gain components affecting the τ_f estimates go to zero. The complete τ_f model is shown below.

$$\dot{\tau}_f(t) = w_3(t) \tag{66}$$

where $E[w_3(t)\ w_3^T(t+\tau)] = Q_3\delta(\tau)$

The value of Q_3 would be chosen during tuning of this filter.

Summary. This Chapter presented the derivation of the equations for the first six states common to all filters. A benchmark filter was designed which gave insight into the important areas of modeling. The development of a fourth order missile filter resulted from this insight. In an attempt to reduce the complexity of the filter's guidance strip model, a first order lag was chosen to approximate the complete guidance strip of the missile.

The time constant, τ_f, of the first order lag was chosen to minimize the error in the state estimates. The design, however, required a detailed analysis concerning the three parameters, n, M/S, and τ_f to completely evaluate its performance. A sensitivity analysis for these uncertain parameters could possibly lead to an adaptive filter that estimates some (most important) or all (depending upon the computational resources available) of the uncertain parameters.

IV. Sensitivity and Parameter Estimation Analysis

Introduction

The modeling effort discussed in Chapter III led to two filters of practical interest; the fourth order missile filter and the first order missile filter. The fourth order filter demonstrated the benefits of including a model of the guidance system and a detailed model of the missile's autopilot. This extensive modeling required perfect knowledge of many parameters which in most cases are uncertain. Implementation of such a filter is, therefore, considered impractical. However, this detailed modeling would be advantageous in determining the sensitivity of the filter design to variations in key parameters of the missile.

The first order filter is more attractive for implementation since it approximates the complete guidance strip as a first order lag. It does not require specific knowledge of the structure and parameters of the particular autopilot, or the time constant of the guidance system. Instead, the significant aspects of the missile are modeled with only three uncertain parameters:

1) n - the proportional navigation constant
2) M/S - the ratio of mass to cross sectional area
3) τ_f - the time constant of the first order lag.

It should be remembered that a fourth uncertain parameter, C_D was redefined in terms of quantities that could be measured or estimated (refer to Chapter III).

The design approach in this analysis considered two possible alternatives for determining each unknown parameter. Either a nominal value would be chosen for the parameter, or the filter would perform on-line estimation to acquire the value of the parameter. The criterion used to decide this issue was the set of results of a sensitivity analysis performed on the fourth order filter.

This study concluded, from the results of this sensitivity analysis, that on-line estimation of each parameter was both possible and beneficial. A systematic approach was then devised which gradually increased the scope of the estimation problem. This approach consisted of a sequence of estimation problems made more complex by the inclusion of additional parameters to be estimated. Eventually, this led to the simultaneous estimation of all five states and all three parameters of the first order missile.

Chapter IV begins with a discussion on the tuning philosophy used throughout this study. This is followed by a presentation which justifies the use of twenty simulation runs for the Monte Carlo analysis. The Monte Carlo analysis was used to determine the performance of each filter design analyzed. Following this is a detailed explanation of the sensitivity analysis of the fourth order filter. The final topic covers the parameter estimation analysis of the first order filter.

Tuning Philosophy

The tuning philosophy used throughout this study can

be expressed as "covariance matching". Basically, this is the matching of the covariance history generated by the filter from the Kalman algorithm to the variances in the filter errors which are calculated in the Monte Carlo analysis. The covariance in the Kalman algorithm is an indication of the confidence of the filter's estimate. Covariance matching, then, tunes the covariance of the filter to reflect the true confidence in its estimates.

The "tuning" of the filter was performed by a proper choice of pseudo noise strength, Q, and the initial filter covariance, P_0, for each state. The initial value of measurement noise strength, modeled by R, was derived from a priori knowledge of the ownship's radar performance. R was also considred a tuning parameter, but its initial value, described above, was used as a lower bound. This was necessary to avoid the condition in which the filter weighted the incoming measurements with more certainty than the radar, as modeled, was capable of providing. These tuning parameters, as well as the initial state estimates, are included with their associated error plots in Appendix B.

During the tuning of the filter for parameter estimation, it became obvious that strict adherence to the philosophy of covariance matching was not advantageous for the parameter estimates. The pseudo noise strength, Q, needed for adequate parameter estimation was too large for matching the filter covariance to the true variance. This resulted in the filter covariance always being larger than the true variance for the parameter estimates.

However, this insured the conservative nature of the filter by never attributing more confidence to its estimates than the filter was actually achieving, thereby reducing the risk of divergence. Since the tuning was performed for one trajectory, adaptive self tuning may be required for an operational system to obtain performance comparable to the results presented in this study.

Variance Convergence

The use of the Monte Carlo analysis requires the determination of an appropriate number of simulations such that the statistics presenting filter performance are generated with a reasonable confidence. The number of simulations was initially chosen as twenty. It was decided that this number would be increased if twenty simulations could not provide valid results.

To confirm that twenty simulations were adequate, the variance of the true error was plotted versus the number of simulation runs. With a proper choice of simulation runs, this plot would show little change in the variance with the addition of each successive run. Figure 25 illustrates such a plot for four time points of the V^I_{mx} velocity variance history. This plot clearly indicates that twenty simulations were an adequate choice for this problem. The addition of successive runs over twenty may mathematically increase the confidence of the statistics but, it is obvious that there will be little change in the value of the variance. Similar plots of other states can be found in

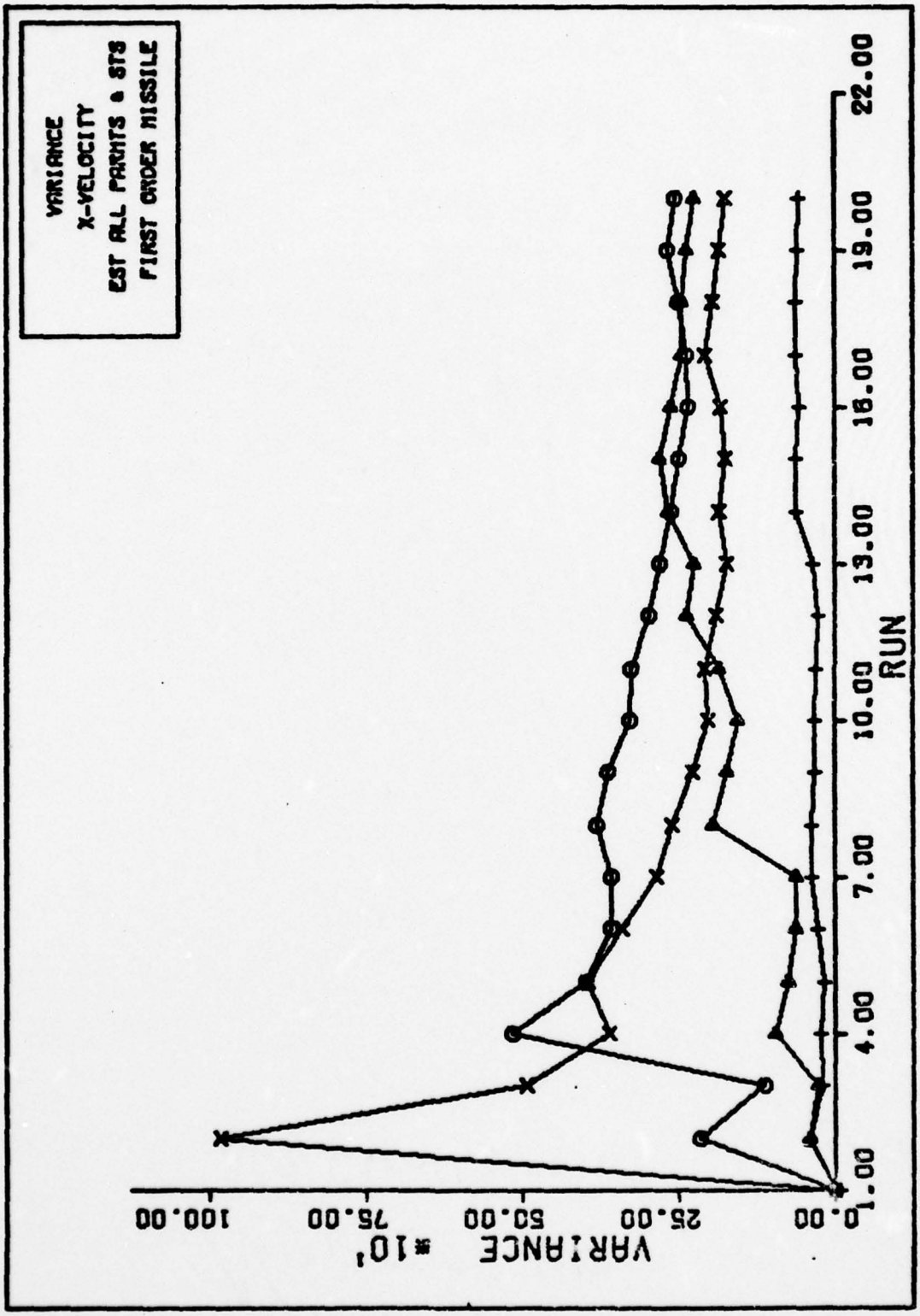

Fig. 25. VARIANCE CONVERGENCE

Appendix B which also illustrates this point.

Sensitivity Analysis

The fourth order filter was used for the sensitivity analysis since the detailed modeling, included in its design of the guidance strip, allowed for an easier interpretation of the filter performance. All states were initialized with zero error and the high-g trajectory was chosen for the simulation. It was suspected, and later observed, that the filter would be less sensitive to parameter variations over the low-g trajectory (discussed further in the section on estimation of n and τ_f). The three parameters, n, M/S, and τ_2, were set in the filter to the original values used in the truth model. The truth model values were then separately varied over what was considered to be their maximum range. The fourth order filter's sensitivity to variations in τ_2 would also be an indication of the first order filter's sensitivity to τ_f, while n, and M/S were modeled directly in this filter.

Table V shows the total mean error squared in the five states of the filter. These numbers were calculated by using Equation (67).

$$\text{Total Mean Error Squared} = \sum_{t=0}^{t_f} \bar{x}_t^2 \qquad (67)$$

where

$\bar{x}_t$ = ensemble average of the state error over twenty simulations made by the filter at time equal to t

Table V

Sensitivity Analysis Total Mean Error Squared

Parameters			θ (10^4)	V_{mx}^I (10^5)	R (10^3)	$\dot{R}$ (10^3)	a_L (10^2)
n	τ_2	M					
Nominals			3.22	0.56	1.74	0.94	1.47
6.0			26.90	4.20	1.93	0.75	7.86
3.0			78.40	13.60	1.76	9.95	25.66
	0.1		4.67	0.49	1.84	1.63	1.25
	0.8		162.00	19.70	1.46	32.80	57.00
		2.0	12.70	3.43	2.20	3.55	10.17
		8.0	7.74	1.22	1.67	11.70	2.23

 - indicates unchanged from nominal values: n = 4.5, τ_2 = .3, M = 4

t_f = final time of the trajectory.

The limits on the proportional navigation constant were chosen based on the discussion by Stallard (Ref 11:13-18). Stallard suggested that for non-optimal guidance the proportional navigation constant should remain between 3 and 5. This analysis considered 6 as a more reasonable upper limit for the sensitivity analysis. The range of the M/S parameter was varied by changing the mass alone. Since the two variables M and S always appear together as the ratio M/S, changing either will produce the needed change in M/S. The range of 2 slugs to 8 slugs was considered to be a large enough variation to test the sensitivity of the filter to this parameter. The minimum value of τ_2 was chosen as 0.1 seconds in consideration of the requirement for the missile to filter the noisy LOS angular rate measurement (Ref 11:1). The maximum value was chosen at 0.8 seconds since missiles using more sluggish guidance systems were considered impractical.

It can be observed from Table V that a greater error is made by the filter at one extreme of each parameter compared to the other extreme of the same parameter. This sensitivity was not as noticeable in the M/S state as in the τ_2 and n channels. The proportional navigation constant was varied equally in both directions yet the larger error committed when n was set to 3, suggests a higher sensitivity in this direction. Similar comparisons can be made with respect to the other two parameters.

These observations can be generalized into a simple relationship between the truth model and the filter. When the parameters of the filter guidance strip are equal to those in the truth model, the dynamics model more accurately accounts for the missile's actual response to changes observed in $\dot{\theta}$. Those changes in the parameters which caused an overall decrease in the bandwidth of the guidance strip in the truth model, resulted in larger estimation errors by the filter. Conversely, those changes which increased the bandwidth caused relatively smaller errors. This bandwidth comparison can also be stated in a lead-lag relationship; more error is made in estimation when the truth model lags the filter, as opposed to the truth model leading the filter. This relationship can be observed in the zero order filter developed by Lutter. The approximation used in the filter modeled the guidance strip with infinite bandwidth. After this analysis, it is obvious that this was the primary reason for the poor performance of this filter. This is also true for the second and third order designs discussed in Chapter III.

The "bandwidth relationship" allows for a heuristic explanation as to why the error is greater when the truth model lags the filter. Figure 26 shows Bode plots of the two possible relationships between the truth model and filter model guidance strips. These plots were not calculated but serve only to demonstrate the main point of the argument. The relatively wider bandwidth of the filter

guidance strip model when the truth model is lagging, makes the filter's model of the missile susceptible to more noise and higher frequency information. Since this high frequency information is not processed by the actual missile, it too is considered noise because of its effect upon the filter estimate. This added noise and high frequency information makes the filter missile appear more erratic when predicting forward to the next measurement. However, two important points lessen the severity of the bandwidth mismatch when the truth model leads the filter:

1) most of the important information is contained in the lower frequencies allowing the filter to predict a fairly accurate trajectory and,
2) the filter is observing less "noise" in its model of the guidance strip.

The total error listed in Table V indicated the filter was sensitive to changes in all three parameters. This fact was also supported by the plots of the filter's error for four of the five states which were generated for the sensitivity analysis. The complete set of these plots are contained in Appendix B of this report.

The results also indicated that the filter was not as sensitive to changes in M/S as it was to n and τ_2. The filter appears to be equally sensitive to n and τ_2. This study did not consider possible limitations upon filter structure during implementation which would restrict the

AD-A055 179 AIR FORCE INST OF TECH WRIGHT-PATTERSON AFB OHIO SCH--ETC F/G 19/5
AN EXTENDED KALMAN FILTER FIRE CONTROL SYSTEM AGAINST AIR-TO-AI--ETC(U)
DEC 77 S J CUSUMANO, M DE PONTE

UNCLASSIFIED AFIT/GE/EE/77-13-VOL-1 NL

2 OF 2
AD A055179

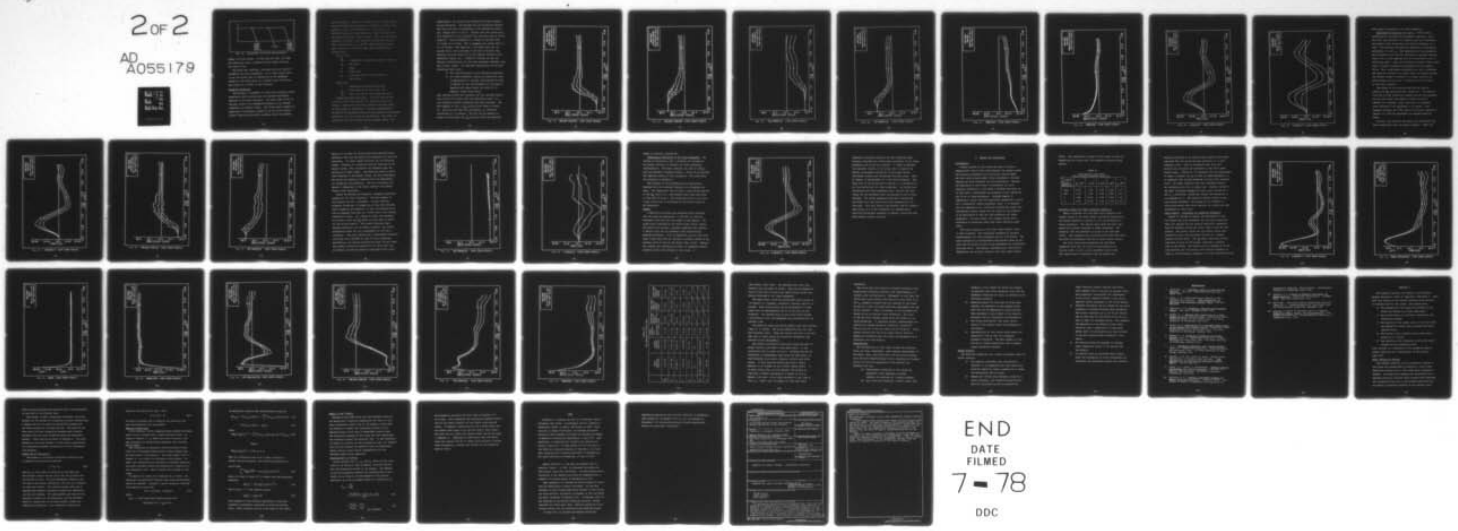

END
DATE FILMED
7-78
DDC

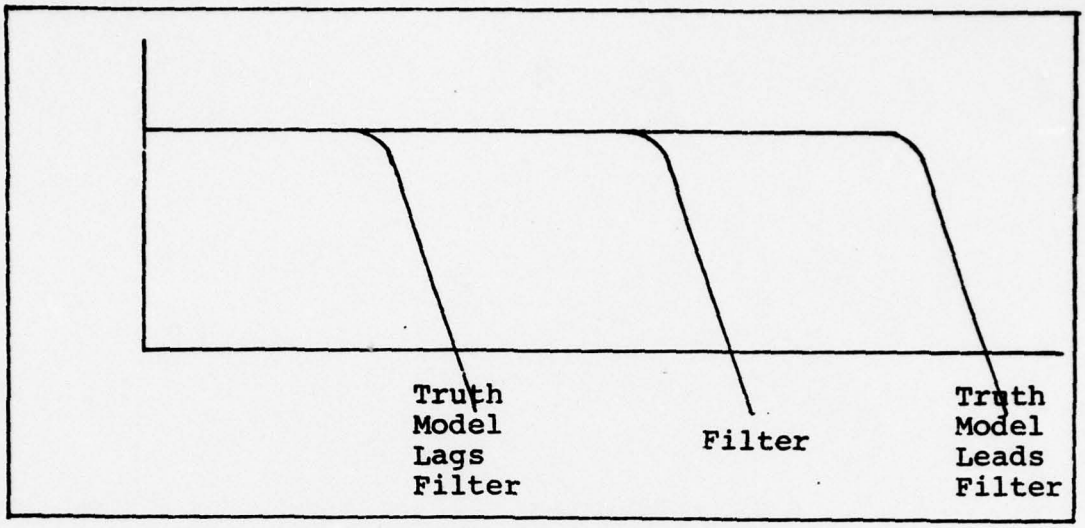

Fig. 26. Truth Model and Filter Relationships

number of filter states. If such were the case, the need for estimating n and τ_2 should be given higher priority than that of M/S.

The study was, therefore, continued with the intent of estimating all three parameters. It is worth noting that, if all the states were as insensitive to the parameter changes as the range state is, a nominal value would have been chosen as a result of this analysis.

Parameter Estimation

The decision to implement a filter which estimates these parameters would be based upon the improved performance observed in the state estimates. The first order filter is the most likely to be implemented because of its reduced complexity and general nature. The filter model attempts to approximate the dominant aspects of an air-to-air missile without requiring particular knowledge about the guidance

strip structure. Instead, it models this as a first order lag which adequately describes the dominant aspects of the guidance strip. The estimation of n, M/S and τ_f, if estimated correctly, help define the overall structure of the particular missile being tracked. This aids the filter algorithm in gleaning the important information from the three measurements θ_T, R, and $\dot{R}$. With estimation of all three parameters, the first order filter estimates are defined below:

Dynamic States

V_{mx}^I - x-component of missile's inertial velocity

θ_T - LOS angle

R - range

$\dot{R}$ - range rate

a_L - developed lateral acceleration of the missile

Parameters

n - proportional navigation constant

τ_f - time constant of first order lag

M/S - ratio of mass to cross sectional area.

Single Parameter Estimation. The first step in the parameter estimation analysis was designed to test the recovery characteristics of the filter to initial errors in each parameter separately. This was accomplished by estimating the parameter which was initialized at its extreme, along with the five states of the missiles. The other two parameters were set at their correct nominal value. For

completeness, the recovery was observed from both extremes of each parameter. The extremes for the navigation constant were kept the same as established in the sensitivity analysis, ranging from 3.0 to 6.0. The M/S ratio was varied from 15.0 slugs/ft^2 to 45.0 slugs/ft^2 with the true value at 29.197 slugs/ft^2. This corresponds to a change in the mass from 2.0 slugs to 6.0 slugs. The τ_f parameter was varied from 0.3 to 1.5 seconds. The range for τ_f was based upon the .85 seconds value, which resulted in the best estimation when matching the first order lag to the complete guidance strip (Reference Chapter III). Figures 27 through 32 show the recovery characteristics of the three parameter estimates from poor initial values. Two important observations can be made concerning these plots:

1) All three parameters can be estimated separately.
2) All three parameters require an acquisition time of approximately 2 seconds (the acquisition time is defined as the time necessary for the mean to approach and remain within one sigma of its apparent steady state value).

Also observed during this procedure was the improved estimation of the five states after the acquisition time (i.e., once adequate parameter estimation had been obtained). The best example of this is V^I_{mx} velocity plot shown in Figure 33. This plot was made while estimating τ_f, which was initialized at 0.3 seconds. The plot can be compared to Figure 34 which shows the V^I_{mx} velocity which was generated

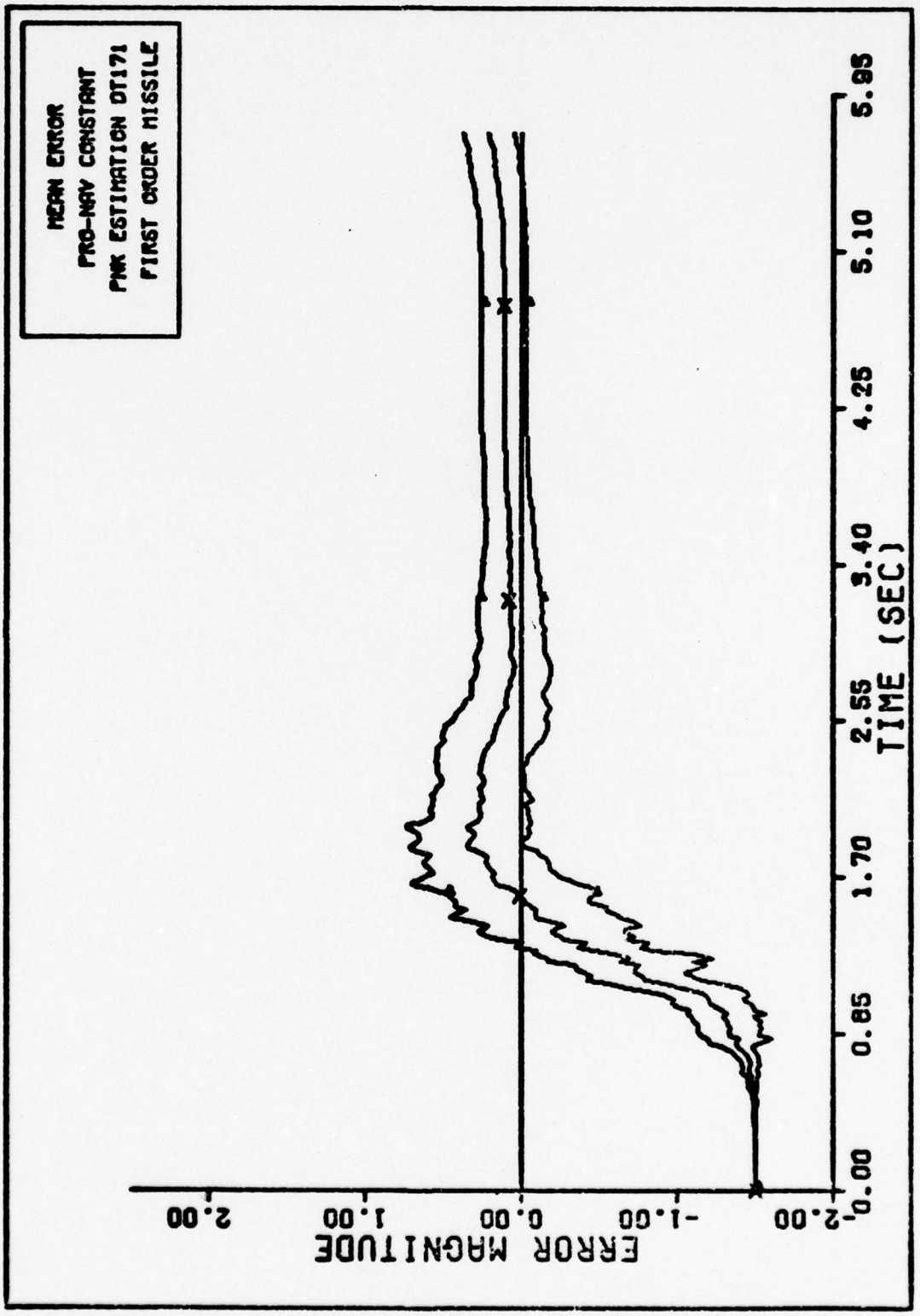

Fig. 27. PRO-NAV CONSTANT FIRST ORDER MISSILE

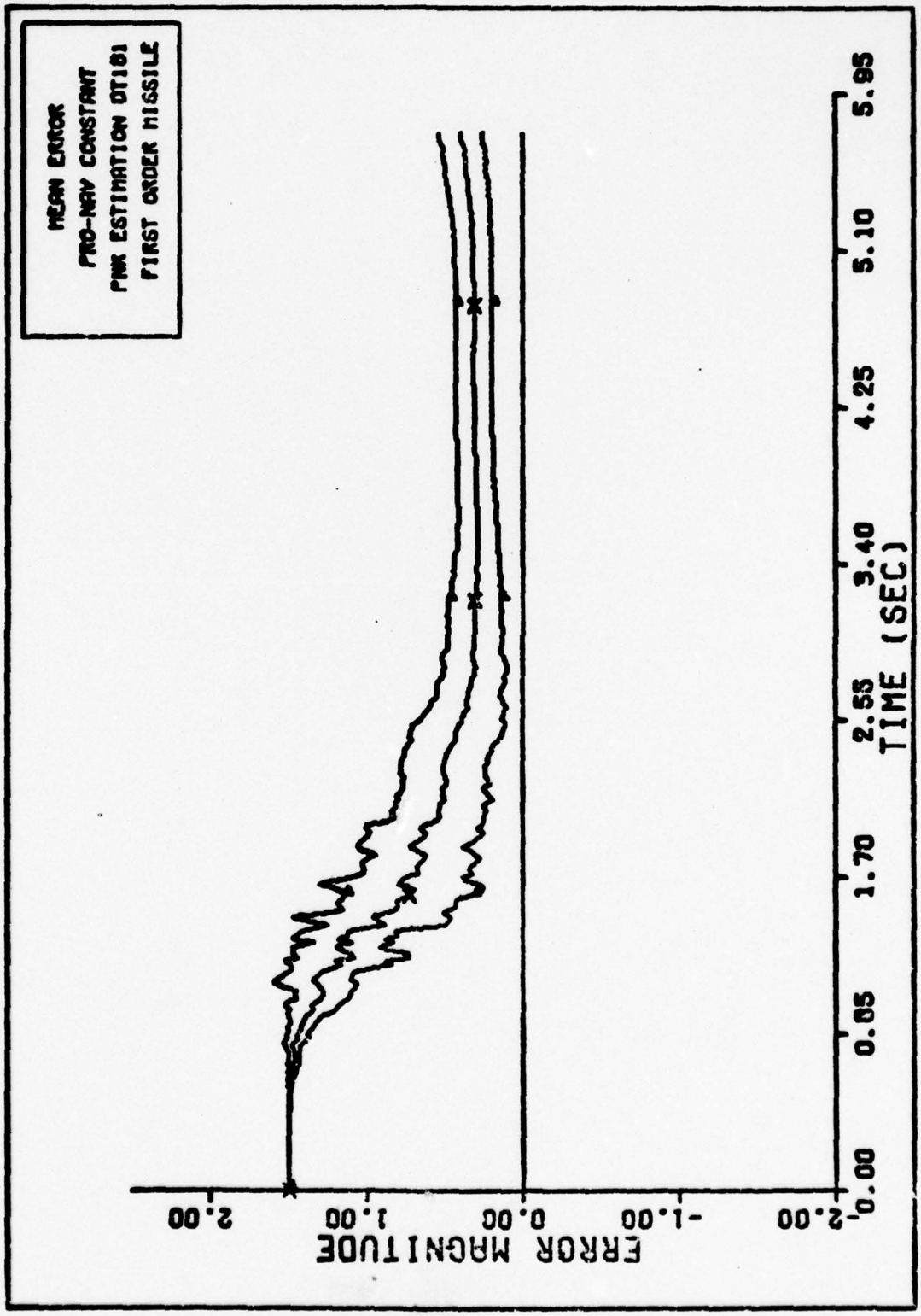

Fig. 28. PRO-NAV CONSTANT FIRST ORDER MISSILE

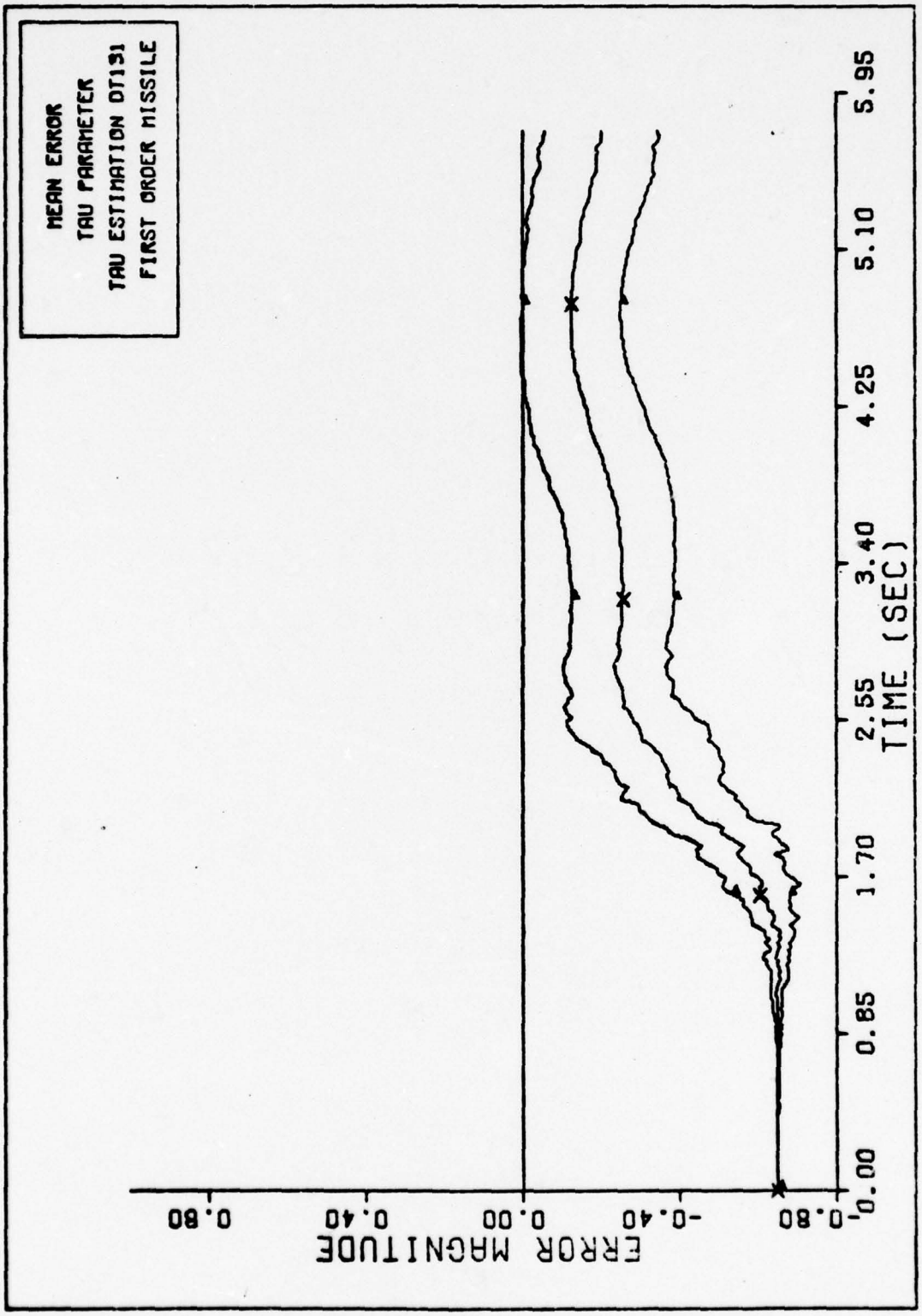

Fig. 29. TAU PARAMETER FIRST ORDER MISSILE

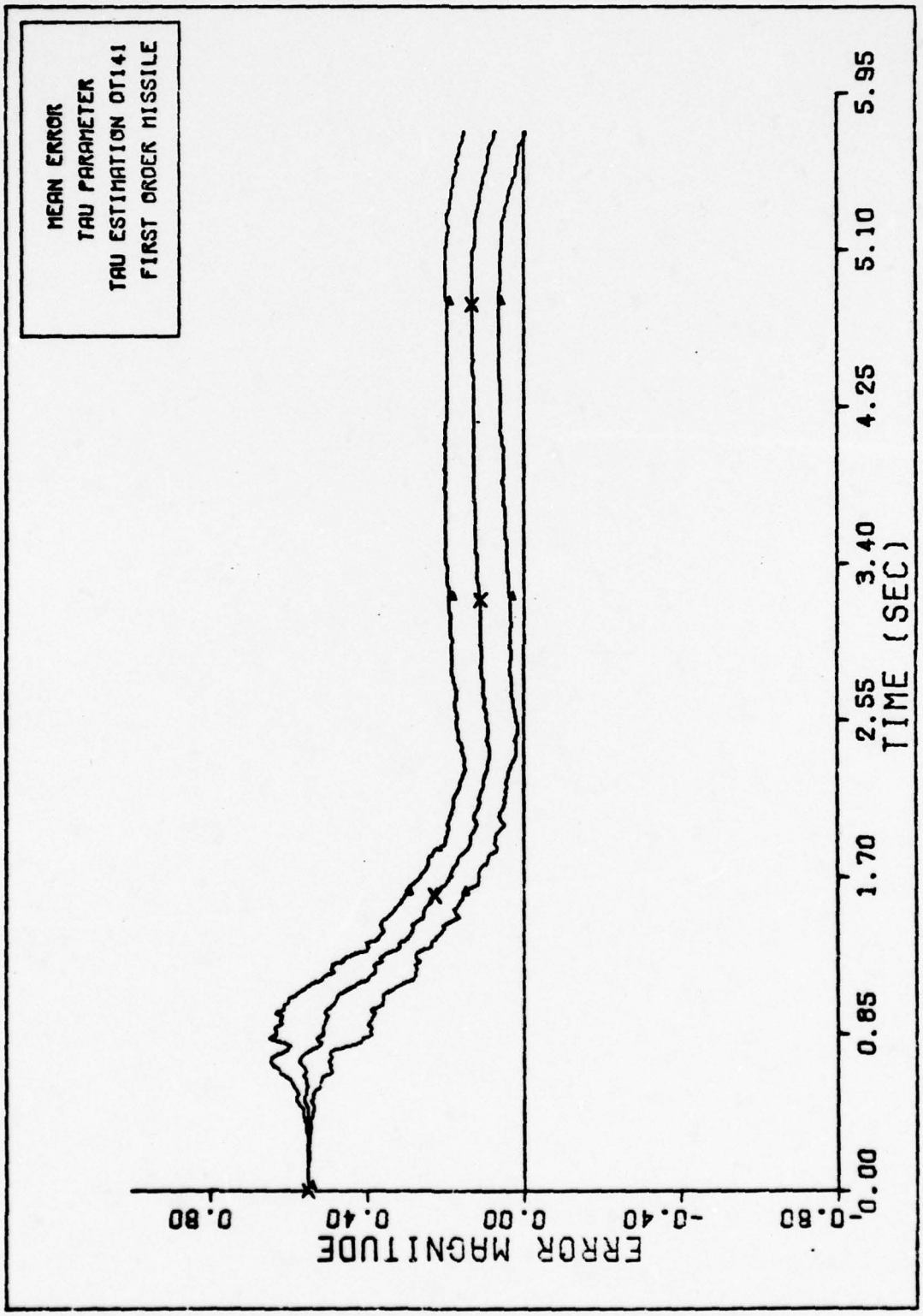

Fig. 30. TAU PARAMETER FIRST ORDER MISSILE

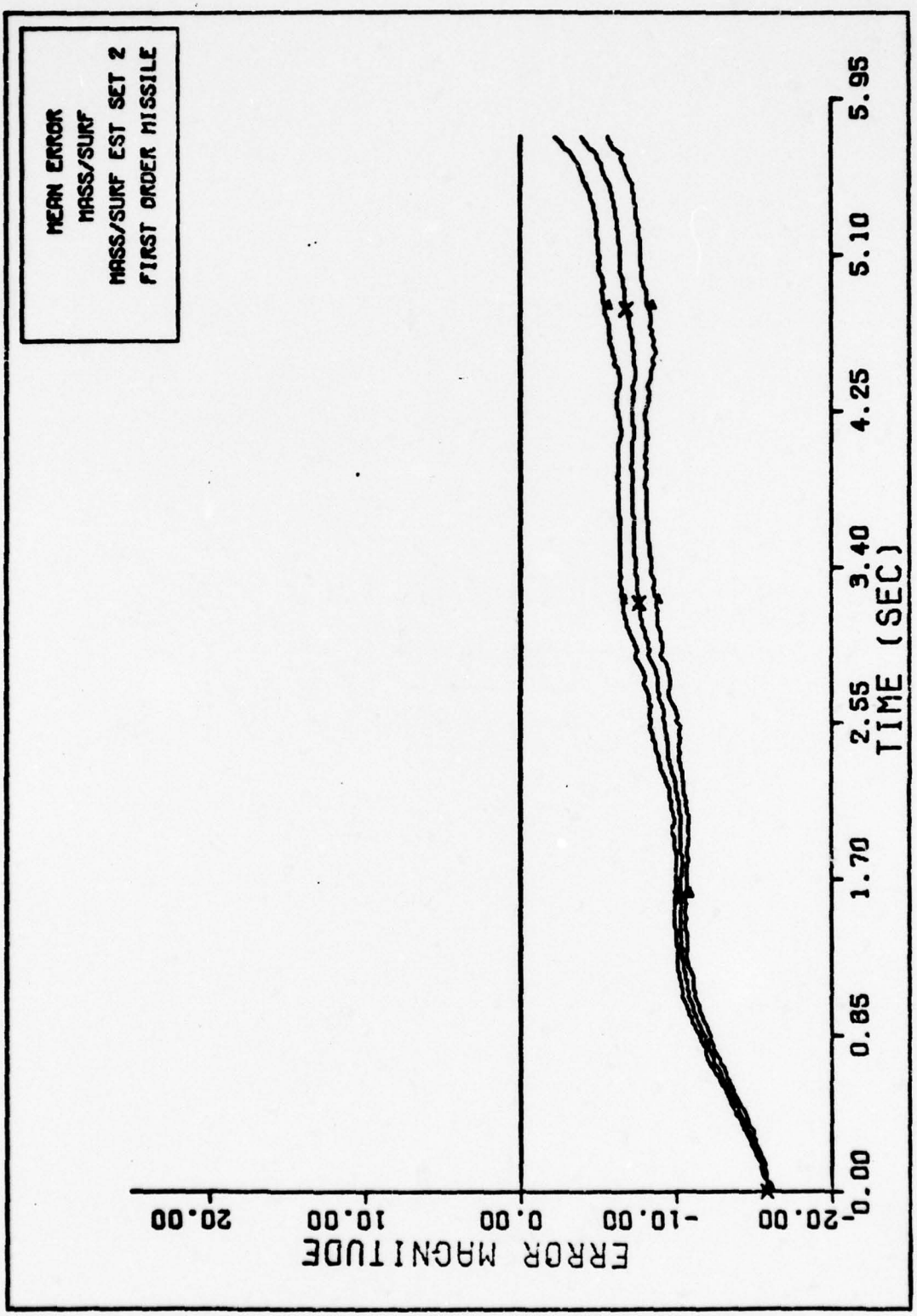

Fig. 31. MASS/SURF FIRST ORDER MISSILE

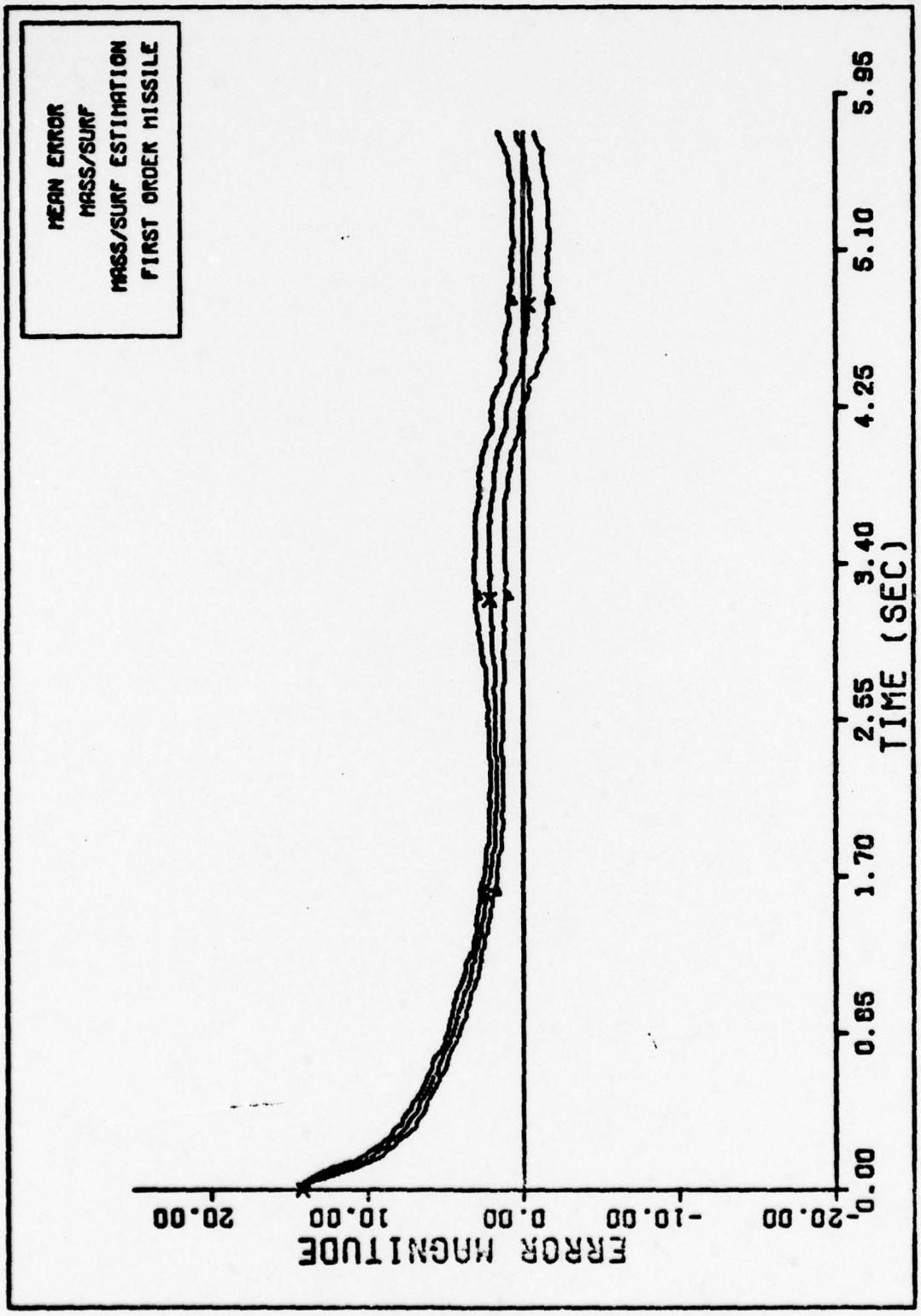

Fig. 32. MASS/SURF FIRST ORDER MISSILE

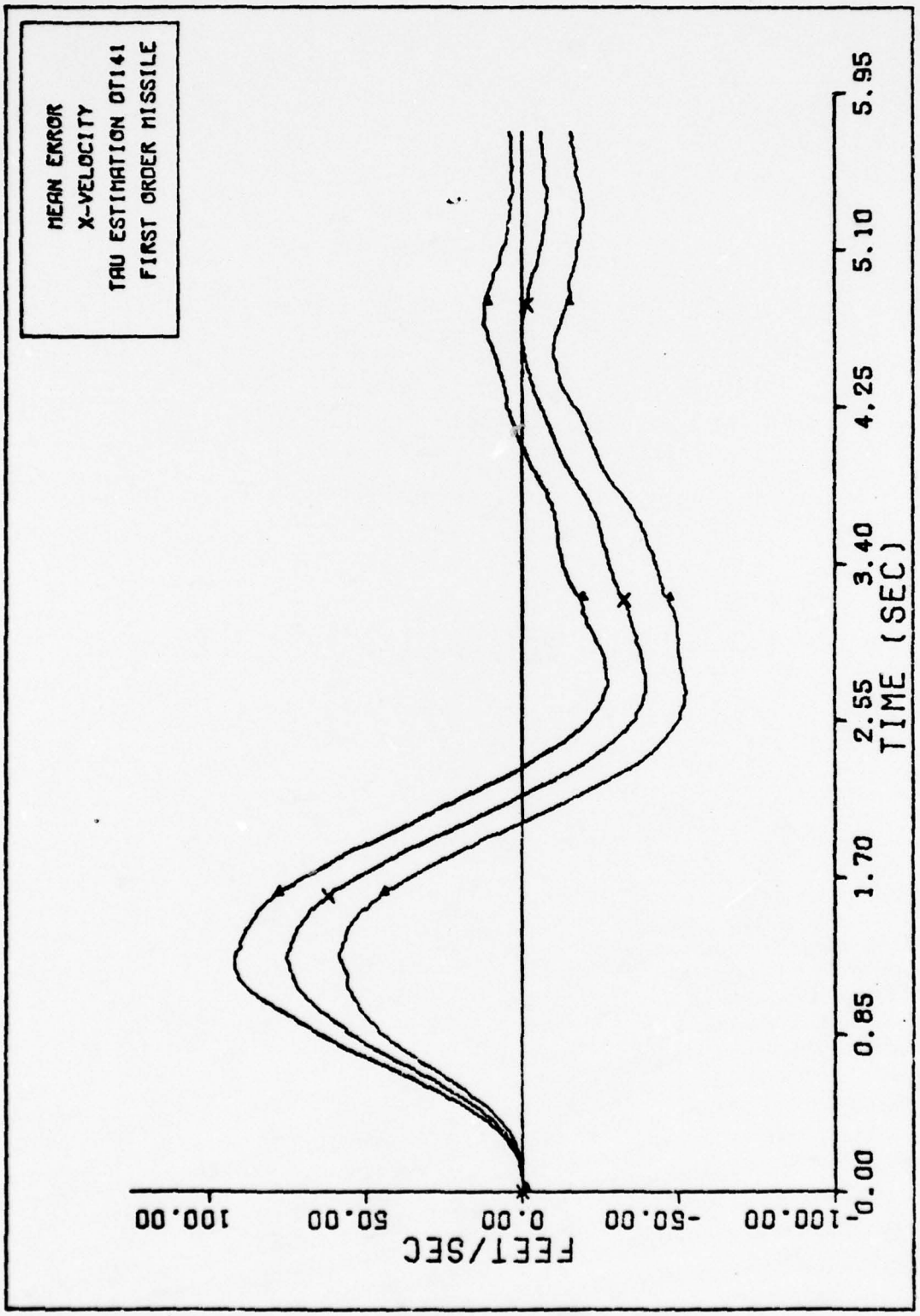

Fig. 33. X-VELOCITY FIRST ORDER MISSILE

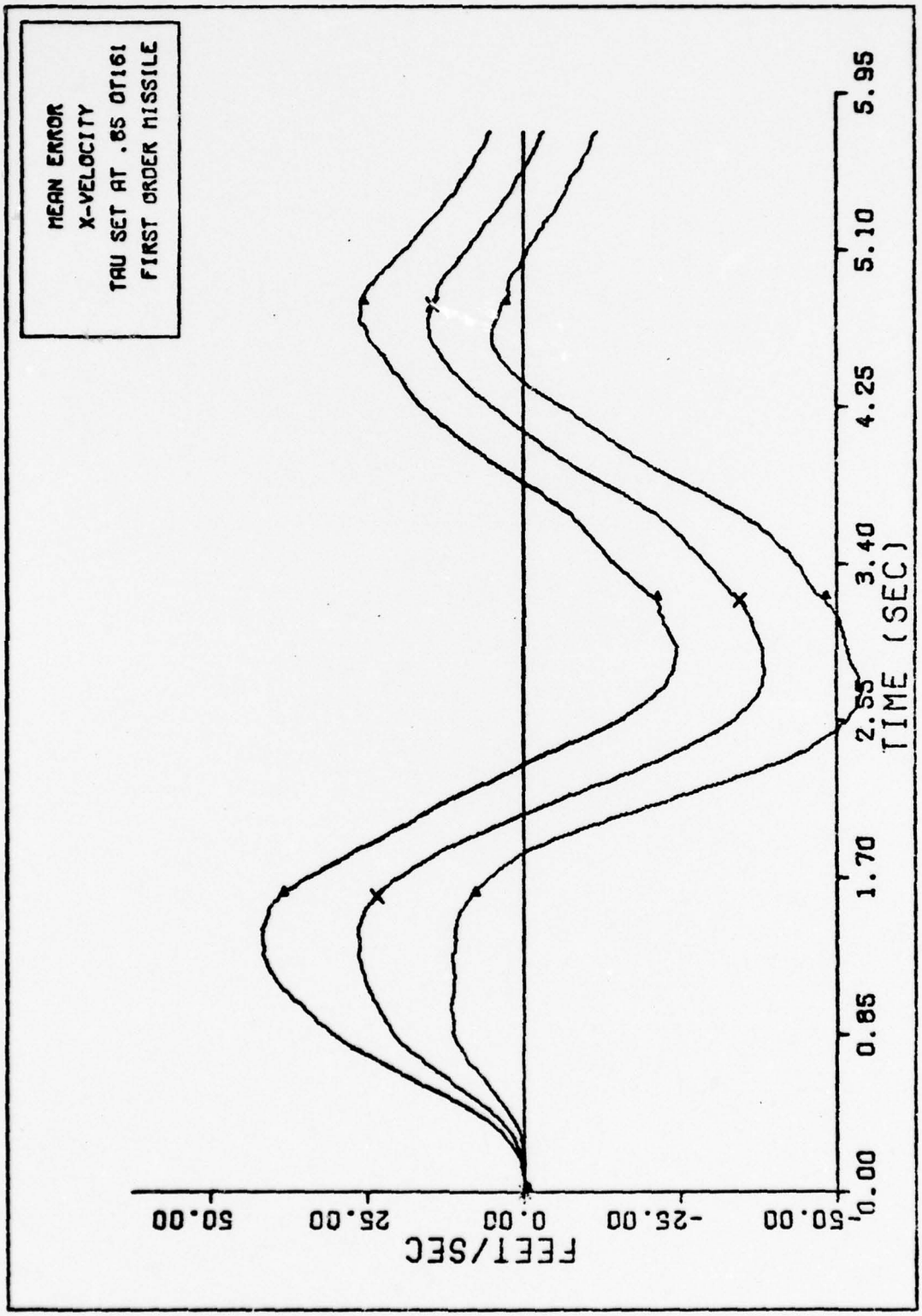

Fig. 34. X-VELOCITY FIRST ORDER MISSILE

with perfect knowledge of all three parameters.

Simultaneous Estimation of n and τ_f. After having satisfactorily estimated each parameter separately, there was still some question as to whether good state estimation was possible when estimating more than one parameter at a time. This question was partially answered by simultaneous estimation of n and τ_f. This combination of two parameters was considered to be the most difficult to estimate together since n and τ_f both appeared only in the guidance strip of the filter model. Also, the variation of each of these parameters strongly influenced the bandwidth of the guidance strip. Thus, simultaneous estimation of n and τ_f addressed the question of whether the filter could distinguish between the changes needed to converge to a proper estimate and those changes possibly made to compensate for the effect of the other parameter.

The answer to this question can best be given by showing the V^I_{mx} estimation plot (Figure 35). The acquisition time for the navigation constant and the time constant for the first order lag (shown in Figure 36 and 37) remained at 2 seconds. After this time, the greatest error observed in the V^I_{mx}channel is 40 ft/sec. This compares favorably with the result of 35 ft/sec reported in Chapter III, when the parameters are assumed perfectly known.

Up until this point in the study, all simulations had been accomplished using the high-g scenario. There was

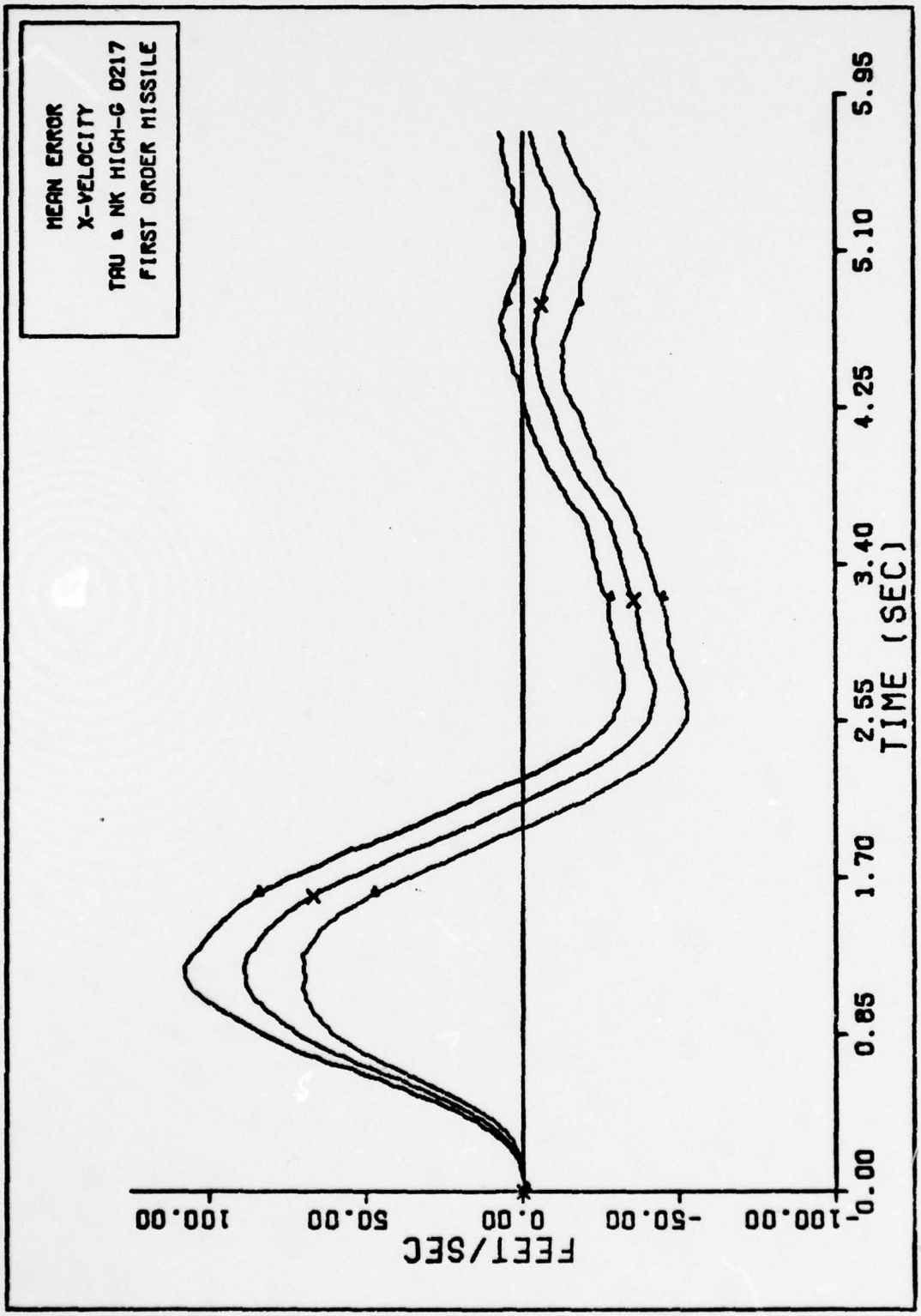

Fig. 35. X-VELOCITY FIRST ORDER MISSILE

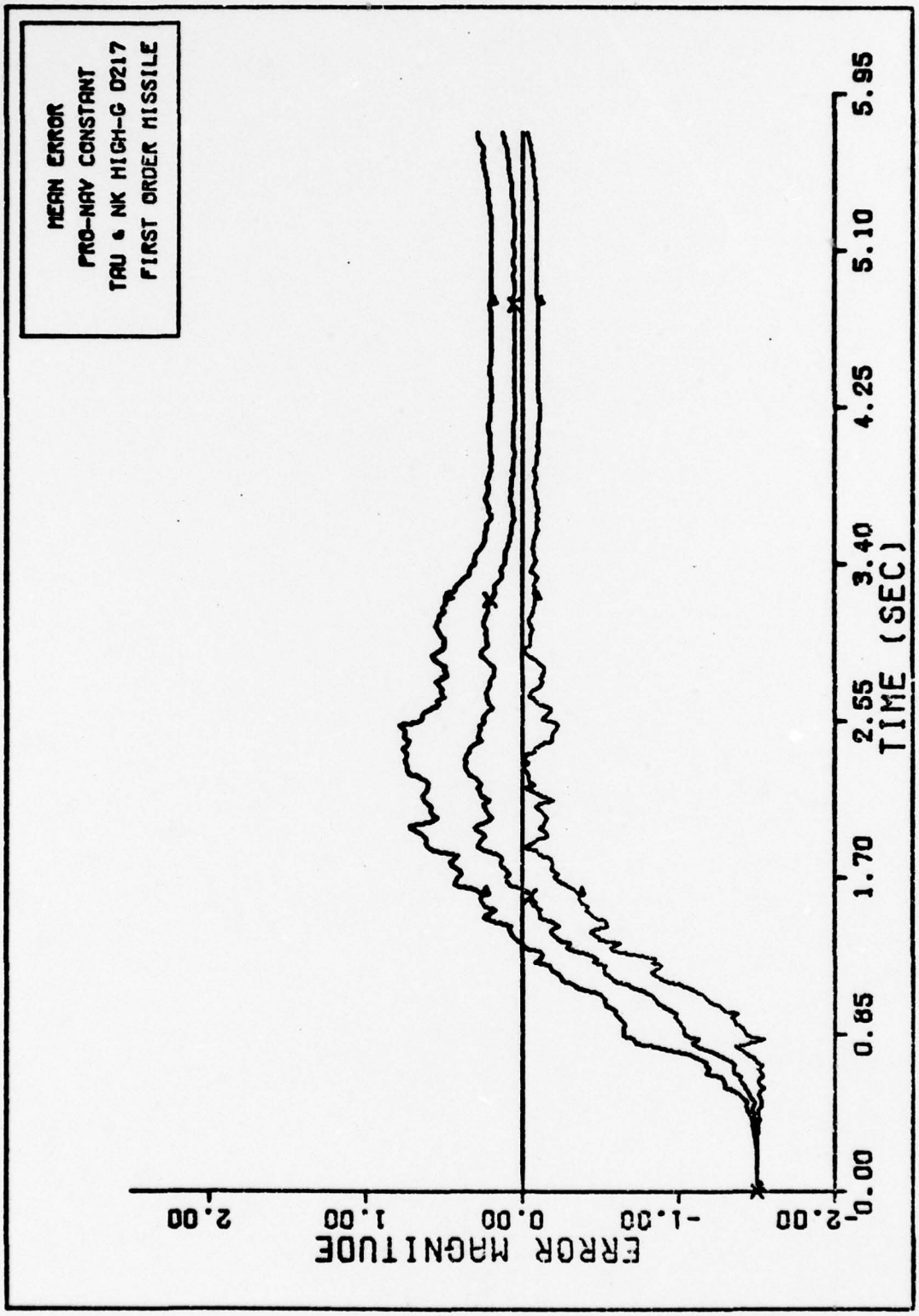

Fig. 36. PRO-NAV CONSTANT FIRST ORDER MISSILE

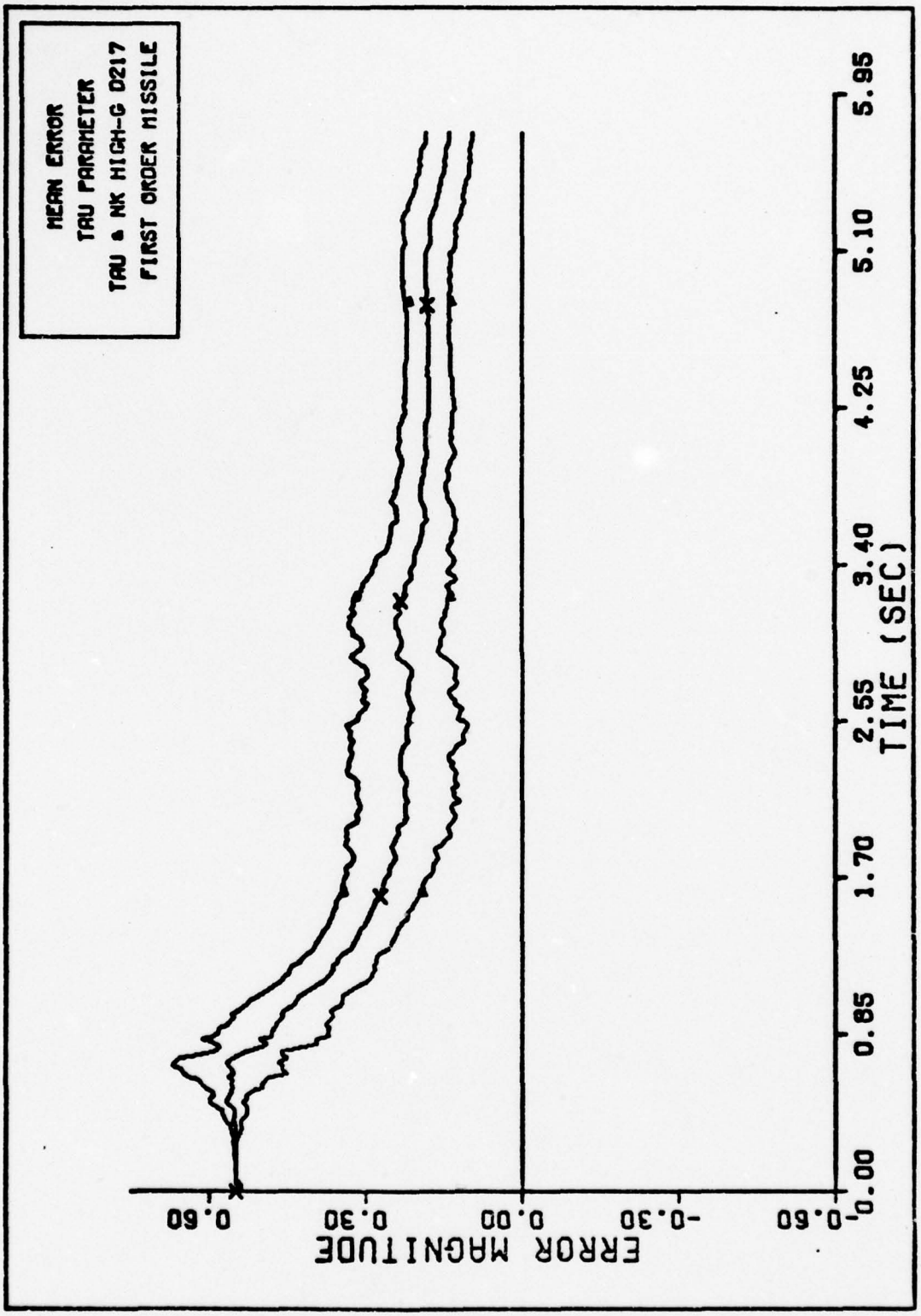

Fig. 37. TAU PARAMETER FIRST ORDER MISSILE

doubt as to whether the filter would yield accurate state estimation when also estimating the parameters for the low-g trajectory. The doubt seemed justified for the following reason. Although the parameters were not functions of the missile states, their estimation was dependent upon the excitation of these states. The wider the range of variations observed in the missile states, the more information the filter was capable of gleaning from the measurements for estimating the parameters. The low-g trajectory was benign in comparison to the high-g scenario and offered minimal state variations.

Figure 38 confirms the suspected parameter estimation problem for the low-g trajectory. The best example of this problem was the τ_f parameter. Without adequate parameter estimation, it seemed less likely that enhanced state estimation was possible; in fact, performance might even be degraded from that of a filter with a less refined acceleration model. Yet, Figure 39 shows this statement to be false, since the V^I_{mx} error was less than 30 ft/sec for the entire scenario. This result indicates that, although beneficial for the high-g scenario, the refined acceleration model was not advantageous for the low-g trajectory. This also implies that a Gauss-Markov acceleration model could possibly be used for low-g scenarios. Nevertheless, the refined acceleration model did not introduce severe estimation problems for the low-g case, and is therefore considered generally applicable over a wide

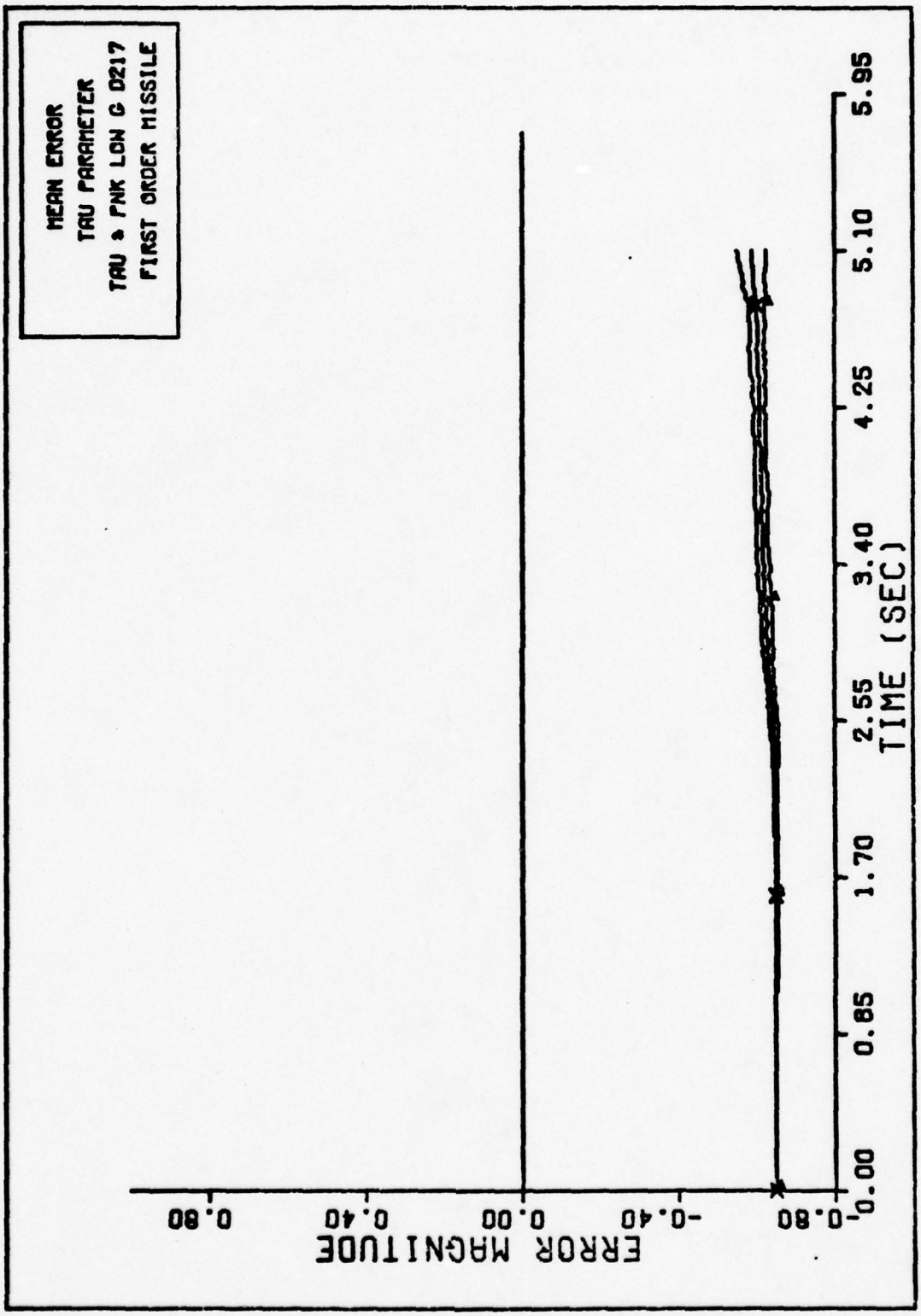

Fig. 38. TAU PARAMETER FIRST ORDER MISSILE

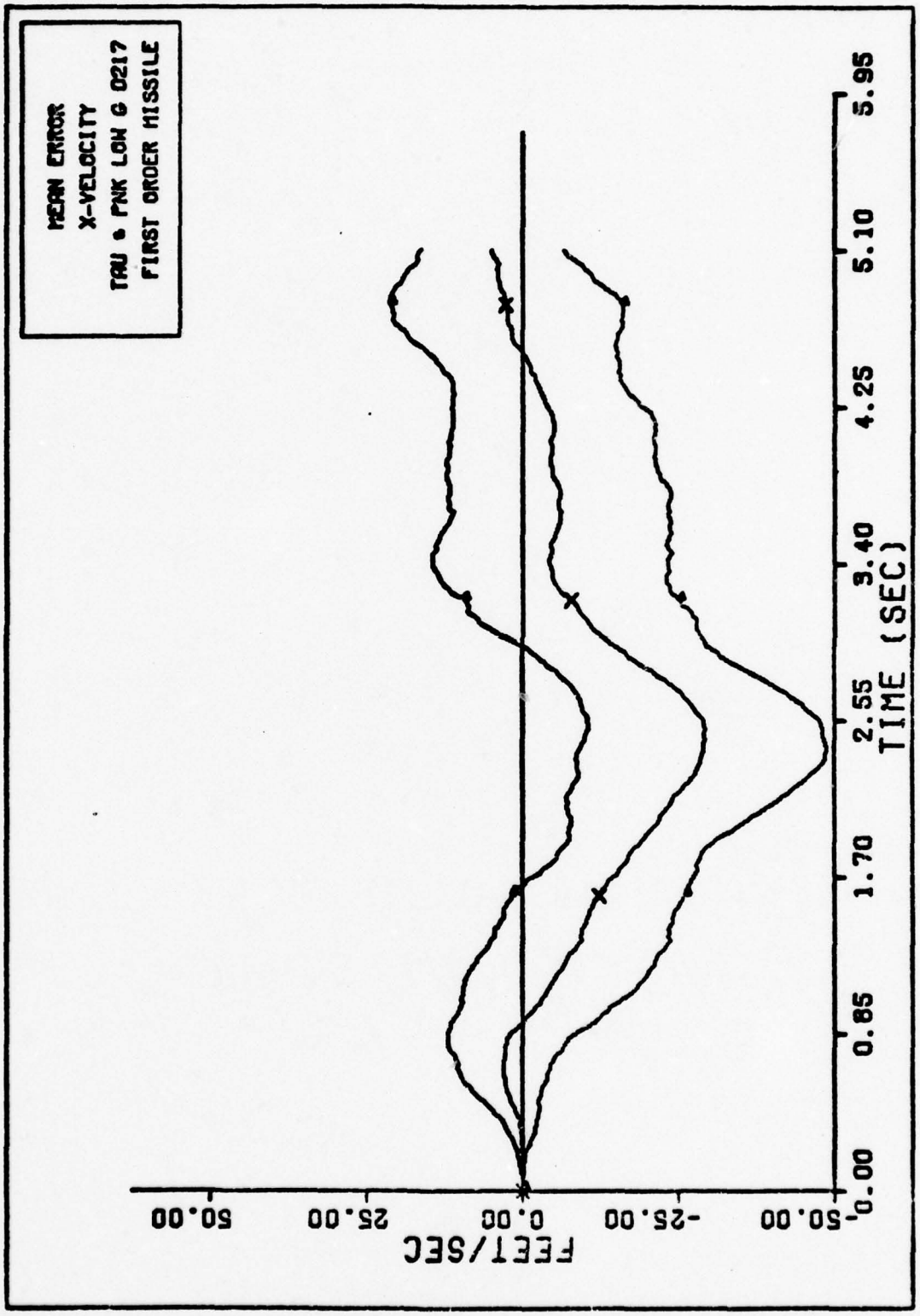

Fig. 39. X-VELOCITY FIRST ORDER MISSILE

range of encounter trajectories.

Simultaneous Estimation of All Three Parameters. The success of estimating n and τ_f together was followed by the logical decision to estimate all three parameters simultaneously. The high-g scenario was used to investigate the parameter estimation better. Figure 40 illustrates the important points of this estimation. The other plots are contained in Appendix B.

The estimate of each parameter was not appreciably degraded with the increased complexity of estimating all three. The acquisition time of about 2 secs can be observed in the V^I_{mx} error plot. The maximum error after this time is less than 50 ft/sec. The increasing error in the first 2 secs of the plot is attributed to the initial error in the parameters.

Summary

A sensitivity analysis was performed which indicated that the three key parameters, n, M/S and τ_2, could be estimated along with the five states of the missile. The large errors committed by the fourth order filter, during the sensitivity analysis, strongly suggested that choosing a nominal value for any parameter would significantly degrade performance. This is especially true for the first order filter which did not include as refined a model of the guidance strip as that of the fourth order filter. Because the tradeoff was considered so great, no suggested nominal parameter values are included in this study. A

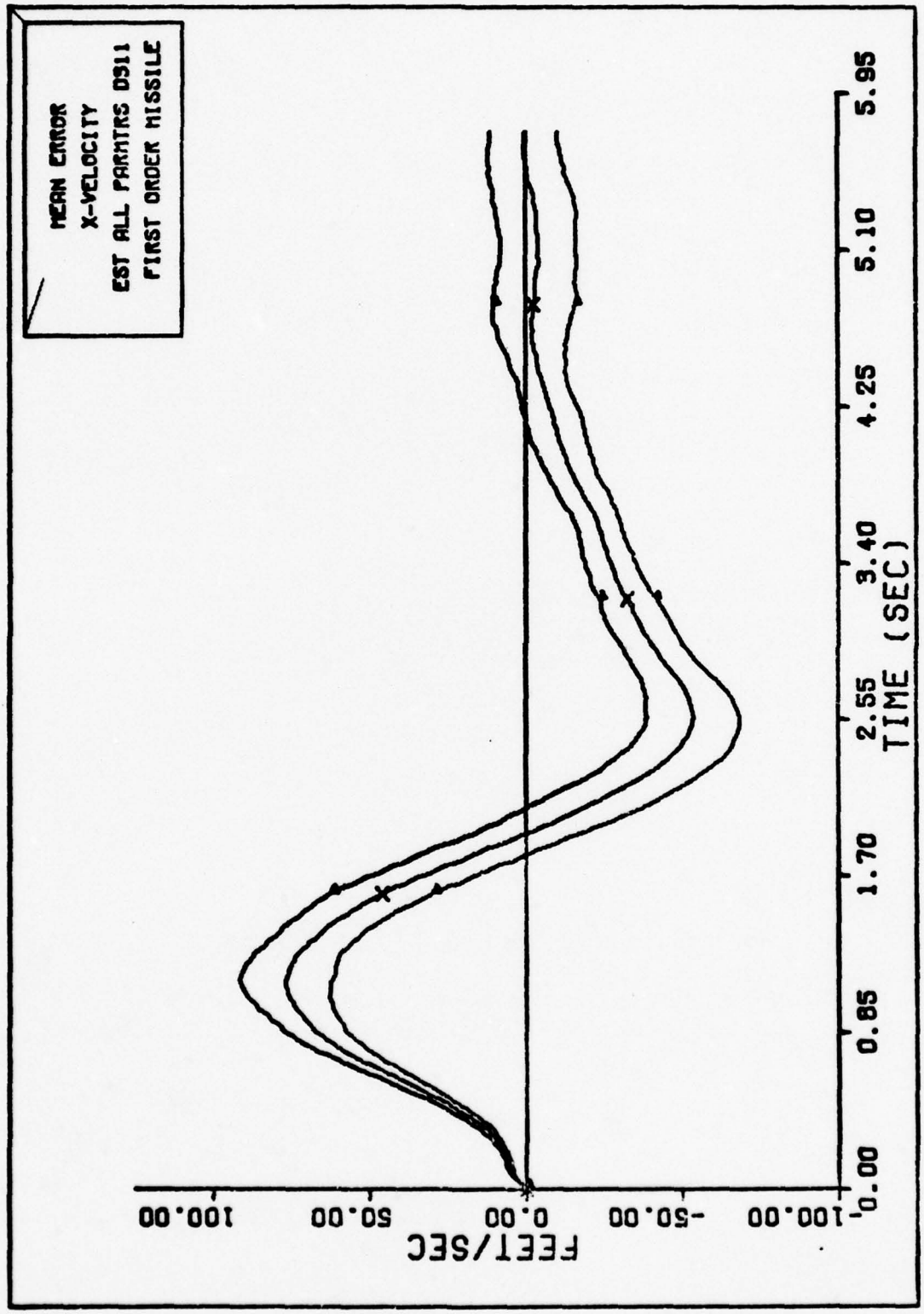

Fig. 40. X-VELOCITY FIRST ORDER MISSILE

systematic estimation analysis was then performed which strongly confirmed that simultaneous estimation of all three parameters and states was possible. In order to diminish the transient effects of the states and, to observe the effects of parameter estimation on the states better, the dynamic states were initialized with zero error. This, of course, is unrealizable in a real world situation. The final test of the filter was to subject it to estimation of all five states and all three parameters. The states were initialized with some reasonable error (10% off the true value) and the parameters were initialized at one of their extremes. The tuning parameters used when initializing the states with zero error were found inappropriate for this case. This also implies the possible need for adaptive self tuning in a filter considered for implementation since the performance presented in Chapter V would not have been achieved without retuning.

V. Results and Conclusions

Introduction

A major purpose of this thesis has been to design a reduced order filter which could estimate the dynamic states and uncertain parameters of an air-to-air missile model. The first order missile model filter developed in the last chapter has great potential for this application. However, the dedication to this effort of estimating all three uncertain parameters in this model's structure may have, up to this point, overshadowed the prospects of only estimating one or two of these parameters. Although Chapter IV emphatically states that the performance degradation is great for a "mismatched" nominal parameter value, it is possible that the composition of a particular problem may either have considerably smaller ranges for the values of the nominals, or be constrained in some way from estimating all three parameters. For this reason, this chapter begins with a discussion on estimating fewer than three uncertain parameters.

The final evaluation of the first order missile filter is then presented. This evaluation attempted to estimate simultaneously all three parameters and all five states. The final evaluation is distinguished from previous cases by the fact that the states as well as the parameters are initialized with some error. The results, presented here, continued to demonstrate the versatile nature of the first order missile

filter. The significant findings of this study, as well as suggestions for future work, are presented following these results.

Table VI

Total Error in Each State
During Single Parameter Estimation

State / Parameter Estimated	V_{mx}^{I} (10^5)	θ (10^{-4})	R (10^3)	$\dot{R}$ (10^3)	a_L (10^2)
none	0.99	3.86	1.82	0.478	3.70
M/S	1.39	5.21	1.85	1.870	5.93
n	2.84	15.20	1.85	0.514	7.23
τ_f	3.45	15.50	1.94	1.370	11.10

Estimating Fewer Than Three Uncertain Parameters

Table VI presents the total mean error squared in the dynamic states of the filter model (calculated according to the method discussed in Chapter IV) for the estimation of single parameters. The initial entry shows the error generated with perfect knowledge of these parameters. The parameter that was estimated is listed in the left hand column. This parameter was initialized with some error while the other two parameters were set at their correct values.

The total errors when estimating the individual parameters show that the filter is more sensitive to initial errors in the τ_f and n parameters than in M/S. This observation is consistent with the sensitivity

analysis performed on the fourth order missile filter which indicated that the filter was more sensitive to τ_2 and n compared to M/S. Table VI delineates more fully the priority for including the parameters in the first order missile model. Therefore, if confronted with the requirement to choose a nominal for one or more of these parameters, it is suggested that the M/S parameter be given first consideration. The table indicates that the n parameter should be considered next with τ_f chosen last. However, because of the small difference between the total errors listed for n and τ_f, a particular problem may justify the estimation of n as opposed to τ_f. The choice of nominal values is very much problem dependent, and because of the tradeoff in filter performance when using nominals, no values have been recommended by this study.

Final Results: Estimating All Uncertain Parameters

Figures 41 through 48 exhibit the performance of the five states and three parameters for the final evaluation. Table VII presents the key results along with information from the benchmark design and fourth order filter for comparison. The initial errors for all missile states were considered within the performance ability of a typical fighter aircraft radar. The V_{mx}^I error, which was initialized with an error of 225 ft/sec, indicates a recovery time of one second. The recovery time is defined to be the time necessary for the initial error induced transient to decay to the performance produced in a filter initialized with

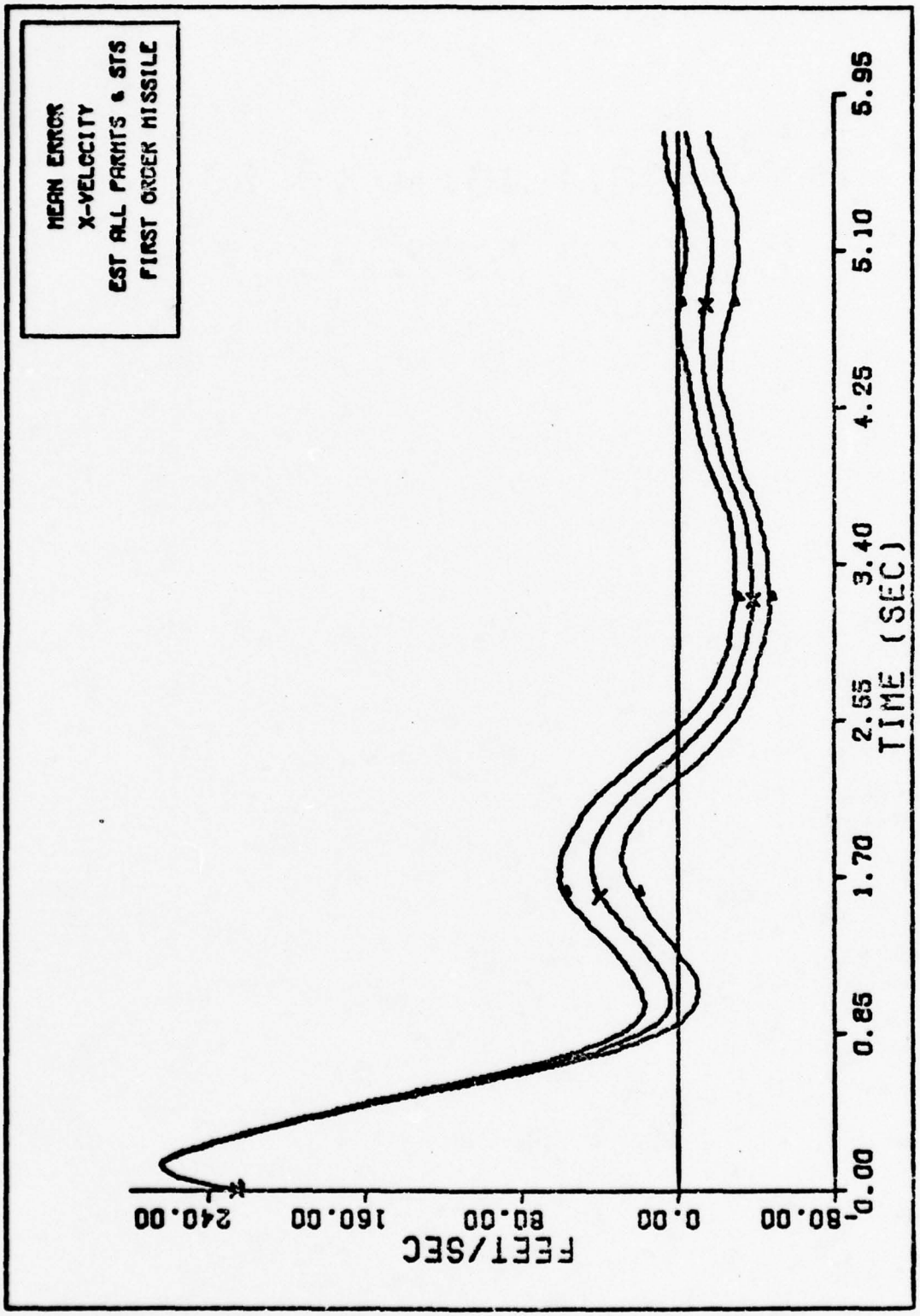

Fig. 41. X-VELOCITY FIRST ORDER MISSILE

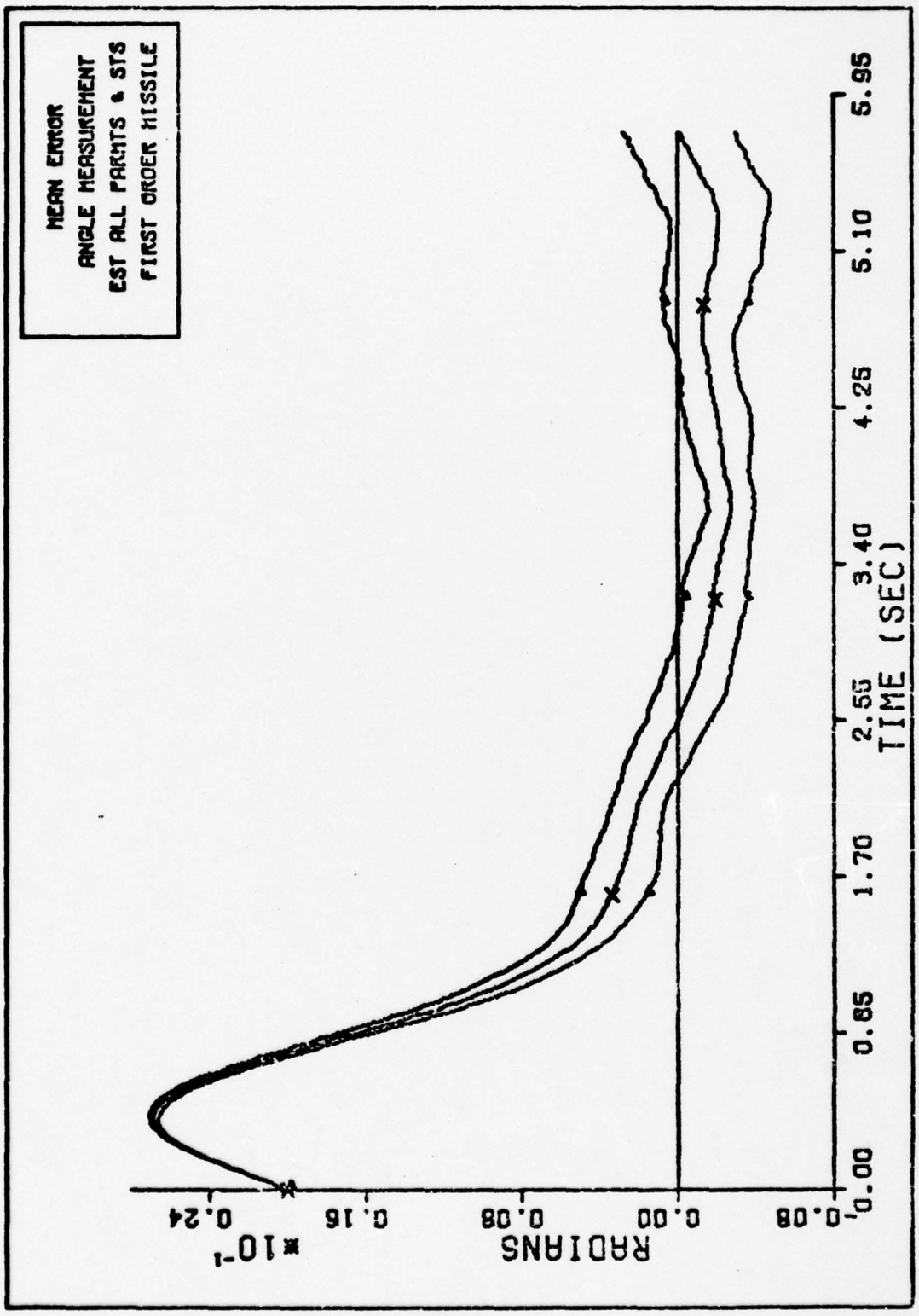

Fig. 42. ANGLE MEASUREMENT FIRST ORDER MISSILE

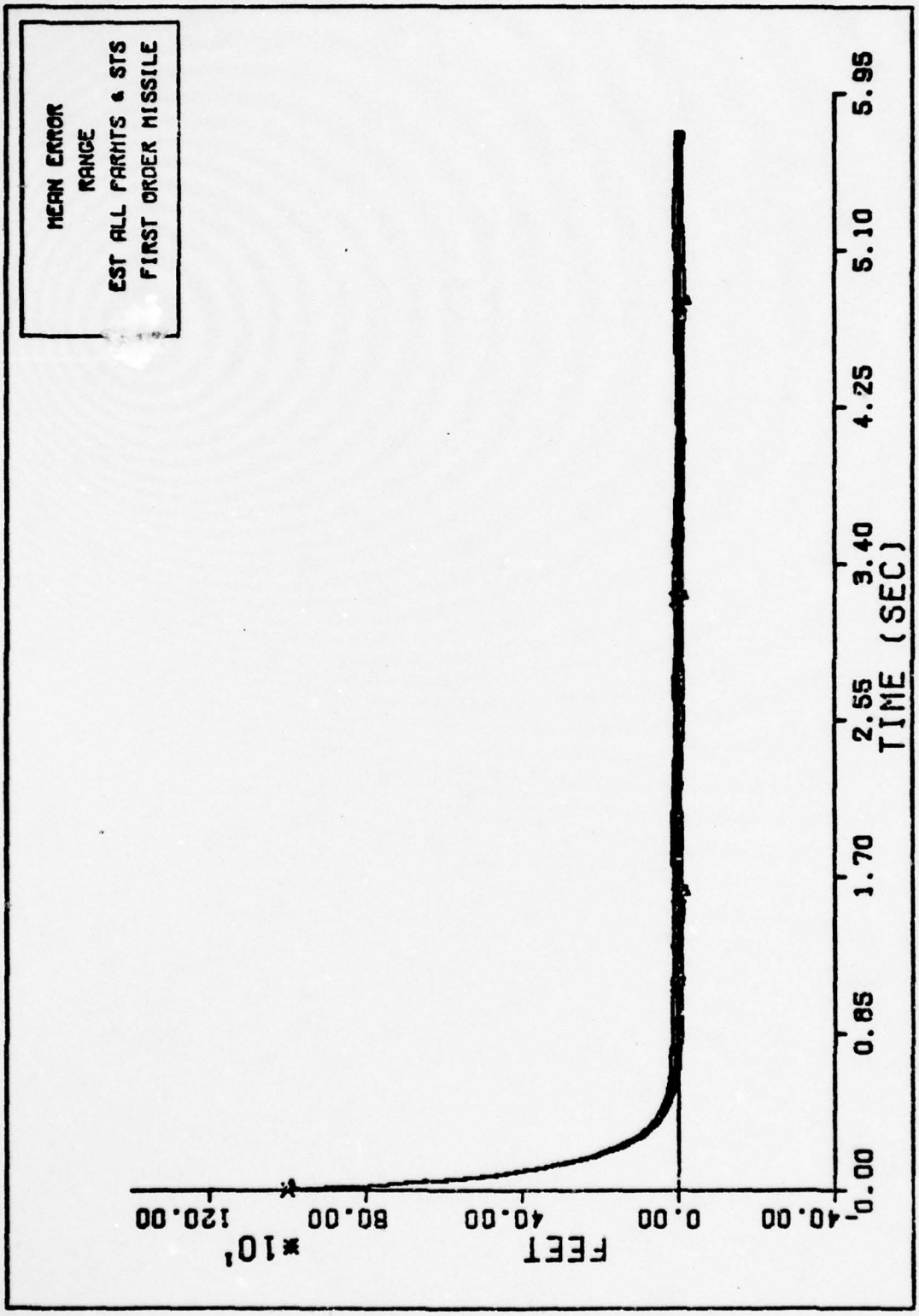

Fig. 43. RANGE FIRST ORDER MISSILE

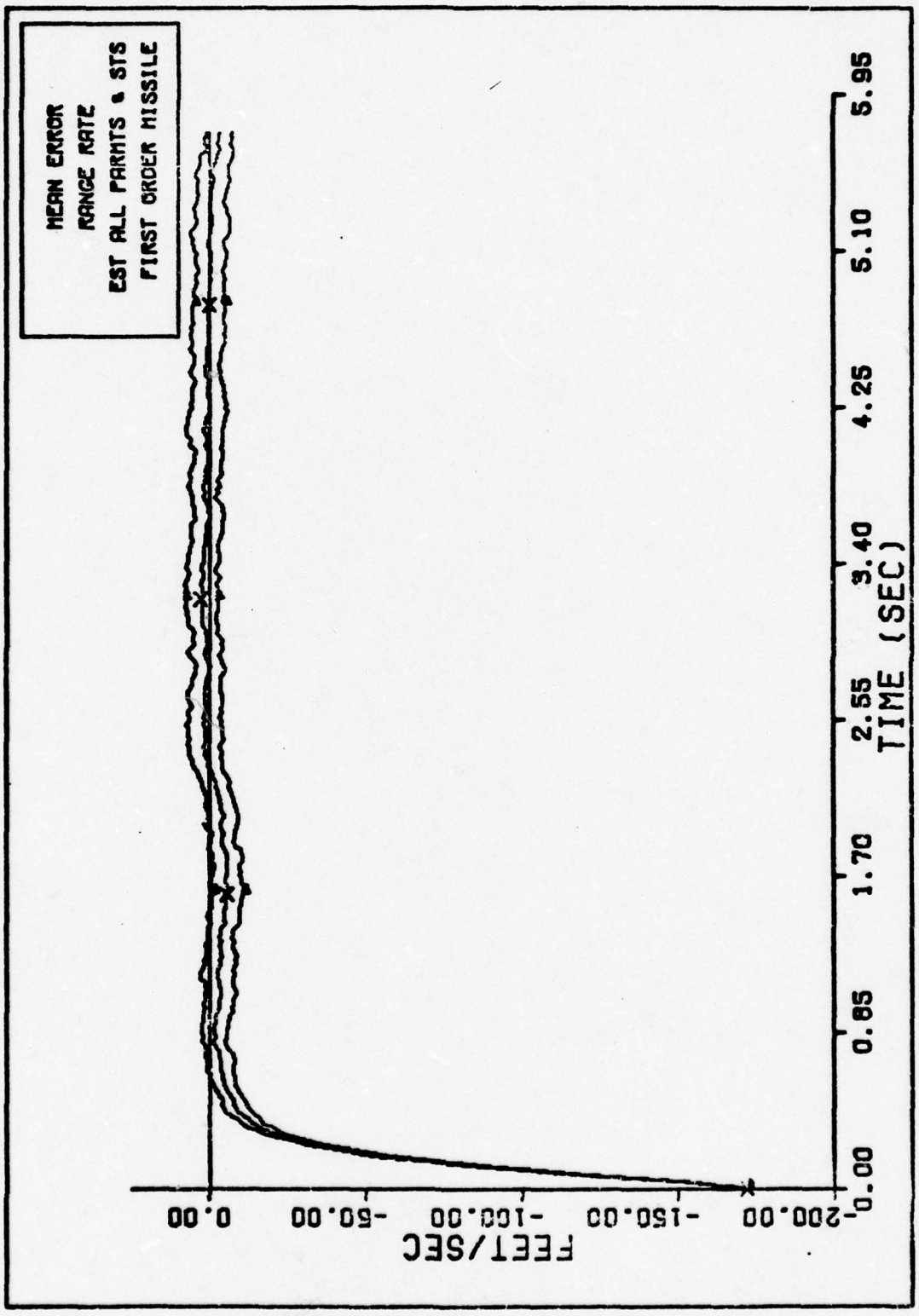

Fig. 44. RANGE RATE FIRST ORDER MISSILE

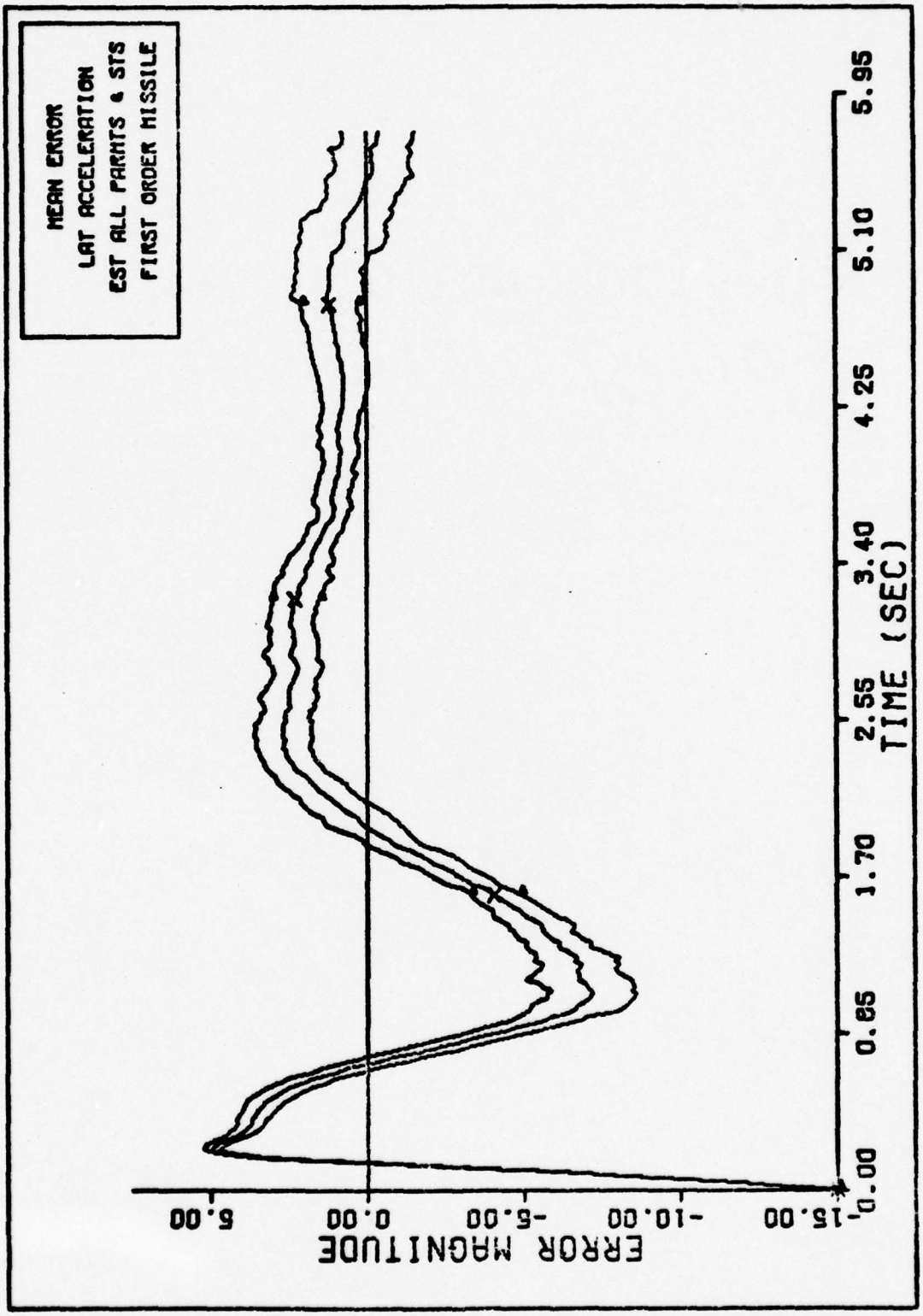

Fig. 45. LAT ACCELERATION FIRST ORDER MISSILE

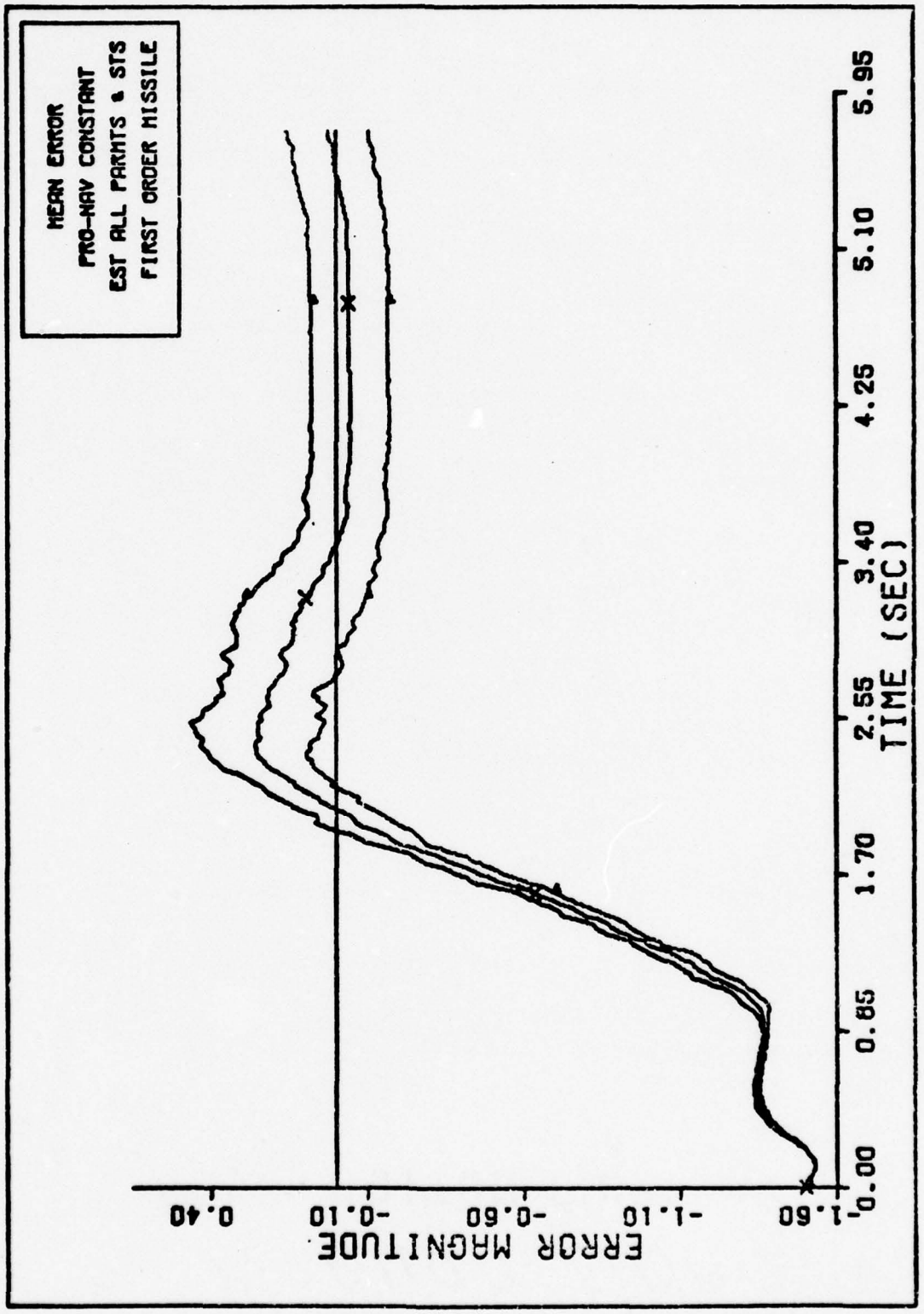

Fig. 46. PRO-NAV CONSTANT FIRST ORDER MISSILE

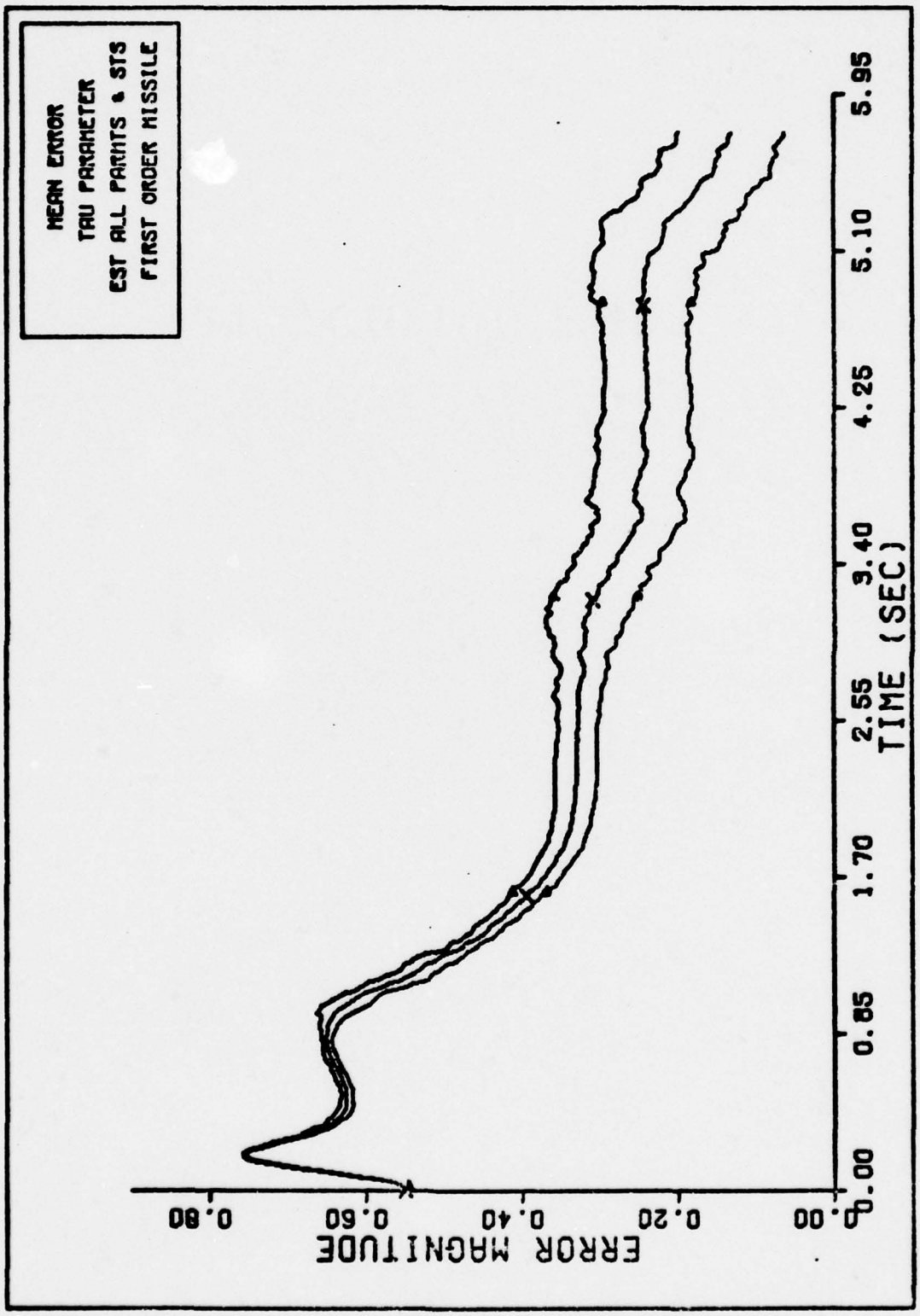

Fig. 47. TAU PARAMETER FIRST ORDER MISSILE

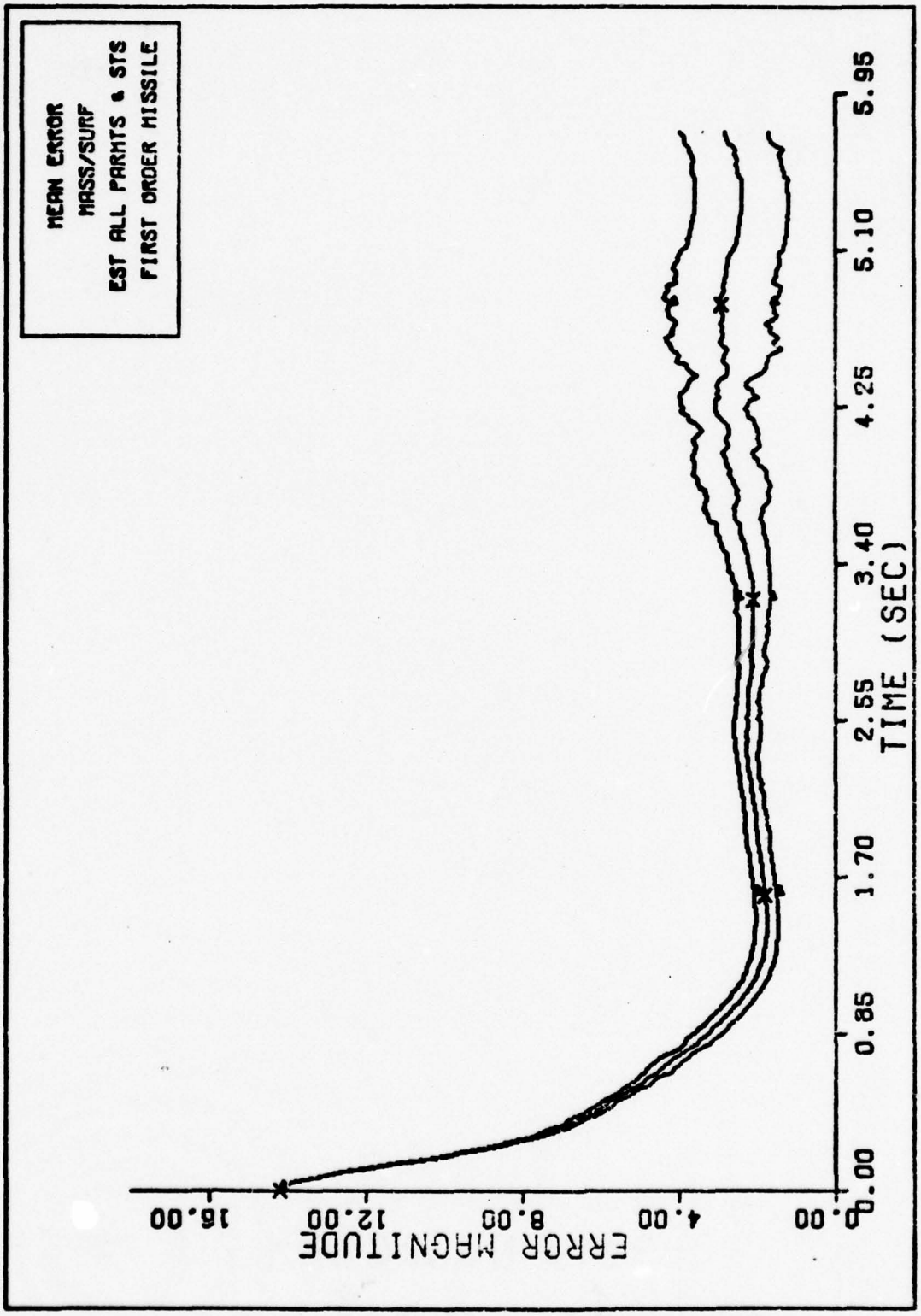

Fig. 48. MASS/SURF FIRST ORDER MISSILE

Table VII

Key Results of Final Test

	True Initial Condition	Assumed Initial Condition	State Recovery Time Parameter Acq. Time	Peak Mean Error of States After Acq. Time	Peak Mean Error of States Fourth Order	Peak Mean Error of States Bench
V^I_{mx}	1,225 fps	1,000 fps	1.0 sec	40 fps	25 fps	10 fps
θ_T	4.363 rad	4.343 rad	1.7 sec	.002 rad	.001 rad	.001 rad
R	10,000 ft	9,000 ft	0.5 sec	10 ft	5 ft	5 ft
$\dot{R}$	2,122 fps	1,900 fps	0.5 sec	15 fps	6 fps	6 fps
a_L	0.0 g's	15. g's	1.7 sec	2.5 g's	1.5 g's	1 g
n	4.5	6.0	2.5 sec			
M/S	29.197 slugs/ft^2	15 slugs/ft^2	1.0 sec			
τ_f	.85 sec	.3 sec	2.5 sec			

zero dynamic state error. The maximum error after this recovery time was about 40 ft/sec. This can be compared to the 35 ft/sec error of the first order missile filter with perfect knowledge of all three parameters.

The angle error, which was initialized with an error of .02 radians (1.1 degrees), indicates a recovery time of 1.7 seconds. This initial error can be considered as a cross range error of approximately 180 ft at the start of the intercept. The maximum error of this state never exceeds 2 milliradians after the engagement has progressed past the recovery time.

The range and range rate errors exhibit very fast recovery times of .5 seconds. The errors committed after this time were extremely small. These two results were due to the fact that both of these states are receiving information from accurate direct measurements.

The lateral acceleration state error shows the same 1.7 second recovery time shown in the angle state. It was initialized with an error of 15 g's. Although this may be considered an unreasonably large error for most cases, it could possibly arise while tracking a missile soon after launch. In this case the missile may enter a high-g maneuver in an attempt to null initial launch errors. It is worth noting that, at five seconds, the missile is achieving a lateral acceleration in excess of 15 g's. However, the error in the filter estimate at this time is only 1 g. Again, this is evidence of very good state

estimation.

The filter does not acquire an accurate estimate of the proportional navigation constant until approximately 2.5 seconds after initialization. Subsequent to this time, the filter mean error remains less than 5% of true value (4.5). The τ_f parameter estimate does not converge to zero error as well as n does, but shows continual improvement over the entire scenario. After 2.5 seconds, it was estimated well enough to aid in accurate state estimation. The error in the M/S ratio reaches steady state the soonest of all three parameters. It converges quickly (approximately one second) but remains biased by a positive 2 slugs/ft^2. This is only 6% of the true value (29.197 slugs/ft). These results confirm that the first order missile filter is capable of estimating both the states and parameters of an attacking air-to-air missile.

Contributions

The contributions of this study include the following. Given the three independent, radar-supplied measurements of LOS angle, range, and range rate of an air-to-air missile, an eight-state Extended Kalman Filter (modeling five dynamic states and three key parameters of the missile) was designed such that:

1a) Simultaneous estimation of the states and parameters, with reasonably accurate results, was possible for a high-g scenario.

1b) The filter was considered "robust" since, when

tracking a low-g target the filter was capable of achieving good state estimation even with the parameter estimation not being as accurate as for the high-g scenario

2) Modeling efforts for this type of filter must consider the bandwidth of the guidance strip. This fact can be emphasized by recalling that even including an exact model of the missile's autopilot did not signficantly aid estimation.

3) The filter could recover from large initial errors in the dynamic states and parameters of the missile.

4) Implementation of this filter would require an acquisition time to lock on to adequate parameter estimates. The best example of this was the 2.5 second acquisition time of proportional navigation constant.

Future Research

The following suggestions are listed as possible areas for future research:

1) The analysis considered only non-thrusting missiles. It is suggested that this restriction could be removed by using a random walk to model the acceleration due to thrust.

2) Because all filters were optimally tuned for a given trajectory, the robustness observed over that one trajectory may not be observed for

other scenarios without retuning the filter. This suggests that an analysis be peformed which more completely investigates the "robustness" of the filter, possibly leading to the use of adaptive tuning techniques in the filter design.

3) Parameter estimation was not needed for the low-g trajectory to achieve accurate state estimates. The initial trajectory of an air-to-air missile may in some cases be this benign since the LOS rate is small for extended ranges. This suggests the possibility of an adaptive filter which initially uses a random walk or first order Markov model for acceleration and then switches to the more complete model presented in this report.

4) The analysis should be expanded to consider three dimensional motion of the missile and the ownship.

5) An analysis could be performed which investigates the degradation of filter performance by increasing the measurement update time interval.

Bibliography

1. Blakelock, J. H. Automatic Control of Aircraft and Missiles. New York: John Wiley and Sons, Inc., April 1965.

2. Fitts, J. M. "Aided Tracking as Applied to High Accuracy Point Systems." IEEE Transactions on Aerospace and Electronic Systems, AES-9: 350-368, May 1973.

3. Jazwinski, A. H. Stochastic Processes and Filtering Theory. New York: Academis Press, 1970.

4. Kjesbo, L. A. Terminal Miss Sensitivity of a Radar Guided Air-to-Air Missile System. Unpublished thesis. Wright-Patterson Air Force Base, Ohio: Air Force Institute of Technology, June 1974.

5. Lutter, R. N. Application of an Extended Kalman Filter to an Advanced Fire Control System. Unpublished thesis. Wright-Patterson Air Force Base, Ohio: Air Force Institute of Technology, December 1976.

6. Maybeck, P. S. Stochastic Estimation and Control Systems (Part I). Unpublished manuscript. Wright-Patterson Air Force Base, Ohio: Air Force Institute of Technology, February 1975.

7. -----. Stochastic Estimation and Control Systems (Part II). Unpublished manuscript. Wright-Patterson Air Force Base, Ohio: Air Force Institute of Technology, February 1975.

8. Pearson, J. B. III. and E. B. Stear. "Kalman Filter Applications in Airborne Radar Tracking." IEEE Transactions on Aerospace and Electronic Systems, AES-10: 319-329, May 1974.

9. Price, C. F. and W. D. Koeningsburg. Adaptive Control and Guidance for Tactical Missiles. TASC TR-170-1. Reading, Massachusetts: The Analytic Sciences Corporation, June 1970.

11. Stallard, D. V. Classical and Modern Guidance of Homing Interceptor Missiles. Technical report. Presented to Seminar of Department of Aeronautics and

Astronautics Cambridge, Massachusettes: Massachusetts Institute of Technology, April 1968.

12. Stockum, L. A. A Study of Guidance Controllers for Homing Missiles. Unpublished dissertation. Columbus, Ohio: Ohio State University, 1974.

13. TR-73-287. "Air-to-Air Control Expoisition Phase III (Expo III). " Wright-Patterson Air Force Base, Ohio: Air Force Avionics Laboratory, September 1973.

14. Wrigley, W. and W. M. Hollister and W. G. Denhard. Gyroscopic Theory, Design, and Instrumentation. Cambridge, Massachusetts: The Massachusetts Institute of Technology Press, 1969.

Appendix A

This appendix contains the changes to the software package designed by Lutter as reported in Reference 5. There were five changes to the original software which resulted in software used for this study. The changes were:

1) The complexity of the integration package of the filter was reduced to a first order Euler.
2) The initialization of the matrix subtraction subroutine was changed.
3) The modeling of the seeker noise in the truth model was changed to include both correlated and uncorrelated noises.
4) The original noise strengths were scaled (multiplied) by a Δt factor.
5) The updating of the lineraized $\underline{F}$ matrix was accomplished at each integration step.

Also included is a discussion on the assumption made by Lutter concerning the linearization of the $\underline{F}$ matrix (Ref 5:65).

Euler Integration Package

The reduced complexity of the integration package of the filter was accomplished by replacing a fourth order Runge-Kutta package with a first order Euler integration package. The Runge-Kutta package was constructed with a backward predictor corrector which automatically decreased the integration step size if the backward prediction was not within a specified tolerance of the starting value.

This one change reduced the execution time of the simulation to one-fifth of its original time.

Even though a simple integration proceedure, the Euler package did not degrade the simulation accuracy substantially. A sample case was run using the Runge-Kutta package and the Euler package for the same data set. The plots of the case using the Euler integration pacakage were indistinguishable from the plots generated using the Runge-Kutta package. These results are shown in Appendix B. The Euler package was also used because it more closely approximated the integration packages available for on-line implementation purposes.

Change Matrix Subtraction

The purpose of the matrix subtraction subroutine was to perform the subtraction operation

$$\underline{C} = \underline{A} + \underline{B} \tag{68}$$

where $\underline{A}$, $\underline{B}$, and $\underline{C}$ were all matrices of the same size. The original routine was set up so that the $\underline{C}$ matrix was initialized at zero. This was unnecessary because $\underline{C}$ was not used in the actual calculation, but just as a location to store the results. The original routine also led to problems when passing information between the subroutine and the main program. The same argument was used for the $\underline{A}$ matrix, passed into the subroutine, and the resultant matrix $\underline{C}$, passed back to the main program, within the subtraction subroutine. This resulted in setting all

values in the matrix $\underline{A}$ to zero. Thus

$$\underline{C} = \underline{0} \; -\underline{B} = -\underline{B} \tag{69}$$

To avoid the problem and to simplify the subroutine the zero initialization of $\underline{C}$ was removed.

Modeling Seeker Noise

In his software, Lutter inappropriately modeled the seeker noise so as to include only a time-correlated noise. As stated in Chapter II, to model this noise correctly, both the correlated and uncorrelated components were included.

The Δt Factor

When developing an equivalent discrete system of equations for the Extended Kalman Filter, noise strength must be given special consideration. The noise sigmas, given in Chapter II, are related to continuous noise sources. To model this continuous noise correctly by discrete equations, the noise strengths should be multiplied by a factor of Δt, the integration time. This Δt factor was included in this study.

To explain the reason for including the Δt factor, the equivalent continuous and discrete time noise relationships should be compared. Consider a linear stochastic differential equation of the form:

$$\dot{\underline{x}}(t) = \underline{F}(t)\underline{x}(t) + \underline{G}(t)\underline{w}(t) \tag{70}$$

where

$\underline{w}(t)$ = a zero mean white Gaussian noise with

$$E\{\underline{w}(t)\underline{w}(t+\tau)^T\} = \underline{Q}_c(t)\delta(t)$$

An equivalent discrete time system equation would be

$$\underline{x}(t_{i+1}) = \underline{\Phi}(t_{i+1},t_i)\underline{x}(t_i) + \int_{t_i}^{t_{i+1}} \underline{\Phi}(t_{i+1},t_i)\underline{G}(\tau)\underline{w}(\tau)d\tau \quad (71)$$

$$= \underline{\Phi}(t_{i+1},t_i)\underline{x}(t_i) \quad \underline{w}_d(t_i) \quad (72)$$

where

$$E\{\underline{w}_d(t_i)\underline{w}_d(t_i)^T\} = \int_{t_i}^{t_{i+1}} \underline{\Phi}(t_{i+1},\tau)\underline{G}(\tau)\underline{Q}_c(\tau)\underline{G}(\tau)^T\underline{\Phi}(t_{i+1},\tau)^T d\tau$$

$$= \underline{Q}_d(t_i)$$

$$E\{\underline{w}_d(t_i)\underline{w}_d(_j)^T\} = \underline{0} \text{ for } t_i \neq t_j$$

When the integration step size is small relative to system time and constants, the following approximation can be made

$$\int_{t_i}^{t_{i+1}} \underline{\Phi G Q}_c G^T \underline{\Phi}^T d\tau = \underline{G}(t_i)\underline{Q}_c(t_i)\underline{G}(t_i)^T\Delta t \quad (73)$$

where all terms of order Δt^2 or higher have been neglected. Therefore

$$\underline{Q}_d(t_i) = \{\underline{G}(t_i)\underline{Q}_c(t_i)\underline{G}(t_i)^T\}\Delta t \quad (74)$$

and for $\underline{G}(t_i) = I$ (the identify matrix)

$$\underline{Q}_d(t_i) = \underline{Q}_c(t_i)\Delta t \quad (75)$$

This argument is also directly applicable to nonlinear stochastic differential equations in which the driving noise enters linearly, and so it was used in this study.

Update of the F Matrix

Because of the complicated and time consuming nature of the Runge-Kutta integration package, and the use of a very short measurement update time of .02 seconds, Lutter made the decision to update the linearized $\underline{F}$ matrix of the Extended Kalman Filter only at measurement update times. The integration package in this study was less complicated and therefore reduced the execution time. It was reasonable to update the $\underline{F}$ matrix at each integration step (.01 seconds). This did not increase the execution time any appreciable amount and was a more correct implementation of the Extended Kalman Filter equations.

Linearization of f-vector

Lutter assumed that $\dot{\theta}_T$, γ_m, and V_m, which are all functions of the filter's state variables, remained constant over the propagation period of .02 seconds. One example of how this assumption affects the linearization of the f-vector can be shown by the development of the partial derivative of $\underline{f}$ for an element which is a function of $\dot{\theta}_T$

$$F_{ij} = \frac{\partial f_i}{\partial x_j}$$

$$= \frac{\partial f_i\{\dot{\theta}_T(x_1,\ldots x_n),\ x_1,\ldots x_n\}}{\partial x_j} \qquad (76)$$

$$= \frac{\partial f_i}{\partial \dot{\theta}_T}\frac{\partial \dot{\theta}_T}{\partial x_j} + \left.\frac{\partial f_i}{\partial x_j}\right| \qquad (77)$$

$\dot{\theta}_T$ = constant

The assumption considers the first term of Equation (77) to be zero. This assumption was verified by computer simulation of the high-g scenario for the fourth order missile filter. A complete linearization of the f-vector which did not assume these terms to be zero was used in this filter. The plots for all states are labeled "comp" and can be found in Appendix B. Comparison of these plots with the fourth order set labeled "A/P EQ 0", whose filter $\underline{F}$-matrix included these assumptions, confirms the validity of the assumption made by Lutter.

Vita

Salvatore J. Cusumano was born on 12 February 1948 in Elizabeth, New Jersey. He graduated from St. Benedict's Preparatory School in Newark, New Jersey in 1966. After one year at Rutgers University, he attended the United States Air Force Academy from which he received the degree of Bachelor of Electrical Engineering in June 1971. Upon graduation, he entered pilot training and received his wings in June 1972. He then served as a KC-135 pilot in the 920th Air Refueling Squadron at Wurtsmith, Air Force Base, Michigan until entering the School of Engineering, Air Force Institute of Technology, in June of 1976.

Manuel De Ponte, Jr. was born 14 December 1949 in Honolulu, Hawaii. In 1967, he graduated from Mater Dei High School, Santa Ana, California. He then entered Loyola University of Los Angeles from where he graduated with a Bachelor of Science degree in Engineering in 1971.

Upon graduation, he entered the United States Air Force and was commissioned a second lieutenant. He was then assigned as Space Systems Operations Officer to Mill Valley Air Force Station, California in December of 1971 and Thule Air Base, Greenland in February 1973. In February 1974, he was assigned to the Foreign Technology Division, Wright-Patterson Air Force Base, Ohio. There he served as a trajectory analyst for the Engineering Data Analysis Branch.

In June 1976, he entered the Graduate Electrical

Engineering program at the Air Force Institute of Technology. Upon graduation in December 1977, he will be assigned to Detachment 1 of the Space and Missile System Organization, Norton Air Force Base, California.

UNCLASSIFIED

SECURITY CLASSIFICATION OF THIS PAGE (When Data Entered)

REPORT DOCUMENTATION PAGE		READ INSTRUCTIONS BEFORE COMPLETING FORM
1. REPORT NUMBER AFIT/GE/EE/77-13	2. GOVT ACCESSION NO.	3. RECIPIENT'S CATALOG NUMBER
4. TITLE (and Subtitle) An Extended Kalman Filter Fire Control System Against Air-to-Air Missiles		5. TYPE OF REPORT & PERIOD COVERED MS Thesis 6. PERFORMING ORG. REPORT NUMBER
7. AUTHOR(s) Salvatore J. Cusumano, Captain, USAF Manuel DePonte, Jr., Captain, USAF		8. CONTRACT OR GRANT NUMBER(s)
9. PERFORMING ORGANIZATION NAME AND ADDRESS Air Force Institute of Technology (AFIT-EN) Wright-Patterson AFB, Ohio 45433		10. PROGRAM ELEMENT, PROJECT, TASK AREA & WORK UNIT NUMBERS
11. CONTROLLING OFFICE NAME AND ADDRESS Laser Analysis Group, Avionic Laboratory Wright-Patterson AFB, Ohio		12. REPORT DATE December 1977 13. NUMBER OF PAGES (Vol I) 142 (Vol II) 352
14. MONITORING AGENCY NAME & ADDRESS(if different from Controlling Office)		15. SECURITY CLASS. (of this report) Unclassified 15a. DECLASSIFICATION/DOWNGRADING SCHEDULE

16. DISTRIBUTION STATEMENT (of this Report)

Approved for public release: distribution unlimited

17. DISTRIBUTION STATEMENT (of the abstract entered in Block 20, if different from Report)

18. SUPPLEMENTARY NOTES

Approved for public release; IAW AFR 190-17

Jerral F. Guess, Captain, USAF
Director of Information

19. KEY WORDS (Continue on reverse side if necessary and identify by block number)

Kalman Filter
Aided Tracking
Fire Control

20. ABSTRACT (Continue on reverse side if necessary and identify by block number)

A previously designed Extended Kalman Filter, based upon the proporational guidance law and an aerodynamic drag equation, is modified to include complete modeling of the autopilot and the guidance system of the missile. A sensitivity analysis of three key parameters is performed to determine the observability of these parameters and the possible need to estimate them in less complex filter models. This analysis establishes the advantages

DD FORM 1 JAN 73 1473 EDITION OF 1 NOV 65 IS OBSOLETE

UNCLASSIFIED

SECURITY CLASSIFICATION OF THIS PAGE (When Data Entered)

Block 20 continued

for reasonable estimates of all three parameters during a high-g trajectory.

A less complex model reduces the number of filter states from eleven to eight. The seeker dynamics, the guidance system, and the autopilot of a missile are approximated by a first order lag. The three parameters estimated include the time constant of the first order lag, the proportional navigation constant of the missile, and the ratio of mass to cross-sectional area of the missile.

Under the high-g scenario, reasonably accurate estimates of the states and the parameters are accomplished. Under the low-g scenario, parameter estimates are degraded due to lack of excitation. This performance of the parameters, however, does not hinder the accurate estimation of the missile states.